Vol. 25, no. 2, 2026 eISSN 2949-4826
PEER-REVIEWED SCIENTIFIC AND PRACTICAL JOURNAL

Russian Journal of Veterinary Pathology

Parasitology / Animal Pathology, Morphology, Physiology, Pharmacology and Toxicology / Sanitation, Hygiene, Ecology, Veterinary and Sanitary Expertise and Biosafety / Zootechnics, Feeding, Technologies of Feed Preparation and Livestock Products Production / Infectious Diseases and Animal Immunology / Breeding, Selection, Genetics and Animal Biotechnology

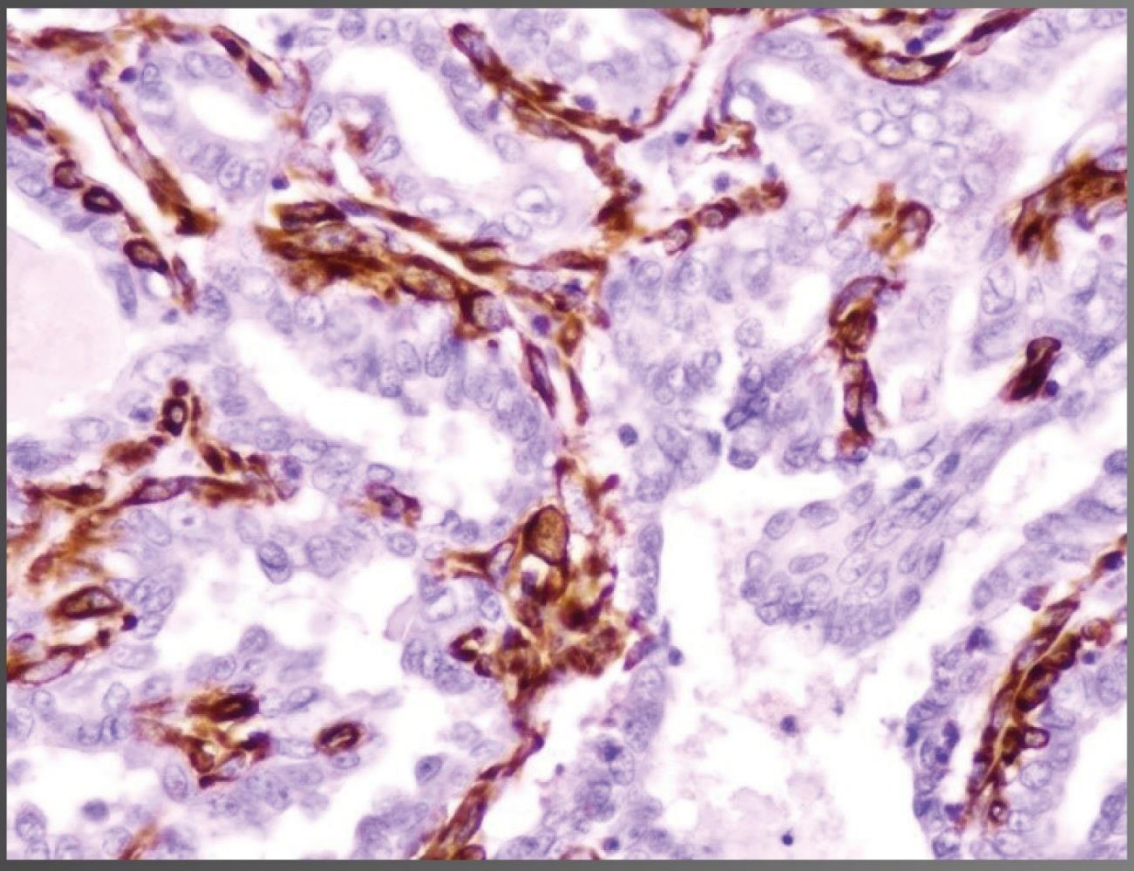

Vimentin expression in fibroblasts. Breast cancer. Immunohistochemical reaction. Magnification ×400.
Authors: Darbisheva A.A., Dilekova O.V.

www.vetpat.ru
DOI 10.23947/2949-4826

Russian Journal of Veterinary Pathology
Veterinarnaya Patologiya

Peer-reviewed scientific and practical journal

The medal "For Achievements in the Field of Veterinary Science" by the Veterinary Medicine Department of the Russian Academy of Agricultural Sciences. Awarded to the editorial board in 2009.

eISSN 2949-4826

Published since 2002

Periodicity – 4 issues per year

DOI: 10.23947/2949-4826

Founder and Publisher — Don State Technical University (DSTU), Rostov-on-Don, Russian Federation

The "Russian Journal of Veterinary Pathology" is a peer-reviewed scientific and practical journal that publishes the results of the original research and review articles in the field of veterinary medicine. It covers the issues of parasitology, physiology, pharmacology, ecology, and considers the aspects of infectious diseases and other matters of veterinary medicine of companion, farm and wild animals.

The journal aims at enhancing the level of professional knowledge of the target audience and to disseminate worldwide the highly efficient, thoroughly verified scientific research in the field of veterinary medicine using an online open access format for maximum accessibility.

The journal is included in the List of the leading peer-reviewed scientific publications (Higher Attestation Commission under the Ministry of Science and Higher Education of the Russian Federation), where the main scientific results of dissertations for the degrees of Doctor and Candidate of Science in the following scientific specialties should be published.

– Parasitology
– Animal Pathology, Morphology, Physiology, Pharmacology and Toxicology
– Sanitation, Hygiene, Ecology, Veterinary and Sanitary Expertise and Biosafety
– Infectious Diseases and Animal Immunology
– Zootechnics, Feeding, Technologies of Feed Preparation and Livestock Products Production
– Breeding, Selection, Genetics and Animal Biotechnology

Registration	Extract from the Register of Registered Mass Media ЭЛ № ФС 77 – 85552 dated June 27, 2023, issued by the Federal Service for Supervision of Communications, Information Technology and Mass Media
Indexing and Archiving	RISC, DOAJ, AGRIS, CyberLeninka, CrossRef, Internet Archive, Google Scholar
Website	http://www.vetpat.ru/
Address of the Editorial Office	1, Gagarin Sq., Rostov-on-Don 344003, Russian Federation
E-mail	vetpat@donstu.ru
Telephone	+7 (863) 273-85-08
Date of Publication No.4,2025	30.06.2026

ДОНСКОЙ ГОСУДАРСТВЕННЫЙ ТЕХНИЧЕСКИЙ УНИВЕРСИТЕТ

Ветеринарная патология

Russian Journal of Veterinary Pathology

Рецензируемый научно-практический журнал

eISSN 2949-4826

Издается с 2002 года

Периодичность – 4 выпуска в год

DOI: 10.23947/2949-4826

Медаль Отделения ветеринарной медицины РАСХН «За достижения в области ветеринарной науки». Вручена редакции журнала в 2009 г.

Учредитель и издатель — Федеральное государственное бюджетное образовательное учреждение высшего образования «Донской государственный технический университет» (ДГТУ), г. Ростов-на-Дону

«Ветеринарная патология» — рецензируемый научно-практический журнал, в котором публикуются результаты оригинальных исследований и обзорные статьи в области ветеринарной медицины. Освещаются вопросы паразитологии, физиологии, фармакологии, экологии, уделяется внимание инфекционным болезням и другим аспектам ветеринарии домашних, сельскохозяйственных и диких животных.

Цель журнала заключается в повышении профессионального уровня знаний профильной аудитории и распространении по всему миру высокоэффективных, тщательно проверенных ветеринарных научных исследований, используя только онлайн-формат открытого доступа для максимальной доступности.

Журнал включен в перечень рецензируемых научных изданий, в котором должны быть опубликованы основные научные результаты диссертаций на соискание ученой степени кандидата наук, на соискание ученой степени доктора наук (Перечень ВАК) по следующим научным специальностям:

1.5.17 – Паразитология (биологические науки, ветеринарные науки)
4.2.1 – Патология животных, морфология, физиология, фармакология и токсикология (биологические науки, ветеринарные науки)
4.2.2 – Санитария, гигиена, экология, ветеринарно-санитарная экспертиза и биобезопасность (биологические науки, ветеринарные науки)
4.2.3 – Инфекционные болезни и иммунология животных (ветеринарные науки, биологические науки)
4.2.4 – Частная зоотехния, кормление, технологии приготовления кормов и производства продукции животноводства (биологические науки, сельскохозяйственные науки)
4.2.5 – Разведение, селекция, генетика и биотехнология животных (биологические науки, сельскохозяйственные науки)

Регистрация:	Выписка из реестра зарегистрированных средств массовой информации ЭЛ № ФС 77-85552 от 27.06.2023 г., выдано Федеральной службой по надзору в сфере связи, информационных технологий и массовых коммуникаций
Индексация и архивация:	РИНЦ, DOAJ, AGRIS, CyberLeninka, CrossRef, Internet Archive, Google Scholar
Сайт:	https://www.vetpat.ru/
Адрес редакции:	344003, Российская Федерация, г. Ростов-на-Дону, пл. Гагарина, 1
E-mail:	vetpat@donstu.ru
Телефон:	+7 (863) 273-85-08
Дата выхода №4,2025 в свет:	30.06.2026

Editorial Board

Редакционная коллегия

Contents

Содержание

ANIMAL PATHOLOGY, MORPHOLOGY, PHYSIOLOGY, PHARMACOLOGY AND TOXICOLOGY

ПАТОЛОГИЯ ЖИВОТНЫХ, МОРФОЛОГИЯ, ФИЗИОЛОГИЯ, ФАРМАКОЛОГИЯ И ТОКСИКОЛОГИЯ

UDC 619:616:591.4:636.2:616.61
https://doi.org/10.23947/2949-4826-2026-25-2-7-13

Original Empirical Research

The Relationship between Caspase-3, -6 Expression and Morphological Changes in Kidneys of Cows

Irina M. Petrova, Maksim V. Bytov, Sergey L. Khatsko, Vladlena D. Zubareva, Lyudmila I. Drozdova, Irina A. Shkuratova

Ural Federal Agrarian Scientific Research Center, Ural Branch of the Russian Academy of Sciences, Ekaterinburg, Russian Federation

✉ bytovmaks@mail.ru

EDN: YNAJTZ

Abstract

Introduction. Cow kidneys are exposed to the impact of industrial factors, which is manifested in development of the various nephropathies with systemic effects on organism. The kidneys are the main organs responsible for homeostasis by regulating osmolarity, mineral balance, and acid-base balance in organism through the excretion of water and inorganic electrolytes. Renal pathology often has latent character and is diagnosed postmortem. Significant destructive changes, including cell death, are often detected in lactating cows due to high metabolic load they undergo. Caspase pathway is one of the pathways in the complex apoptotic signaling cascade. Unfortunately, the expression of caspases in bovine kidneys has not been yet described in the literature. The aim of the study is to describe the relationship between the expression of caspase-3 and caspase-6 and the pathological changes in the kidneys of high-yielding cows.

Materials and Methods. A morphological study of renal samples from high-yielding cows (4–6 lactations, 7–8 years old, n=4) was conducted at the Ural Federal Agrarian Scientific Research Center, Ural Branch of the Russian Academy of Sciences in the period from 2023 to 2025. Standard histological techniques including hematoxylin and eosin staining and Mallory's trichrome staining were used. Immunohistochemical analysis of the samples using antibodies to caspase-3, and -6 was performed.

Results. It was found that in the kidneys of 7–8-year-old cows there develop the destructive processes including renal failure, inflammatory reactions, and sclerotic and microcirculatory disorders. The observed conditions are associated with high expression of caspase-6 at the level of the renal tubules, which confirms damage to the renal parenchyma. Caspase-3 is expressed primarily in the renal tubules and in renal stroma elements, which indicates intensification of apoptotic processes across the entire organ.

Discussion and Conclusion. The destructive processes revealed in the kidneys of high-yielding cows are likely to be associated not only with the age but also with the high metabolic load imposed on the organism during lactation. The research findings substantiate the need for further study of pro-apoptotic factors due to their influence on the development of various pathologies in cattle.

Keywords: caspase-3, caspase-6, apoptosis, cows, nephrosclerosis, polycystic kidney disease, morphological study

Declaration on Compliance with the Principles of the European Convention for the Protection of Vertebrate Animals Used for Experimental and Other Scientific Purposes: the authors declare that all the studies were conducted in compliance with the principles of Good Laboratory Practice.

Funding. The work was carried out in the frame of the Russian Science Foundation project No. 23-16-00117 of 2023 "Spatial characterization of transcriptomic and metabolomic features of premature structural and functional degeneration of tissues in farm animal and poultry organs".

For Citation: Petrova IM, Bytov MV, Khatsko SL, Zubareva VD, Drozdova LI, Shkuratova IA. The Relationship between Caspase-3, -6 Expression and Morphological Changes in Kidneys of Cows. *Russian Journal of Veterinary Pathology*. 2026;25(2):7–13. https://doi.org/10.23947/2949-4826-2026-25-2-7-13

Оригинальное эмпирическое исследование

Взаимосвязь экспрессии каспазы-3 и -6 с морфологическими изменениями в почках коров

И.М. Петрова, М.В. Бытов ✉, С.Л. Хацко, В.Д. Зубарева, Л.И. Дроздова, И.А. Шкуратова

[1] Уральский федеральный аграрный научно-исследовательский центр Уральского отделения Российской академии наук, г. Екатеринбург, Российская Федерация

✉ bytovmaks@mail.ru

Аннотация

Введение. Почки коров подвержены воздействию факторов промышленного содержания, что проявляется развитием различных нефропатий, оказывающих системное действие на организм. Почки — основной орган, обеспечивающий гомеостаз путем регуляции осмолярности, минерального и кислотно-основного состояния организма посредством экскреции воды и неорганических электролитов. Патология почек зачастую носит латентный характер и диагностируется постмортально. У лактирующих коров в связи с высокой метаболической нагрузкой часто выявляются значительные деструктивные изменения, проявляющиеся в том числе гибелью клеток. Одним из путей в сложном каскаде сигналинга апоптоза является каспазный. К сожалению, на сегодняшний день для крупного рогатого скота экспрессия ферментов-каспаз в почках не описана. Цель работы — описание взаимосвязи экспрессии каспазы-3 и каспазы-6 с патологическими изменениями в почках высокопродуктивных коров.

Материалы и методы. Морфологическое исследование образцов почек высокопродуктивных коров (4–6 лактаций, возраст 7-8 лет, n=4) проведено в ФГБНУ УрФАНИЦ УрО РАН в период с 2023 по 2025 г. Использованы стандартные методы гистотехники с окрашиванием препаратов гематоксилином и эозином, а также по Маллори. Проведено иммуногистохимическое исследование образцов с антителами к каспазе-3 и -6.

Результаты исследования. Выявлено, что у коров в возрасте 7-8 лет в почках развиваются деструктивные процессы в виде почечной недостаточности, воспалительных реакций, склеротических и микроциркуляторных изменений. Обнаруженные явления ассоциированы с высокой экспрессией каспазы-6 на уровне почечных канальцев, что подтверждает повреждение почечной паренхимы. Каспаза-3 экспрессируется преимущественно в канальцах почки, а также в элементах ее стромы, что указывает на интенсификацию апоптических процессов по всему органу.

Обсуждение и заключение. Обнаруженные деструктивные процессы в почках высокопродуктивных коров ассоциированы, вероятно, не только с возрастом, но также с высокой метаболической нагрузкой на организм во время лактаций. Полученные данные обосновывают дальнейшее изучение проапоптических факторов в свете их влияния на развитие различных патологий у крупного рогатого скота.

Ключевые слова: каспаза-3, каспаза-6, апоптоз, коровы, нефросклероз, поликистоз, почки, морфологическое исследование

Декларация о соблюдении принципов Европейской конвенции о защите позвоночных животных, используемых для экспериментов и других научных целей: авторы заявляют, что все проведенные исследования соответствовали принципам конвенции и правилам надлежащей лабораторной практики.

Финансирование. Работа выполнена в рамках проекта Российского научного фонда 2023 г. «Пространственная характеристика транскриптомных и метаболомных особенностей преждевременной структурно-функциональной дегенерации тканей органов сельскохозяйственных животных и птицы» (№ 23-16-00117).

Для цитирования: Петрова И.М., Бытов М.В., Хацко С.Л., Зубарева В.Д., Дроздова Л.И., Шкуратова И.А. Взаимосвязь экспрессии каспазы-3 и -6 с морфологическими изменениями в почках коров. *Ветеринарная патология*. 2026;25(2):7–13. https://doi.org/10.23947/2949-4826-2026-25-2-7-13

Introduction. The organism of high-yielding dairy cows is susceptible to metabolic imbalances. One of the consequences of milk production stress is the development of acidotic syndrome, which negatively effects the kidneys [1]. Ketosis, which cows are particularly susceptible to during lactation, can also lead to various nephropathies [2]. The pathological processes developed in the kidneys inhibit organ functioning, have a systemic nature and affect the overall condition of an animal. In the scientific community the role of apoptosis in the pathogenesis of various kidney diseases has long been actively discussed [3]. For example, it has been established that programmed death of tubular epithelial cells, along with necrosis, are the basic signs of acute renal failure [4]. In addition to nephrocyte damage, renal vascular damage and endothelial cell apoptosis are important factors in the development of renal dysfunction. The loss of endothelial

cells by apoptosis is deemed to play a significant role in changing the microvascular network observed during renal damage [5]. Apoptosis has also been described in renal interstitial cells following ischemic renal injury [6].

Caspases are enzymes belonging to a group of proteases that are involved in cell apoptosis. 12 caspases have been described for humans and rodents, however for cattle, the exact number of enzymes from this group has to be determined yet. Caspases are divided into 3 groups: executioners, initiators and inflammatory caspases. Caspase-3 represents the executive caspase group, and caspase-6 — the initiator caspase group. Studies on the role of caspases in the development of various pathologies in the organs of cattle are extremely few. For example, the role of caspase-3 in the apoptosis of mammary gland cells in cows fed with concentrated feed has been described [7]. Data on the role of caspases in the development of renal pathologies in cattle are not available in the literature. However, caspases are known to be involved in inflammatory responses, apoptosis, vasoconstriction, and tubular necrosis in various kidney diseases in humans and rodents [8]. Furthermore, the important role of caspases in renal damage makes them a favourable target for therapy. For example, on the example of polycystic kidney disease in rats, it was demonstrated that caspase inhibition can reduce apoptosis in renal tubules and slow disease progression [9].

Therefore, the aim of the present study is to describe the relationship between caspase-3 and caspase-6 expression and morphological changes in the kidneys of high-yielding cows with pathologies.

Materials and Methods. The work was carried out at the Ural Federal Agrarian Scientific Research Center, Ural Branch of the Russian Academy of Sciences (Ekaterinburg) in the period from 2023 to 2025. To study the morphological changes in the kidneys of cows, the material was collected postmortem from animals aged 7–8 years old, that had 4–6 lactations (n=4). For histological examination, tissue specimens of no more than 0.5 cm thick were fixed in 10% Neutral Buffered Formalin (NBF) in a proportion of 1:20. After fixation, the specimens were rinsed in running water, dehydrated, then soaked in paraffin, and paraffin blocks were prepared. Paraffin sections of 3–4 μm thickness were made. Sections were deparaffinized and stained using hematoxylin and eosin and Mallory's trichrome staining techniques.

Immunohistochemical staining of the samples with antibodies to caspase-3 and caspase-6 was performed to assess the intensity of apoptosis in the organ. For immunohistochemical analysis, sections were placed on the adhesive slides (Superfrost), then placed on a slide drying bench (+60°C) until the paraffin was visibly melted. Immunohistochemical analysis was performed in compliance with the following protocol:

1. The sections were placed in a Tris-EDTA buffer solution heated in a water-bath up to 96°C for 12 min for heat-induced epitope retrieval (HIER, pH 6; "PrimeBio-Med", Russia).

2. After 12 minute incubation in a water-bath, the sections were left in the buffer solution to cool to indoor temperature and then rinsed with distilled water.

3. The sections were incubated in an H_2O_2 solution for 10 min, then placed in distilled water for 2 min.

4. The sections were dried and outlined with a hydrophobic pen.

5. The sections were soaked in TBST buffer solution for 1 min.

6. Primary antibodies were applied to the sections, which were then placed in the humidified incubator for 1 hour at 30°C.

7. Sections were rinsed three times with TBST buffer solution.

8. Secondary antibodies were applied to the sections, which were then placed in the humidified incubator for 30 minutes at 30°C.

9. Sections were rinsed three times with TBST buffer solution.

10. DAB chromogen was applied to the sections, which were incubated until darkening, approximately during 30–60 seconds.

11. Sections were rinsed in distilled water and then counterstained with hematoxylin for 10 seconds.

12. Sections were rinsed in distilled water, decolorized, and placed in balsam.

Antibodies to caspase-3 (PAA626Bo01, Cloud-Clone Corp., China) and caspase-6 (PAC340Bo02, Cloud-Clone Corp., China) were used as primary antibodies at a 1:100 dilution. Antibodies to rabbit IgG (SAA544Rb19, Cloud-Clone Corp., China) were used as secondary antibodies with DAB (Bio-Rad Laboratories, Inc., USA) as a horseradish peroxidase substrate in accordance with the manufacturer's instructions.

Histological description of the specimens was made, and the intensity of immunohistochemical staining was visually assessed.

Research Results. Examination of the cows' renal specimens has revealed significant changes in the organ. The dilation in Shumlyansky Bowman capsule of renal corpuscles was seen in the renal cortex. Endothelial proliferation was visible in the Juxtaglomerular apparatus, indicating the development of intracapillary glomerulonephritis (Fig. 1.1). Cystic cavities of varying sizes were found throughout the cortex, indicating renal failure (Fig. 1.2). Protein casts were deposited in the lumen of the proximal tubules, indicating a protein metabolism disorder. Nephrocytes with degenerative changes, and a number of cells exhibiting structural abnormalities were observed. The renal tubules demonstrated narrowing of the lumen, swelling of the nephrocytes, and changes in their structure (Figs. 1.1 and 1.2).

Mallory's trichrome staining has revealed increased connective tissue patterns in the Shumlyansky Bowman capsule and between the proximal convoluted tubules, indicating productive inflammation (Fig. 1.3). Foci of nephrosclerosis were found in renal interstitium between the tubules (Fig. 1.4). In the area of blood vessels, particularly near the perivascular zone of arcuate arteries, the pronounced sclerotic processes were observed — the extensive areas of connective tissue proliferation, stained in various shades of blue (Fig. 1.5). Within the vessels themselves, the active processes of disorganization and proliferation of vascular wall elements, and sharp narrowing of the arterial lumen were observed (Fig. 1.6).

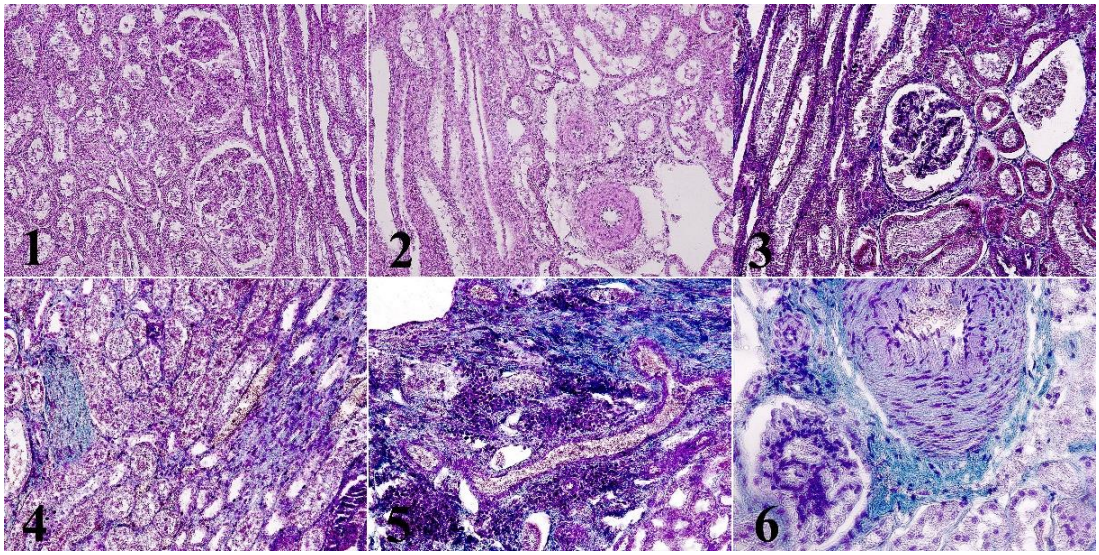

Fig. 1. Morphological structure of the kidneys of high-yielding cows aged 7–8 years:
1, 2 — hematoxylin and eosin staining, 200× magnification; 3–5 — Mallory's trichrome staining, 200× magnification;
6 — Mallory's trichrome staining, 400× magnification

Along with the morphological changes, expression of the proapoptotic proteins caspase-3 and caspase-6 was observed in the kidneys of the cows studied. Moderate expression of caspase-3 was revealed in the nephrocytes of the cortical tubules (Fig. 2.1), as well as in the cells of the parietal layer of the Shumlyansky-Bowman capsule of deformed glomeruli (Fig. 2.2). A large number of caspase-3-positive cells were also detected in the interstitium around the cystic cavities (Fig. 2.3). Nephrocytes in both the renal cortex and medulla tubules were intensely colored in brown, which indicates a high degree of caspase-6 expression in them (Fig. 2.4 and 2.5). At the same time, renal corpuscles that retained their structure were not expressing caspase-6, unlike the deformed glomeruli (Fig. 2.6). It is worth noting that not all the tubules had a caspase-positive reaction, which may be due to the possibility of cell death not only by apoptosis, but also by necrosis, and is discussed in the literature [4].

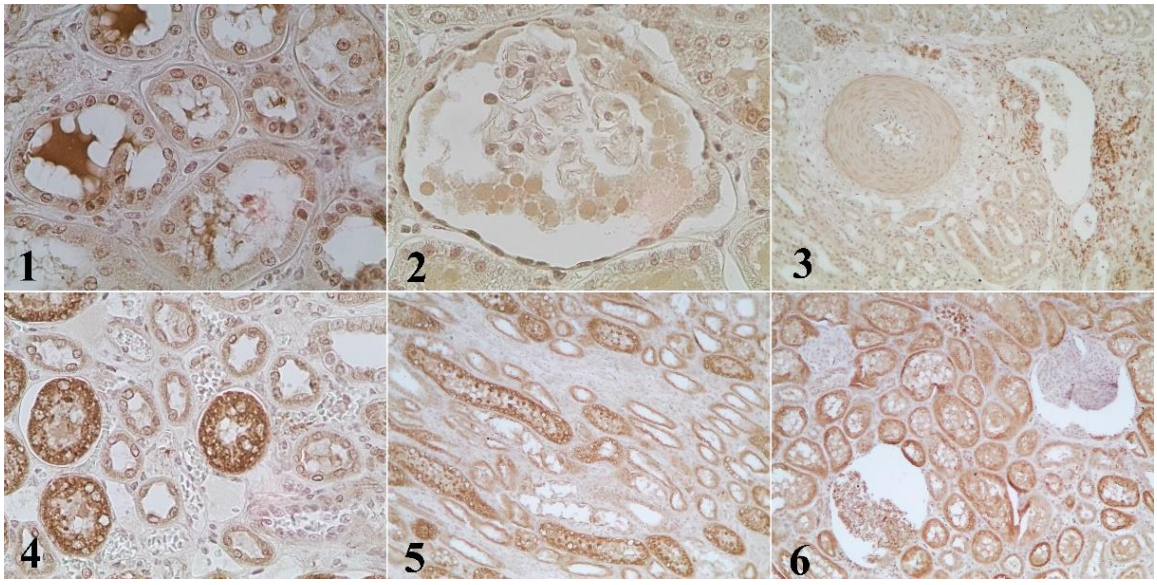

Fig. 2. Immunohistochemical detection of caspase-3 (1–3) and caspase-6 (4–6) in kidney tissues of high-yielding cows aged 7–8 years, hematoxylin counterstaining: 1, 2, 4, 5 – 400× magnification; 3 and 6 – 200× magnification

Discussion and Conclusion. Morphological examination of kidney tissues in cows aged from 7- to 8-year-old reveals the development of destructive processes in the organ, which are likely related not only to the age but also to the high metabolic load endured by the organism during lactation. Changes affect not only functioning of the organ parenchyma but also the stroma and microvasculature. The formation of cystic cavities, the presence of deformed glomeruli, and abnormalities in the structure of the Juxtaglomerular apparatus indicate the development of renal failure. The deposition of protein casts in the renal tubules and the death of nephrocytes indicate the development of degenerative processes. Foci of nephrosclerosis and significant microcirculatory disorders indicate the presence of inflammatory reactions and fibrotic changes in the organ.

The described changes are accompanied by the expression of apoptotic factors—caspase-3 and caspase-6. Caspase-6 is predominantly expressed by renal tubular cells, which, judging by morphological description, undergo degenerative processes caused by the protein metabolism disorder. Thus, the elevated caspase-6 expression is a marker of renal cell damage and pre-apoptotic state triggering the caspase cascade. Caspase-3 expression is observed not only in renal parenchyma functioning, but also in the stromal elements of the organ —in the interstitium and vascular wall cells. Thus, due to the executive role of caspase-3, the conclusion about extensive apoptotic processes occurring in various tissues of the organ can be drawn. The obtained data provide a profound basis for further in-depth study of pro-apoptotic factors in the context of their effect on the development of various pathologies in cattle.

References

1. Evglevsky AA, Evglevskaya EP, Mikhaylova II, Vanina NV, Erigenskaya NF, Suleimanova TA. Disturbance of Acid-Base Balance in the Cow: Causes, Consequences and Treatment. *Veterinary Pathology*. 2017;(1(59)):53–58. (In Russ.).

2. İssi M, Gül Y, Başbuğ O. Evaluation of Renal and Hepatic Functions in Cattle with Subclinical and Clinical Ketosis. *Turkish Journal of Veterinary and Animal Sciences*. 2016;40:47–52. https://doi.org/10.3906/vet-1505-16

3. Pak LB, Dubikov AI, Kabanceva TA, Vasilyuk AA, Grigoryan OM. Apoptosis and Nephropathies. *Nephrology*. 2013;17(4):36–43. (In Russ.).

4. Yang B, Lan S, Dieudé M, Sabo-Vatasescu JP, Karakeussian-Rimbaud A, Turgeon J, et al. Caspase-3 is a Pivotal Regulator of Microvascular Rarefaction and Renal Fibrosis after Ischemia-Reperfusion Injury. *Journal of the American Society of Nephrology*. 2018;29(7):1900–1916. http://doi.org/10.1681/ASN.2017050581

5. Hörbelt M., Lee S.Y., Mang H.E., Knipe N.L., Sado Y., Kribben A., Sutton T.A. Acute and chronic microvascular alterations in a mouse model of ischemic acute kidney injury. *American Journal of Physiology*. 2007;293(3):688–695. https://doi.org/10.1152/ajprenal.00452.2006

6. Forbes JM, Hewitson TD, Becker GJ, Jones CL. Ischemic Acute Renal Failure: Long-Term Histology of Cell and Matrix Changes in the Rat. *Kidney International*. 2000;57(6):2375–2385. https://doi.org/10.1046/j.1523-1755.2000.00097.x

7. Ul Aabdin Z, Cheng X, Dai H, Wang Y, Sahito B, Roy AC, et al. High-Concentrate Feeding to Dairy Cows Induces Apoptosis via the NOD1/Caspase-8 Pathway in Mammary Epithelial Cells. *Genes*. 2020;11(1):107. https://doi.org/10.3390/genes11010107

8. Homsi E, Janino P, de Faria JBL. Role of Caspases on Cell Death, Inflammation, and Cell Cycle in Glycerol-Induced Acute Renal Failure. *Kidney International*. 2006;69(8):1385–1392. https://doi.org/10.1038/sj.ki.5000315

9. Tao Y, Zafar I, Kim J, Schrier RW, Edelstein CL. Caspase-3 Gene Deletion Prolongs Survival in Polycystic Kidney Disease. *Journal of the American Society of Nephrology*. 2008;19(4):749–755. https://doi.org/10.1681/ASN.2006121378

About the Authors:

Irina M. Petrova, Laboratory Technician of the Genomic Research and Animal Breeding Department, Ural Federal Agrarian Research Center of the Ural Branch of the Russian Academy of Sciences (112a, Belinsky Str, P.O. Box 269, Ekaterinburg, 620142, Russian Federation), ORCID, Scopus ID, SPIN-code, marygane6@mail.ru

Maksim V. Bytov, Postgraduate Student, Junior Research Associate of the Genomic Research and Animal Breeding Department, Ural Federal Agrarian Research Center of the Ural Branch of the Russian Academy of Sciences (112a, Belinsky Str, P.O. Box 269, Ekaterinburg, 620142, Russian Federation), ORCID, Researcher ID, Scopus ID, SPIN-code, bytovmaks@mail.ru

Sergey L. Khatsko, Laboratory Technician of the Genomic Research and Animal Breeding Department, Ural Federal Agrarian Research Center of the Ural Branch of the Russian Academy of Sciences (112a, Belinsky Str, P.O. Box 269, Ekaterinburg, 620142, Russian Federation), ORCID, Scopus ID, SPIN-code, hardscore@mail.ru

Vladlena D. Zubareva, Cand.Sci. (Veterinary), Senior Research Associate of the Genomic Research and Animal Breeding Department, Ural Federal Agrarian Research Center of the Ural Branch of the Russian Academy of Sciences

(112a, Belinsky Str., P.O. Box 269, Ekaterinburg, 620142, Russian Federation), ORCID, Scopus ID, SPIN-code, zzub97@mail.ru

Lyudmila I. Drozdova, Dr.Sci. (Veterinary), Professor, Lead Research Associate of the Ecology and Noncontagious Animal Pathology Department, Ural Federal Agrarian Research Center of the Ural Branch of the Russian Academy of Sciences (112a, Belinsky Str., P.O. Box 269, Ekaterinburg, 620142, Russian Federation), ORCID, SPIN-code, drozdova43@mail.ru

Irina A. Shkuratova, Corresponding Member of the Russian Academy of Sciences, Dr.Sci. (Veterinary), Professor, Chief Research Associate of the Ecology and Noncontagious Animal Pathology Department, Ural Federal Agrarian Research Center of the Ural Branch of the Russian Academy of Sciences (112a, Belinsky Str., P.O. Box 269, Ekaterinburg, 620142, Russian Federation), ORCID, Scopus ID, SPIN-code, shkuratova@bk.ru

Claimed Contributorship:

IM Petrova: formulating the main concept, search for publications, analysis of the research results, formulating the conclusions

MV Bytov: development of research methodology, formal analysis, writing the manuscript.

SL Khatsko: conducting experiments and collecting data; preparing the initial draft of the manuscript.

VD. Zubareva: editing and refining the manuscript.

LI Drozdova: analysis and validation of the obtained results, preparing a draft of the manuscript.

IA Shkuratova: scientific supervision, developing the concept and methodology of research, preparing a draft of the manuscript.

***Conflict of Interest Statement:* the authors declare no conflict of interest.**

All authors have read and approved the final manuscript.

Об авторах:

Петрова Ирина Михайловна, лаборант Отдела геномных исследований и селекции животных, Уральский федеральный аграрный научно-исследовательский центр Уральского отделения Российской академии наук (620142, Российская Федерация, г. Екатеринбург, а/я 269, ул. Белинского, 112а), ORCID, Scopus ID, SPIN-код, marygane6@mail.ru

Бытов Максим Владимирович, аспирант, младший научный сотрудник Отдела геномных исследований и селекции животных, Уральский федеральный аграрный научно-исследовательский центр Уральского отделения Российской академии наук (620142, Российская Федерация, г. Екатеринбург, а/я 269, ул. Белинского, 112а), , ORCID, Researcher ID, Scopus ID, SPIN-код, bytovmaks@mail.ru

Хацко Сергей Леонидович, лаборант Отдела геномных исследований и селекции животных, Уральский федеральный аграрный научно-исследовательский центр Уральского отделения Российской академии наук (620142, Российская Федерация, г. Екатеринбург, а/я 269, ул. Белинского, 112а), ORCID, Scopus ID, SPIN-код, hardscore@mail.ru

Зубарева Владлена Дмитриевна, кандидат ветеринарных наук, старший научный сотрудник Отдела геномных исследований и селекции животных, Уральский федеральный аграрный научно-исследовательский центр Уральского отделения Российской академии наук (620142, Российская Федерация, г. Екатеринбург, а/я 269, ул. Белинского, 112а), ORCID, Scopus ID, SPIN-код, zzub97@mail.ru

Дроздова Людмила Ивановна, доктор ветеринарных наук, профессор, ведущий научный сотрудник Отдела экологии и незаразной патологии животных, Уральский федеральный аграрный научно-исследовательский центр Уральского отделения Российской академии наук (620142, Российская Федерация, г. Екатеринбург, а/я 269, ул. Белинского, 112а), ORCID, SPIN-код, drozdova43@mail.ru

Шкуратова Ирина Алексеевна, член-корреспондент РАН, доктор ветеринарных наук, профессор, главный научный сотрудник Отдела экологии и незаразной патологии животных, Уральский федеральный аграрный научно-исследовательский центр Уральского отделения Российской академии наук (620142, Российская Федерация, г. Екатеринбург, а/я 269, ул. Белинского, 112а), ORCID, Scopus ID, SPIN-код, shkuratova@bk.ru

Заявленный вклад авторов:

И.М. Петрова: формирование основной концепции, поиск литературы, анализ результатов, формирование выводов.

М.В. Бытов: разработка методологии, формальный анализ; написание рукописи.

С.Л. Хацко: проведение экспериментов и сбор данных; подготовка первоначального варианта рукописи.

В.Д. Зубарева: редактирование и доработка рукописи.

Л.И. Дроздова: анализ полученных результатов, валидация, написание черновика рукописи.

И.А. Шкуратова: научное руководство, разработка концепции, разработка методологии, написание черновика рукописи.

Конфликт интересов: **авторы заявляют об отсутствии конфликта интересов.**

Все авторы прочитали и одобрили окончательный вариант рукописи.

Received / Поступила в редакцию 15.04.2026
Reviewed / Поступила после рецензирования 13.05.2026
Accepted / Принята к публикации 24.05.2026

ANIMAL PATHOLOGY, MORPHOLOGY, PHYSIOLOGY, PHARMACOLOGY AND TOXICOLOGY

ПАТОЛОГИЯ ЖИВОТНЫХ, МОРФОЛОГИЯ, ФИЗИОЛОГИЯ, ФАРМАКОЛОГИЯ И ТОКСИКОЛОГИЯ

UDC 577.218:575.1:577.1
https://doi.org/10.23947/2949-4826-2026-25-2-14-24

Literature Review

DAT Knockout Rat Models: Dopamine Dysfunction, Epigenetic Mechanisms, and Approaches to Gene Therapy: A Literature Review

Albert R. Khakimov[1] ✉, **Anna I. Lebedeva**[1], **Lyalya A. Musina**[1], **Zukhra R. Khismatullina**[2]

EDN: TYPQWH

[1]Russian Eye and Plastic Surgery Center of Bashkir State Medical University of the Ministry of Healthcare of the Russian Federation, Ufa, Russian Federation

[2]Ufa University of Science and Technology, Ufa, Russian Federation

✉ shershakov2015a@mail.ru

Abstract

Introduction. Dopamine transporter gene knockout (DAT-KO) animal model is a valuable experimental tool for studying the pathophysiology of diseases associated with dopamine dysfunction, such as attention-deficit/hyperactivity disorder, schizophrenia, and Parkinson's disease. The aim of the present review is to systematize the scientific data on using the DAT-KO rat models for studying dopaminergic dysfunction, epigenetic mechanisms, and gene therapy approaches.

Materials and Methods. Literary sources were searched for in PubMed, Scopus, Web of Science, and Google Scholar scientific citation databases. The original studies (n=49) on the structure and function of DAT, knockout models, epigenetic mechanisms, and gene therapy published from 1991 to 2025 in English language only were included into the review. The results have been presented in a PRISMA flow chart and in the illustrations.

Results. DAT knockout rat models exhibit a 5–7-fold increase of extracellular dopamine level, hyperactivity and structural changes in the basal ganglia, which indicates dopamine dysfunction. Homozygous knockout animals are found to completely lack functional DAT protein, whereas animals with heterozygous knockout retain approximately half of its function and exhibit intermediate phenotypes. Epigenetic regulation of SLC6A3 gene expression is mediated by DNA methylation, histone modifications (including H3K9/K14 acetylation and H3K27 methylation) and microRNA modifications. Moreover, the DAT promoter remains hypomethylated during postnatal ontogenesis in rats, resulting in its age-related expression increase. Gene therapy using viral vectors has demonstrated the potential to restore DAT function.

Discussion and Conclusion. The DAT-KO rat models reliably reproduce the key neurochemical and morphological features of dopaminergic dysfunction. However, the picture seems much incomplete due to the fragmentary character of data on the dynamics of epigenetic regulation of dopamine transporter expression during disease progression and insufficient evidence base on dose-dependent effects and long-term safety of gene therapy. The epigenetic mechanisms open the new tracks for biomarker search and personalization of therapy. Gene therapy using adeno-associated viral and lentiviral vectors demonstrates the potential to restore DAT function in the preclinical models, however, further clarification on dose-dependent effects and minimization of the immune response is required. The integration of epigenetic markers into the clinical protocols, development of combinatory strategies, and validation of the DAT-KO models for comorbid conditions continue to be the promising tracks for further research.

Keywords*:* literature review, dopamine (dopaminergic) dysfunction, dopamine transporter, DAT, DAT gene knockout, rats, mice, DAT-KO, SLC6A3, epigenetic regulation, gene therapy, viral vectors

For Citation: Khakimov AR, Lebedeva AI, Musina LA, Khismatullina ZR. DAT Knockout Rat Models: Dopamine Dysfunction, Epigenetic Mechanisms, and Approaches to Gene Therapy: A Literature Review. *Russian Journal of Veterinary Pathology*. 2026;25(2):14–24. https://doi.org/10.23947/2949-4826-2026-25-2-14-24

Обзор научной литературы

Модель крыс с нокаутом гена DAT: дофаминовая дисфункция, эпигенетические механизмы и подходы к генной терапии. Обзор научной литературы

А.Р. Хакимов[1] ✉, **А.И. Лебедева**[1], **Л.А. Мусина**[1], **З.Р. Хисматуллина**[2]

[1]ФГБОУ ВО «Башкирский государственный медицинский университет» Минздрава России «Всероссийский центр глазной и пластической хирургии», г. Уфа, Российская Федерация

[2]ФГБОУ ВО «Уфимский университет науки и технологий», г. Уфа, Российская Федерация

✉ shershakov2015a@mail.ru

Аннотация

Введение. Модель животных с нокаутом кодирующего гена (DAT-KO) представляет собой ценный экспериментальный инструмент для изучения патофизиологии заболеваний, связанных с нарушением дофаминовой функции, таких как синдром дефицита внимания и гиперактивности, шизофрения, болезнь Паркинсона. Целью обзора является систематизация научных данных о дофаминергической дисфункции, эпигенетических механизмах и подходах к генной терапии на модели крыс с нокаутом гена DAT (DAT-KO).

Материалы и методы. Поиск литературных источников проводился в базах данных PubMed, Scopus, Web of Science и Google Scholar. В обзор включены оригинальные исследования только на английском языке (n=49), опубликованные в период с 1991 по 2025 гг. и посвященные структуре и функциям DAT, моделям нокаута, эпигенетическим механизмам и генной терапии. Результаты представлены в виде блок-схемы PRISMA и рисунков.

Результаты исследования. В моделях нокаута DAT у крыс наблюдается 5–7-кратное повышение внеклеточного уровня дофамина, гиперактивность и структурные изменения в базальных ганглиях, что отражает дофаминовую дисфункцию. Гомозиготные нокаутные животные полностью лишены функционального белка DAT, тогда как гетерозиготы сохраняют около половины его активности и демонстрируют промежуточные фенотипы. Эпигенетическая регуляция экспрессии гена *Slc6a3* осуществляется через метилирование ДНК, модификации гистонов (включая ацетилирование H3K9/K14 и метилирование H3K27) и микроРНК, причем в постнатальном онтогенезе крыс промотор DAT остается гипометилированным, что обеспечивает возрастное повышение его экспрессии. Генная терапия с использованием вирусных векторов демонстрирует потенциал восстановления функции DAT.

Обсуждение и заключение. Модель DAT-KO у крыс достоверно воспроизводит ключевые нейрохимические и морфологические особенности дофаминергической дисфункции. Полнота картины, однако, во многом ограничена фрагментарностью данных о динамике эпигенетической регуляции экспрессии дофаминового транспортера в ходе прогрессирования заболеваний и недостаточной доказательной базой по дозозависимым эффектам и долгосрочной безопасности генной терапии. Эпигенетические механизмы открывают новые направления для поиска биомаркеров и персонализированной терапии. Применение генной терапии с использованием аденоассоциированных и лентивирусных векторов демонстрирует потенциал восстановления функции DAT в доклинических моделях, однако требует дальнейшего уточнения дозозависимых эффектов и минимизации иммунного ответа. Перспективными направлениями остаются интеграция эпигенетических маркеров в клинические протоколы, разработка комбинированных стратегий и валидация модели DAT-KO при коморбидных состояниях.

Ключевые слова: обзор научной литературы, дофаминовая (дофаминергическая) дисфункция, дофаминовый транспортер, DAT, нокаут гена DAT, крысы, мыши, DAT-KO, *SLC6A3*, эпигенетическая регуляция, генная терапия, вирусные векторы

Для цитирования: Хакимов А.Р., Лебедева А.И., Мусина Л.А., Хисматуллина З.Р. Модель крыс с нокаутом гена DAT: дофаминовая дисфункция, эпигенетические механизмы и подходы к генной терапии. Обзор научной литературы. *Ветеринарная патология*. 2026;25(2):14–24. https://doi.org/10.23947/2949-4826-2026-25-2-14-24

Introduction. Rats and mice with knockout of dopamine transporter (DAT) protein encoded by SLC6A3 gene, represent a valuable experimental DAT-KO model for studying the pathophysiology of diseases associated with dopamine dysfunction. The dopamine transporter plays a key role in regulation of the dopaminergic neurotransmission, ensuring reuptake of dopamine from the synaptic cleft into presynaptic neurons, which controls the intensity and duration of signals on dopamine receptors [1, 2]. DAT is expressed predominantly in dopaminergic neurons of the

substantia nigra and ventral tegmental area, with the highest degree of expression in the striatum and nucleus accumbens, where it regulates up to 80% of dopaminergic signaling [1]. In the prefrontal cortex, crusial for higher cognitive control and social interactions, DAT, in conjunction with the norepinephrine transporter, modulates dopamine activity influencing social behavior [2, 3]. Dysregulation in DAT-mediated dopamine homeostasis is associated with depression, bipolar disorder, attention-deficit/hyperactivity disorder (ADHD), schizophrenia, and Parkinson's disease. Due to DAT being a target for psychostimulants such as cocaine and methylphenidate, it is associated with disorders caused by the use of psychoactive substances [1, 4].

The DAT-KO animal model is characterized by a complete absence of functional protein, which induces a hyperdopaminergic condition characterised by a 5–7-fold increase of extracellular dopamine level and a decrease in presynaptic dopamine [5]. This results in hyperactivity, motor stereotypies, cognitive deficits and disorders of diminished motivation, as well as in neuroanatomical changes including reduced striatal volume, increased volume of prefrontal cortex and cerebellum, decreased GABAergic interneuron density and dysfunctions in the serotonergic system [2, 4, 6]. With regard to physiology, DAT-KO rats exhibit reduction of body weight and impaired motor coordination, making the model relevant for studying ADHD and schizophrenia [1, 2]. Heterozygous DAT-KO rats with partial reduction in DAT activity, also exhibit patterns of altered behavior. Therefore, even partial loss of DAT function can cause significant neurochemical and behavioral changes [6].

The aim of the present review is to systematize scientific data on using the DAT knockout (DAT-KO) rat models for studying the dopamine dysregulation, epigenetic mechanisms, and gene therapy approaches.

Materials and Methods. Search for literature was performed in PubMed, Scopus, Web of Science, and Google Scholar science citation databases by the keywords: dopamine transporter, DAT-KO, SLC6A3, dopamine dysregulation, epigenetic regulation, gene therapy, dopamine signaling, DAT knockout rats, DAT knockout mice, neurotransmitter transporters. The latest search was performed on October 5, 2025. The following publications were included in the analysis: the original studies, reviews, and meta-analyses in the English language only, published from 1991 to 2025. The sample included publications (n=49) containing data on: dopamine dysregulation (neurochemical and behavioral phenotypes) in DAT-KO rat models; epigenetic mechanisms of dopamine transporter regulation; gene therapy approaches to DAT deficiency using viral vectors. The results have been systematized and presented in the PRISMA flow chart and in the figures.

Research Results

Selection of references. As a result of the search across all scientific citation databases and other sources, 253 publications were found. After removal of 43 duplicates, 210 articles were selected for further analysis. After screening titles and abstracts, 115 articles were excluded. Potentially eligible full texts (n=95) were uploaded to cloud storage and reviewed by a wide range of experts to assess their relevance. At this stage, another 46 publications were excluded as they did not contain information on methodology, results, or interpretation thereof in the context of dopaminergic dysfunction. Thus, 49 articles were eventually selected to undergo the review. A summary of the literary sources' verification process for inclusion into the review is presented in the PRISMA flowchart (Fig. 1).

The SLC6A3 gene and its role in dopamine dysfunction. The SLC6A3 gene encoding DAT belongs to the family of Na^+- and Cl^--dependent neurotransmitter transporters (Fig. 2). In humans, it is localized on the chromosome 5p15.33 and covers approximately 52.5 kbp, including 15 coding exons [7, 8]. The DAT protein consists of 620 amino acids, has a molecular mass of approximately 69 kDa, and includes 12 transmembrane domains. The N-terminus and C-terminus are oriented toward the cytoplasm, and a large extracellular loop with N-glycosylation sites is located between the third and fourth domains [9].

In mice, the SLC6A3 gene is localized on chromosome 13 and has a highly conserved gene sequence: the gene also consists of 15 exons, and the boundaries of the intron-exon junctions in the coding regions are completely identical to those in humans [10]. The size of the mouse gene is significantly smaller—approximately 24.5 kbp—and the nucleotide sequences are 85% identic with that of human DAT (amino acid sequences are 93% identic). However, mice lack the Variable Number Tandem Repeat (VNTR) in the 3'-untranslated region characteristic of humans, and their full-length mRNA is 10% shorter [10, 11].

The rat SLC6A3 gene also contains 15 exons, and its cDNA was cloned and sequenced in the early 1990s [12, 13]. The amino acid sequence of rat DAT exhibits 97% identity with the human protein within the transmembrane domains

and 87% — in the extramembrane regions [11]. The rat protein, like the mouse protein, consists of 619 amino acids (one less than the human protein due to the absence of the CAG codon encoding glycine at position 198) and has a molecular mass of approximately 69 kDa [11].

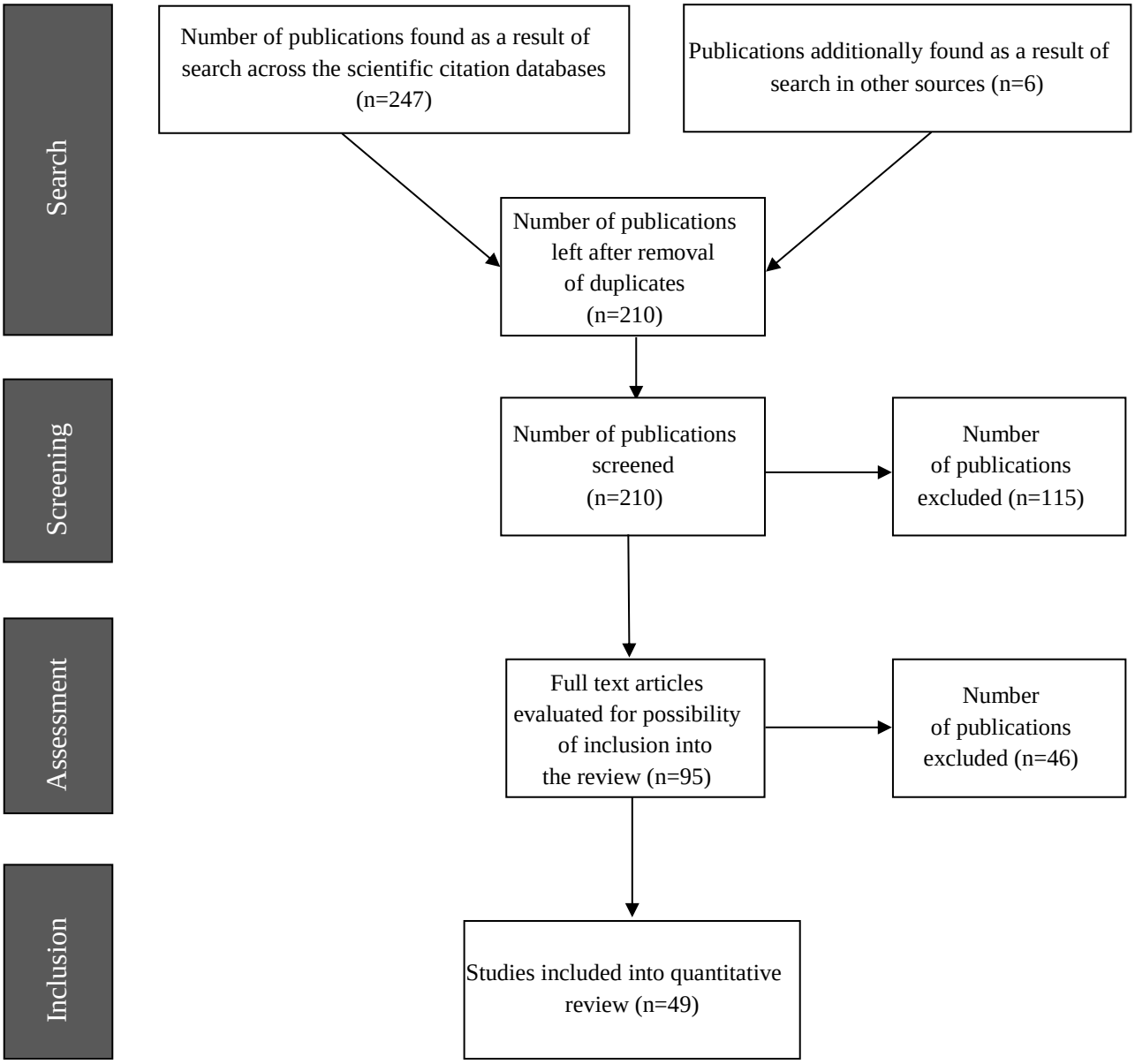

Fig. 1. Flow chart for selecting the publications in compliance with the PRISMA guidelines

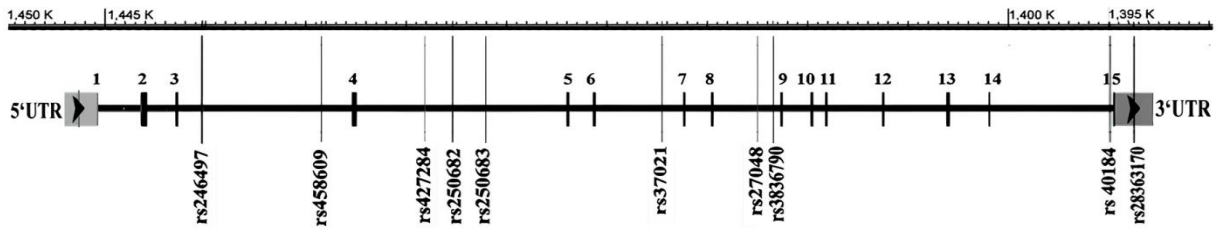

Fig. 2. Schematic representation of the human SLC6A3 gene sequence. Dark vertical blocks represent exons (1–15), with introns located between them. The positions of polymorphic markers (rs-numbers) are indicated along the gene sequence. The grey arrow indicates the 5'-untranslated region (5'UTR), and the black arrow indicates the 3'-untranslated region (3'UTR). The scale bar at the top corresponds to the gene localization on the chromosome [14]

The main function of DAT is the Na^+- and Cl^--dependent reuptake of dopamine from the synaptic cleft back to the presynaptic terminal (Fig. 3). It is less efficient in transporting norepinephrine [15, 16]. The highest expression is observed in dopaminergic neurons of the

substantia nigra and ventral tegmental area [1], whereas the highest protein density is observed in axonal terminals of the striatum and nucleus accumbens [17, 18]. In the prefrontal cortex, the amount of DAT is significantly lower, and its functions are partially compensated by the norepinephrine transporter [19].

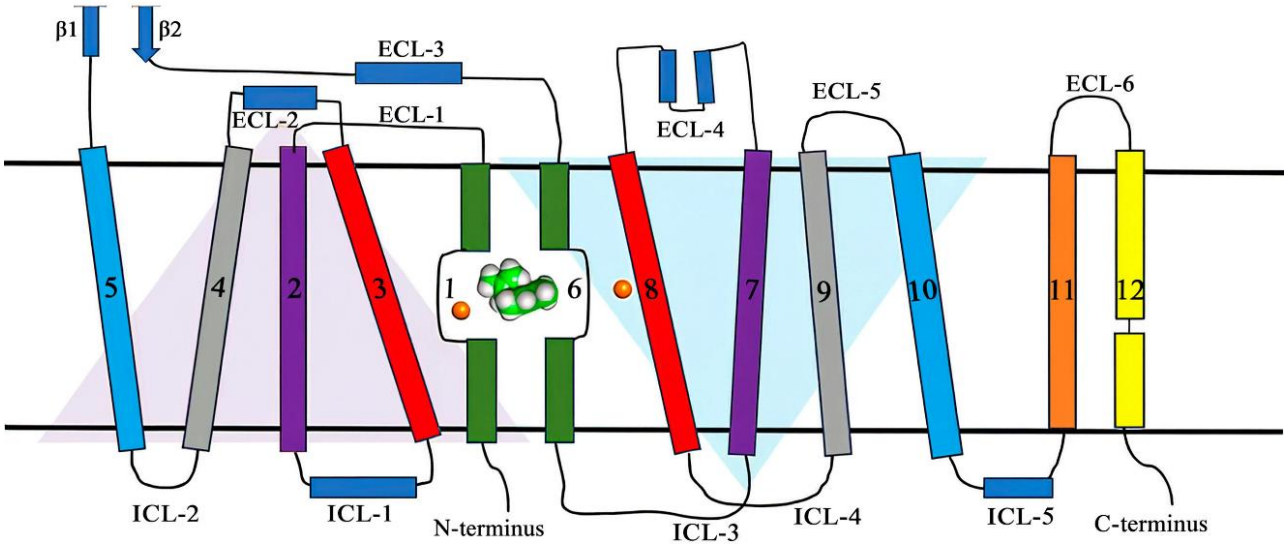

Fig. 3. Topological structure of DAT. Rectangles represent transmembrane domains (1–12) connected by intracellular (ICL) and extracellular (ECL) loops. The N-terminus and C-terminus are located in the cytoplasm. Orange-colour spheres correspond to Na^+ ions, and the green-and-white model corresponds to the substrate molecule in the binding site. Two domains with an inverted symmetry axis form the substrate binding site [15].

The functional activity of the protein is regulated by post-translational modifications. Phosphorylation of serine residues in the C-terminus affects intracellular transport and the rate of dopamine reuptake [20]. Cysteine palmitoylation in the second and fifth transmembrane domains promotes oligomer formation [21]. Lysine ubiquitination in the C-terminus determines the rate of protein degradation [22], and N-glycosylation of asparagines in the extracellular loop stabilizes the structure of DAT and regulates its expression on the membrane [23].

Genetic variants of SLC6A3 include a 40-bp VNTR polymorphism in the 3'-untranslated region. The number of repeats can vary from three to eleven, with the most common allele having ten repeats, occurring in approximately 70% of the population [24, 25]. Shorter variants, such as the 9R allele, are associated with an increased risk of schizophrenia, as well as with the development of cocaine and alcohol dependences. The 10R allele, on the contrary, is more often associated with Parkinson's disease and ADHD, as well as a lower susceptibility to nicotine dependence [8].

Alongside, the pathogenic mutations, including missense substitutions (e.g., p.Leu368GIn) and splicing abnormalities (c.1269+1G→A), which lead to the development of DAT deficiency syndrome, also known as infantile parkinsonism-dystonia 1, were found to be described [26]. This condition is characterized by a complete loss of protein function and pronounced hyperdopaminergia [26, 27]. The gene damage tolerance assessment (GDI=0.90) indicates its moderate sensitivity to mutations [28]. Among the known protein partners of DAT, the following ones have been described: PRKCABP and TGFB1I1 [29], involved in the regulation of phosphorylation; SYNGR3, binding to the N-terminus [30]; and TOR1A, affecting intracellular localization [31].

Animal models with knockout of DAT-encoding gene. The homology between human SLC6A3 and its rat ortholog is high. The coding sequence of nucleotide sequence is approximately 85% convergent, and the amino acid sequence of DAT is 92% convergent [32]. This proximity ensures preservation of key structural and functional properties of the protein across species. Therefore, gene knockout in rats replicates the key manifestations of DAT deficiency in humans, including hyperdopaminergia and motor impairments. Thus, the DAT-KO rats represent the robust models for studying the pathogenetic mechanisms associated with DAT dysfunction.

The study of the physiological role of DAT began with the creation of the first animal models with the respective gene being knocked out. Among the first such models were DAT knockout mice genetically engineered by homologous recombination *in vivo*. To construct a targeting vector, dopamine transporter cDNA was used: a 2.0 kbp region including exons 6–8 was replaced with the PGK-Neo cassette. The vector was administered into embryonic stem cells by electroporation, and homologous recombinants were selected by

double selection and confirmed by Southern blotting. Embryonic cells with correct integration were used to engineer the chimeric individuals, from which the heterozygous $DAT^{+/-}$ and homozygous $DAT^{-/-}$ mice were reared—the first experimental models with DAT deficiency [33].

Rat SLC6A3 knockout was obtained using targeted mutagenesis. This model was first engineered in 2018 in Wistar-Han rats using the "zinc fingers" method. Removal of five base pairs in the second exon resulted in the premature formation of a stop codon and the absence of DAT mRNA in the striatum [5].

In 2022, an alternative Sprague-Dawley rat strain was engineered with the identical mutation obtained by CRISPR/Cas9 method. In homozygous animals the protein was completely absent, extracellular dopamine level was 5–7 times higher, the tyrosine hydroxylase expression was observed to increase in the substantia nigra, whereas normal regulation of other genes of dopamine system was maintained [34]. Heterozygous animals preserved approximately half of the DAT function and exhibited intermediate behavioral phenotypes [35].

Epigenetic mechanisms of dopamine transporter gene regulation. Expression is regulated by epigenetic mechanisms, including DNA methylation, histone modifications, and activity of non-coding RNAs [36]. These processes determine the level of transcription in dopaminergic neurons and thereby influence dopamine reuptake and DAT endocytosis. Disruptions in these mechanisms are likely to be the factors of neurodegenerative and psychiatric disease pathogeneses.

DNA methylation is performed by DNA methyltransferase enzymes and usually reduces promoter function due to the incorporation of 5-methylcytosine into CpG islands [37]. In the brains of patients with Parkinson's disease, hypermethylation of the SLC6A3 gene promoter has been observed, which leads to reduced DAT expression and reduced efficiency of its endocytosis, increasing dopamine deficiency. The use of demethylating agents, such as 5-Aza-2'-deoxycytidine, fosters the restoration of expression and stimulates the differentiation of dopaminergic neurons [36]. In the norm, in rats in early postnatal development, DAT promoter remains hypomethylated, which ensures an age-related increase of mRNA levels in the midbrain and reflects the dynamics of the dopaminergic system maturation [38].

Histone modifications also regulate DNA accessibility for transcription factors. Acetylation of H3K9/K14 residues increases significantly by 56th postnatal day, which is accompanied by an increase in DAT mRNA levels in the midbrain and striatum. A 71.3% decrease in Dnmt1 expression and 84.3% decrease in Dnmt3a expression by 56th postnatal day are accompanied by an increase in DAT level. During the same period, the Nurr1 and Pitx3 transcription factors enhance binding to the gene promoter region, with 6- and 8-fold increase of activity, respectively. These interactions with epigenetic markers ensure age-related regulation of DAT expression [38]. Histone deacetylases HDAC1 and HDAC2 supress the transcription, whereas their inhibitors, such as vorinostat, increase acetylation and enhance protein endocytosis [36]. H3K27 methylation by EZH2 inhibits DAT expression in Parkinson's disease and reduces the levels of genes involved in endocytosis, such as clathrin and dynamin. Changes in methylation levels of H3K4 and H3K27 histones in this disease are associated with activation of neuroinflammation and death of neurons [39].

MicroRNAs and long non-coding RNAs regulate post-transcriptional DAT expression. An additional level of control is provided by mRNA modifications, such as N6-methyladenine. These modifications determine the stability and efficiency of mRNA translation and influence endocytosis via signaling pathways mediated by protein kinase C and dopamine D2 receptors [36, 40]. Demethylases reduce DAT expression and foster α-synuclein accumulation in Parkinson's disease. Moreover, RNA editing by ADAR enzymes and pseudouridylation affect the function of endocytic proteins and, consequently, dopamine reuptake processes [36].

Disruption of these mechanisms is likely to be associated with ADHD, schizophrenia, and Parkinson's disease. Whereas, according to some data, the epigenetic inhibitors, such as GSK126 and STM2457, may be considered as potential therapeutic agents [36, 41, 42].

Gene therapy for DAT deficiency. Research into gene therapy for DAT deficiency has begun relatively recently. Therapy is based on the administration of a functional copy of the SLC6A3 gene using viral vectors—mostly adeno-associated viruses (AAV) and lentiviruses (LV) [26].

Administration of AAV2 or AAV9 with the synapsin promoter into the substantia nigra or intraventricularly ensures expression of human DAT in dopaminergic neurons, followed by protein transport to the striatum. During experiments in DAT-KO mice, the therapy demonstrated distinct dose dependence: administration of 2×10^{10} vg per mouse ensured complete restoration of motor function, normalized the descent time along the vertical pole and

other motor activity indices, and resulted in 100% survival by 12th week. Similar results were obtained after administration of AAV9 on 0 postnatal day. However, excess of the therapeutic dose by an order of magnitude caused toxicity with tremor and bradykinesia in half of the animals [43].

In adult mice, administration of AAV2 or AAV2/10 with different constructs (hSyn1-hDAT, TH-iCre/CMV-DIO-mDAT) also resulted in dose-dependent recovery: walking distance and time spent in the central zone during the open field test were observed to normalize, motor skills in the vertical pole test — to improve, gait parameters — to restore and hyperlocomotion — to reduce [44].

Combinatory approaches to DAT deficiency gene therapy involve the use of multiple vectors to ensure selective expression in dopaminergic neurons or the combination of viral delivery with pharmacological agents. In the DAT-KO mouse models, combined delivery of two AAV vectors was performed: AAV2/10 packaged with Cre-recombinase under the control of the tyrosine hydroxylase (TH) promoter and AAV2/10 packaged with Cre-dependent rat DAT expression cassette were administered into the substantia nigra. This approach ensured DAT expression only in TH-positive neurons. By 48th day after injection, a decrease in hyperlocomotion in the open field test, normalization of performance in the vertical pole test, and restoration of gait parameters were observed. Biochemical analysis showed partial restoration of dopamine uptake and normalization of the ratio of metabolites of the dopaminergic and serotonergic systems [44].

Similar therapy with a dual-AAV-vector-system administered to adult mice confirmed reaching the stable effect. Tyrosine hydroxylase expression was maintained without undesirable activation in other structures, such as the locus coeruleus [44, 45].

Lentiviral vectors (LV) are used in DAT deficiency gene therapy primarily in *in vitro* models based on iPSCs differentiated into midbrain dopaminergic neurons. In such systems, LV is used to correct mutations in the target gene that cause loss of DAT function. LV transduction restores dopamine uptake, reduces apoptosis, and increases the survival of TH-positive cells. The combination of LVs with an Hsp70 protein inhibitor enhances the effect, increasing dopamine uptake by 50–100% and reducing apoptosis to 20–30% of the control level. However, for some mutations, the effect is determined predominantly by viral transduction [43]. Therapy with LV is less commonly used in *in vivo* models, including DAT-KO mice, but LVs demonstrate the potential for selective expression in dopaminergic neurons and restoration of motor function [45].

Compared to AAV systems, lentiviral vectors provide more stable integration into the host genome but are associated with a risk of insertional mutagenesis, which limits their clinical application [46]. At the same time, analysis of available data shows that the main track of research is targeted at AAV due to their low immunogenicity and high efficacy of certain serotypes (AAV2, AAV5, AAV8, AAV9) for the central nervous system [47, 48]. Studies using other viral platforms (in particular, adenovirus or herpesvirus) for the correction of DAT deficiency are not available yet, which highlights the limitations of the current experimental database.

Discussion and Conclusion. A significant amount of data on studying the dopamine dysfunction, epigenetic mechanisms, and gene therapy approaches in the DAT-KO rat models is accumulated in the scientific literature and has been systematized by the authors. However, the completeness of this dataset is limited by several factors: homozygous models are used quite oftener in research than the heterozygous ones, which limits the understanding of the full range of consequences of partial DAT dysfunction. Data on the dynamics in epigenetic regulation of the dopamine transporter remain fragmented [32, 34], and preclinical gene therapy studies are not supported by a sufficient number of studies on long-term safety [39, 42].

The literature review has shown that homozygous DAT gene knockout models can replicate certain aspects of dopaminergic transmission dysregulation [1, 5]. The complete absence of the transporter functions represents an extreme form of pathology, whereas heterozygous specimens exhibit intermediate phenotypic manifestations, and therefore their parallel study is increasingly valuable.

In addition, neuroanatomical and behavioral changes in knockout models may reflect both direct consequences of DAT deficiency and secondary conditions in other neurotransmitter networks [49]. Therefore, multimodal approaches are required to separate primary and secondary effects: high-field MRI for quantitative morphometry, targeted transcriptomic and proteomic analyses to identify cascades of compensatory changes, and time-related assessment of phenotypes at different ages. Epigenetic data on SLC6A3 regulation provide an important but still fragmentary addition to the understanding of dopaminergic dysfunction. Single studies indicate

hypermethylation of the SLC6A3 promoter in Parkinson's disease and age-dependent changes in histone methylation and modifications in rodent models [38, 39]. However, these scattered data do not allow building a comprehensive picture, since this requires establishing an exact correspondence between epigenetic markers, DAT expression and the clinical picture.

At the same time, the prospects for therapeutic correction of DAT deficiency appear encouraging. AAV-mediated delivery of SLC6A3 has shown dose-dependent restoration of motor parameters in animal models [43, 44, 45]. However, the use of AAV vectors has certain difficulties due to a narrow therapeutic index in terms of time and dose [46], which requires precision of the parameters of administration and spatiotemporal control of transgene expression.

Alongside, two-vector approaches ensuring selective expression in TH neurons and LV strategies for *in vitro* correction in iPSCs demonstrate functional efficacy [43]. But LV vectors are a priori less safe compared to AAV [48]. Therefore, research priority should be given to optimising targeting, control of expression levels and long-term monitoring of side effects.

Thus, the SLC6A3 gene knockout rat model represents a valuable experimental model for studying the pathophysiology of dopaminergic dysfunctions. Its high homology to the human SLC6A3 gene ensures the replicability of key phenotypes, including hyperdopaminergia, motor and cognitive disorders, and makes it relevant for studying ADHD, schizophrenia, Parkinson's disease, and DAT deficiency syndrome.

Advanced gene therapy strategies based on AAV and LV vectors demonstrate high efficacy in restoring DAT function and correcting motor and behavioral disorders in experimental models. However, the specific nature of gene therapy using viral vectors, particularly the narrow therapeutic dose range and the need to prevent side effects, as well as the limited available data, emphasise the importance of further research.

References

1. Savchenko A, Targa G, Fesenko Z, Leo D, Gainetdinov RR, Sukhanov I. Dopamine Transporter Deficient Rodents: Perspectives and Limitations for Neuroscience. *Biomolecules*. 2023;13(5):806. https://doi.org/10.3390/biom13050806

2. Puzzo C, Festucci F, Curcio G, Gigantesco A, Adriani W. Exploring Transgenerational Inheritance in Epigenotypes of DAT Heterozygous Rats: Circadian Anomalies and Attentional Vulnerability. *Behavioural Brain Research*. 2024;464:114921. https://doi.org/10.1016/j.bbr.2024.114921

3. Petrelli F, Dallérac G, Pucci L, Calì C, Zehnder T, Sultan S, et al. Dysfunction of Homeostatic Control of Dopamine by Astrocytes in the Developing Prefrontal Cortex Leads to Cognitive Impairments. *Molecular Psychiatry*. 2020;25(4):732–749. https://doi.org/10.1038/s41380-018-0226-y

4. Adinolfi A, Zelli S, Leo D, Carbone C, Mus L, Illiano P, et al. Behavioral Characterization of DAT-KO Rats and Evidence of Asocial-Like Phenotypes in DAT-HET Rats: The Potential Involvement of Norepinephrine System. *Behavioural Brain Research*. 2019;359:516–527. https://doi.org/10.1016/j.bbr.2018.11.028

5. Leo D, Sukhanov I, Zoratto F, Illiano P, Caffino L, Sanna F, et al. Pronounced Hyperactivity, Cognitive Dysfunctions, and BDNF Dysregulation in Dopamine Transporter Knock-out Rats. *Journal of Neuroscience*. 2018;38(8):1959–1972. https://doi.org/10.1523/JNEUROSCI.1931-17.2018

6. Cinque S, Zoratto F, Poleggi A, Leo D, Cerniglia L, Cimino S, et al. Behavioral Phenotyping of Dopamine Transporter Knockout Rats: Compulsive Traits, Motor Stereotypies, and Anhedonia. *Frontiers in Psychiatry*. 2018;9:43. https://doi.org/10.3389/fpsyt.2018.00043

7. Apsley AT, Domico ER, Verbiest MA, Brogan CA, Buck ER, Burich AJ, et al. A Novel Hypervariable Variable Number Tandem Repeat in the Dopamine Transporter Gene (SLC6A3). *Life Science Alliance*. 2023;6(4):e202201677. https://doi.org/10.26508/lsa.202201677

8. Reith MEA, Kortagere S, Wiers CE, Sun Hui, Kurian MA, Galli A, et al. The Dopamine Transporter Gene SLC6A3: Multidisease Risks. *Molecular Psychiatry*. 2022;27(2):1031–1046. https://doi.org/10.1038/s41380-021-01341-5

9. Nguyen H, Cheng MH, Lee JY, Aggarwal S, Mortensen OV, Bahar I. Allosteric Modulation of Serotonin and Dopamine Transporters: New Insights from Computations and Experiments. *Current Research in Physiology*. 2024;7:100125. https://doi.org/10.1016/j.crphys.2024.100125

10. Donovan DM, Vandenbergh DJ, Perry MP, Bird GS, Ingersoll R, Nanthakumar E, et al. Human and Mouse Dopamine Transporter Genes: Conservation of 5′-Flanking Sequence Elements and Gene Structures. *Molecular Brain Research*. 1995;30(2):327–335. https://doi.org/10.1016/0169-328x(95)00018-n

11. Vandenbergh DJ, Persico AM, Uhl GR. A Human Dopamine Transporter cDNA Predicts Reduced Glycosylation, Displays a Novel Repetitive Element and Provides Racially-Dimorphic TaqI RFLPs. *Molecular Brain Research*. 1992;15(1–2):161–166. https://doi.org/10.1016/0169-328x(92)90165-8

12. Shimada S, Kitayama S, Lin CL, Patel A, Nanthakumar E, Gregor P, et al. Cloning and Expression of a Cocaine-Sensitive Dopamine Transporter Complementary DNA. *Science*. 1991;254(5031):576-578. https://doi.org/10.1126/science.1948034

13. Kilty JE, Lorang D, Amara SG. Cloning and Expression of a Cocaine-Sensitive Rat Dopamine Transporter. *Science*. 1991;254(5031):578–579. https://doi.org/10.1126/science.1948035

14. Koijam AS, Hijam AC, Singh AS, Jaiswal P, Mukhopadhyay K, Rajamma U, et al. Association of Dopamine Transporter Gene with Heroin Dependence in an Indian Subpopulation from Manipur. *Journal of Molecular Neuroscience*. 2021;71(1):122-136. https://doi.org/10.1007/s12031-020-01633-5

15. Nepal B, Das S, Reith ME, Kortagere S. Overview of the Structure and Function of the Dopamine Transporter and Its Protein Interactions. *Frontiers in Physiology*. 2023;14:1150355. https://doi.org/10.3389/fphys.2023.1150355

16. Pidathala S, Mallela AK, Joseph D, Penmatsa A. Structural Basis of Norepinephrine Recognition and Transport Inhibition in Neurotransmitter Transporters. *Nature Communications*. 2021;12(1):2199. https://doi.org/10.1038/s41467-021-22385-9

17. Nirenberg MJ, Chan J, Pohorille A, Vaughan RA, Uhl GR, Kuhar MJ, et al. The Dopamine Transporter: Comparative Ultrastructure of Dopaminergic Axons in Limbic and Motor Compartments of the Nucleus Accumbens. *Journal of Neuroscience*. 1997;17(18):6899–6907. https://doi.org/10.1523/JNEUROSCI.17-18-06899.1997

18. Basso V, Döbrössy MD, Thompson LH, Kirik D, Fuller HR, Gates MA. State of the Art in Sub-Phenotyping Midbrain Dopamine Neurons. *Biology*. 2024;13(9):690. https://doi.org/10.3390/biology13090690

19. Sugimoto A, Suzuki Y, Yoshinaga K, Orime N, Hayashi T, Egawa J, et al. Influence of Atomoxetine on Relationship Between ADHD Symptoms and Prefrontal Cortex Activity During Task Execution in Adult Patients. *Frontiers in Human Neuroscie*nce. 2021;15:755025. https://doi.org/10.3389/fnhum.2021.755025

20. Granas C, Ferrer J, Loland CJ, Javitch JA, Gether U. N-Terminal Truncation of the Dopamine Transporter Abolishes Phorbol Ester- and Substance P Receptor-Stimulated Phosphorylation without Impairing Transporter Internalization. *Journal of Biological Chemistry*. 2003;278(7):4990–5000. https://doi.org/10.1074/jbc.M205058200

21. Zeppelin T, Pedersen KB, Berglund NA, Periole X, Schiøtt B. Effect of Palmitoylation on the Dimer Formation of the Human Dopamine Transporter. *Scientific Reports*. 2021;11(1):4164. https://doi.org/10.1038/s41598-021-83374-y

22. Daniels GM, Amara SG. Regulated Trafficking of the Human Dopamine Transporter: Clathrin-Mediated Internalization and Lysosomal Degradation in Response to Phorbol Esters. *Journal of Biological Chemistry*. 1999;274(50):35794-35801. https://doi.org/10.1074/jbc.274.50.35794

23. Afonso-Oramas D, Cruz-Muros I, de la Rosa DA, Abreu P, Giráldez T, Castro-Hernández J, et al. Dopamine Transporter Glycosylation Correlates with the Vulnerability of Midbrain Dopaminergic Cells in Parkinson's Disease. *Neurobiology of Disease*. 2009;36(3):494–508. https://doi.org/10.1016/j.nbd.2009.09.002

24. Olasore HS, Osuntoki AA, Magbagbeola OA, Awesu AB, Olashore AA. Association of Dopamine Transporter Gene (DAT1) 40 bp 3' UTR VNTR Polymorphism (rs28363170) and Cannabis Use Disorder. *Substance Use: Research and Treatment*. 2023;17:1–7. https://doi.org/10.1177/11782218231163696

25. Zeng Q, Ning F, Gu S, Zeng Q, Chen R, Peng L, et al. The 10-Repeat 3'-UTR VNTR Polymorphism in the SLC6A3 Gene May Confer Protection against Parkinson's Disease: A Meta-Analysis. *Frontiers in Genetics*. 2021;12:789112. https://doi.org/10.3389/fgene.2021.789112

26. Ng J, Barral S, Waddington SN, Kurian MA. Dopamine Transporter Deficiency Syndrome (DTDS): Expanding the Clinical Phenotype and Precision Medicine Approaches. *Cells*. 2023;12(13):1737. https://doi.org/10.3390/cells12131737

27. Madduluri B, Garapati D, Yareeda S. Dopamine Transporter Deficiency Syndrome: A Rare Case of Infantile-Onset Dystonia-Parkinsonism. *Journal of Movement Disorders*. 2025;18(3):280–282. https://doi.org/10.14802/jmd.25057

28. Itan Yuval, Shang Lei, Boisson B, Patin E, Bolze A, Moncada-Vélez M, et al. The Human Gene Damage Index as a Gene-Level Approach to Prioritizing Exome Variants. *Proceedings of the National Academy of Sciences of the United States of America*. 2015;112(44):13615-13620. https://doi.org/10.1073/pnas.1518646112

29. Torres GE, Yao WD, Mohn AR, Quan H, Kim KM, Levey AI, et al. Functional Interaction between Monoamine Plasma Membrane Transporters and the Synaptic PDZ Domain-Containing Protein PICK1. *Neuron*. 2001;30(1):121–34. https://doi.org/10.1016/s0896-6273(01)00267-7

30. Egaña LA, Cuevas RA, Baust TB, Parra LA, Leak RK, Hochendoner S, et al. Physical and Functional Interaction between the Dopamine Transporter and the Synaptic Vesicle Protein Synaptogyrin-3. *Journal of Neuroscience*. 2009;29(14):4592-4604. https://doi.org/10.1523/JNEUROSCI.4559-08.2009

31. Torres GE, Sweeney AL, Beaulieu JM, Shashidharan P, Caron MG. Effect of TorsinA on Membrane Proteins Reveals a Loss of Function and a Dominant-Negative Phenotype of the Dystonia-Associated DeltaE-TorsinA Mutant. *Proceedings of the National Academy of Sciences of the United States of America*. 2004;101(44):15650–15655. https://doi.org/10.1073/pnas.0308088101

32. Giros B, el Mestikawy S, Godinot N, Zheng K, Han H, Yang-Feng T, et al. Cloning, Pharmacological Characterization, and Chromosome Assignment of the Human Dopamine Transporter. *Molecular Pharmacology*. 1992;42(3):383–390. https://doi.org/10.1016/S0026-895X(25)08925-4

33. Kurzina NP, Volnova AB, Aristova IY, Gainetdinov RR. A New Paradigm for Training Hyperactive Dopamine Transporter Knockout Rats: Influence of Novel Stimuli on Object Recognition. *Frontier in Behavioral Neuroscience*. 2021;15:654469. https://doi.org/10.3389/fnbeh.2021.654469

34. Lloyd JT, Yee AG, Kalligappa PK, Jabed A, Cheung PY, Todd KL, et al. Dopamine Dysregulation and Altered Responses to Drugs Affecting Dopaminergic Transmission in a New Dopamine Transporter Knockout (DAT-KO) Rat Model. *Neuroscience*. 2022;491:43–64. https://doi.org/10.1016/j.neuroscience.2022.03.019

35. Vaganova AN, Fesenko ZS, Volnova AB, Gainetdinov RR. Stable Dopamine-Signaling mRNA Co-Expression in the Substantia Nigra is Deregulated in Pathological Conditions, but Not in Dopamine Transporter Knockout Rats. *Biomolecules*. 2025;15(8):1117. https://doi.org/10.3390/biom15081117

36. Liang Z, Liu W, Cao M, Cui J, Lan J, Ding Y, et al. Epigenetic Regulation-Mediated Disorders in Dopamine Transporter Endocytosis: A Novel Mechanism for the Pathogenesis of Parkinson's Disease. *Theranostics*. 2025;15(6):2250–2278. https://doi.org/10.7150/thno.107436

37. Moore LD, Le T, Fan G. DNA Methylation and Its Basic Function. *Neuropsychopharmacology*. 2013;38(1):23–38. https://doi.org/10.1038/npp.2012.112

38. Green AL, Eid A, Zhan L, Zarbl H, Guo GL, Richardson JR. Epigenetic Regulation of the Ontogenic Expression of the Dopamine Transporter. *Frontiers in Genetics*. 2019;10:1099. https://doi.org/10.3389/fgene.2019.01099

39. Song H, Chen J, Huang J, Sun P, Liu Y, Xu L, et al. Epigenetic Modification in Parkinson's Disease. *Frontiers in Cell and Developmental Biology*. 2023;11:1123621. https://doi.org/10.3389/fcell.2023.1123621

40. Jiang X, Liu B, Nie Z, Duan L, Xiong Q, Jin Z, et al. The Role of M6a Modification in the Biological Functions and Diseases. *Signal Transduction and Targeted Therapy*. 2021;6(1):74. https://doi.org/10.1038/s41392-020-00450-x

41. Yankova E, Blackaby W, Albertella M, Rak J, De Braekeleer E, Tsagkogeorga G, et al. Small-Molecule Inhibition of METTL3 as a Strategy against Myeloid Leukaemia. *Nature*. 2021;593:597–601. https://doi.org/10.1038/s41586-021-03536-w

42. Li Y, Gan Y, Liu J, Li J, Zhou Z, Tian R, et al. Downregulation of MEIS1 Mediated by ELFN1-AS1/EZH2/DNMT3a Axis Promotes Tumorigenesis and Oxaliplatin Resistance in Colorectal Cancer. *Signal Transduction and Targeted Therapy*. 2022;7(1):87. https://doi.org/10.1038/s41392-022-00902-6

43. Ng J, Barral S, De La Fuente Barrigon C, Lignani G, Erdem FA, Wallings R, et al. Gene Therapy Restores Dopamine Transporter Expression and Ameliorates Pathology in iPSC and Mouse Models of Infantile Parkinsonism. *Science Translational Medicine*. 2021;13(594):eaaw1564. https://doi.org/10.1126/scitranslmed.aaw1564

44. Illiano P, Bass CE, Fichera L, Mus L, Budygin EA, Sotnikova TD, et al. Recombinant Adeno-Associated Virus-Mediated Rescue of Function in a Mouse Model of Dopamine Transporter Deficiency Syndrome. *Scientific Reports*. 2017;7:46280. https://doi.org/10.1038/srep46280

45. Ng J, Barral S, Waddington SN, Kurian MA. Gene Therapy for Dopamine Dyshomeostasis: From Parkinson's to Primary Neurotransmitter Diseases. *Movement Disorders*. 2023;38(6):924–936. https://doi.org/10.1002/mds.29416

46. Escors D, Breckpot K. Lentiviral Vectors in Gene Therapy: Their Current Status and Future Potential. *Archivum Immunologiae et Therapiae Experimentalis*. 2010;58(2):107–119. https://doi.org/10.1007/s00005-010-0063-4

47. Xu L, Yao S, Ding YE, Xie M, Feng D, Sha P. Designing and Optimizing AAV-Mediated Gene Therapy for Neurodegenerative Diseases: From Bench to Bedside. *Journal of Translational Medicine*. 2024;22(1):866. https://doi.org/10.1186/s12967-024-05661-2

48. Wang Y, Mu S, Liu F. Viral Vectors in Neurodegenerative Diseases: Immune Responses and Therapeutic Applications. *Frontiers in Neurology*. 2025;16:1603125. https://doi.org/10.3389/fneur.2025.1603125

49. Belskaya A, Kurzina N, Savchenko A, Sukhanov I, Gromova A, Gainetdinov RR. Rats Lacking the Dopamine Transporter Display Inflexibility in Innate and Learned Behavior. *Biomedicines*. 2024;12(6):1270. https://doi.org/10.3390/biomedicines12061270

About the Authors:

Albert R. Khakimov, Junior Research Associate of the Morphology Research Department, Russian Eye and Plastic Surgery Center of Bashkir State Medical University of the Ministry of Healthcare of the Russian Federation (67/1, R. Zorge Str., Ufa, 450075, Russian Federation), SPIN-code, ORCID, shershakov2015a@mail.ru

Anna I. Lebedeva, Dr.Sci. (Biology), Lead Research Associate, Head of the Morphology Research Department, Russian Eye and Plastic Surgery Center of Bashkir State Medical University of the Ministry of Healthcare of the Russian Federation (67/1, R. Zorge Str., Ufa, 450075, Russian Federation), SPIN-code, ORCID, jeol02@mail.ru

Lyalya A. Musina, Dr.Sci. (Biology), Lead Research Associate of the Morphology Research Department, Russian Eye and Plastic Surgery Center of Bashkir State Medical University of the Ministry of Healthcare of the Russian Federation (67/1, R. Zorge Str., Ufa, 450075, Russian Federation), SPIN-code, ORCID, morphoplant@mail.ru

Zukhra R. Khismatullina, Dr.Sci.(Biology), Professor of the Department of Biochemistry, Biotechnology and Physiology, Ufa University of Science and Technology (32, Zaki Validi Str., Ufa, 450008, Russian Federation), SPIN-code, ORCID, hismatullinazr@mail.ru

Claimed Contributorship:

AR Khakimov: collecting and analyzing data from literary sources, writing the manuscript

AI Lebedeva: editing the manuscript, validating the final version of the article.

LA Musina: analysis of the obtained data, editing the manuscript.

ZR Khismatullina: formulating the idea of the article, editing the manuscript.

Conflict of Interest Statement: **the authors declare no conflict of interest.**

All authors have read and approved the final manuscript.

Об авторах:

Хакимов Альберт Рузилевич, младший научный сотрудник научно-исследовательского отдела морфологии ФГБОУ ВО «Башкирский государственный медицинский университет» Минздрава России «Всероссийский центр глазной и пластической хирургии» (450075, Российская Федерация, г. Уфа, ул. Р. Зорге, д. 67/1), SPIN-код, ORCID, shershakov2015a@mail.ru

Лебедева Анна Ивановна, доктор биологических наук, ведущий научный сотрудник, заведующий научно-исследовательского отдела морфологии ФГБОУ ВО «Башкирский государственный медицинский университет» Минздрава России «Всероссийский центр глазной и пластической хирургии» (450075, Российская Федерация, г. Уфа, ул. Р. Зорге, д. 67/1), SPIN-код, ORCID, jeol02@mail.ru

Мусина Ляля Ахияровна, доктор биологических наук, ведущий научный сотрудник научно-исследовательского отдела морфологии ФГБОУ ВО «Башкирский государственный медицинский университет» Минздрава России «Всероссийский центр глазной и пластической хирургии», (450075, Российская Федерация, г. Уфа, ул. Р. Зорге, д. 67/1), SPIN-код, ORCID, morphoplant@mail.ru

Хисматуллина Зухра Рашидовна, доктор биологических наук, профессор кафедры биохимии, биотехнологии и физиологии Уфимского университета науки и технологий (450008, российская Федерация, г. Уфа, ул. Заки Валиди, д. 32) , SPIN-код, ORCID, hismatullinazr@mail.ru

Заявленный вклад авторов:

А.Р. Хакимов: сбор и анализ данных литературы, написание текста рукописи.

А.И. Лебедева: редактирование текста рукописи, утверждение окончательного варианта статьи.

Л.А. Мусина: анализ полученных данных, редактирование текста рукописи.

З.Р. Хисматуллина: идея, редактирование текста рукописи.

Конфликт интересов: **авторы заявляют об отсутствии конфликта интересов.**

Все авторы прочитали и одобрили окончательный вариант рукописи.

Received / Поступила в редакцию 10.02.2026
Reviewed / Поступила после рецензирования 03.03.2026
Accepted / Принята к публикации 09.03.2026

ANIMAL PATHOLOGY, MORPHOLOGY, PHYSIOLOGY, PHARMACOLOGY AND TOXICOLOGY

ПАТОЛОГИЯ ЖИВОТНЫХ, МОРФОЛОГИЯ, ФИЗИОЛОГИЯ, ФАРМАКОЛОГИЯ И ТОКСИКОЛОГИЯ

Original Empirical Research

UDC 619:616-089.5-092.4
https://doi.org/10.23947/2949-4826-2026-25-2-25-33

Optimization of General Anesthesia Monitoring Methods Used in Laboratory Animals during Development and Experimental Study of Veterinary Drugs

Sergei K. Shebeko ✉
Don State Technical University, Rostov-on-Don, Russian Federation
✉ shebeko_sk@mail.ru

EDN: RCHCEF

Abstract

Introduction. Giving general anesthesia to animals is an important element of experimental research during the development and study of new veterinary drugs. Due to specific nature of general anesthesia and the need to use the potent sedatives and hypnotics, it has always been posing a risk to laboratory animals. In the frame of present-day veterinary research, the problem of proficient monitoring of anesthesia is extremely relevant, especially with regard to research involving laboratory rodents. The aim of the study is to develop and optimize laboratory monitoring methods of general anesthesia in animals during experimental studies of new veterinary drugs.

Materials and Methods. The study was conducted at the research laboratory of the Institute of Living Systems, DSTU, from January to May 2024. The experiment involved 20 Wistar rats of both sexes weighing 300–400 g that were subjected to inhalation anesthesia with isoflurane, using an RWD R520 anesthesia machine. The laboratory monitoring protocols were developed based on the electroencephalography (EEG), electrocardiography (ECG), respiratory rate, blood pressure, and body temperature parameters. The condition of animal organs and systems was assessed by means of biochemical blood and urine tests, as well as excretory function tests.

Results. An inhalation chamber connected to an anesthesia machine was designed for the study in rats. It allowed laboratory monitoring of animals' condition during inhalation anesthesia by electrophysiological and functional methods. A trial mode of the chamber using 2.0% isoflurane gas supply, at a flow rate of 2.0 l/min, and a withdrawal rate of 8.0 l/min had proved to be the optimal protocol for administering general anesthesia to laboratory rats. Electrophysiological, biochemical, and functional parameters demonstrated high tolerability of the anesthesia protocol used.

Discussion and Conclusion. The development proposed by the authors optimizes laboratory monitoring in animals during general anesthesia, contributes to improvement of quality of experimental research results, facilitates the work of researchers, and can be used during the development of new veterinary drugs.

Key words: general anesthesia, laboratory monitoring, experimental studies, laboratory rats, inhalation anesthesia, inhalation chamber, electrophysiological parameters

For Citation. Shebeko SK. Optimization of General Anesthesia Monitoring Methods Used in Laboratory Animals during Development and Experimental Study of Veterinary Drugs. *Russian Journal of Veterinary Pathology*. 2026;25(2):25–33. https://doi.org/10.23947/2949-4826-2026-25-2-25-33

Оригинальное эмпирическое исследование

Оптимизация методов контроля общей анестезии лабораторных животных при разработке и экспериментальном изучении ветеринарных препаратов

С.К Шебеко ✉

Донской государственный технический университет, г. Ростов-на-Дону, Российская Федерация

✉ shebeko_sk@mail.ru

Аннотация

Введение. Общая анестезия животных является важным элементом экспериментальных исследований при разработке и изучении новых ветеринарных препаратов. В силу своей специфики, необходимости применения сильнодействующих седативных и гипнотических средств, анестезия всегда представляет собой риск для лабораторных животных. В настоящее время в ветеринарных исследованиях остро стоит проблема грамотного анестезиологического сопровождения, особенно при работе с лабораторными грызунами. Цель данного исследования — разработка и оптимизация методов лабораторного контроля общей анестезии животных при проведении экспериментальных исследований новых ветеринарных препаратов.

Материалы и методы. Исследование проведено на базе научно-исследовательской лаборатории Института живых систем ДГТУ в период с января по май 2024 г. В эксперименте участвовало 20 крыс линии Wistar обоих полов массой 300–400 г, которых подвергали общей ингаляционной анестезии с использованием изофлурана и наркозного аппарата RWD R520. Протоколы лабораторного контроля разрабатывали на основе показателей электроэнцефалографии, электрокардиографии, частоты дыхания, артериального давления и температуры тела. Оценку состояния органов и систем животных проводили с помощью биохимических исследований крови, мочи и показателей выделительной функции животных.

Результаты исследования. В ходе исследований была сконструирована ингаляционная камера для крыс, подключаемая к наркозному аппарату, позволяющая проводить лабораторный контроль электрофизиологическими и функциональными методами в условиях ингаляционной анестезии. Апробация камеры при режиме подачи газа с концентрацией изофлурана 2,0 %, скоростью подачи 2,0 л/мин и отбора 8,0 л/мин, показала, что это оптимальный протокол осуществления общей анестезии у лабораторных крыс. Данные электрофизиологических, биохимических и функциональных параметров свидетельствовали о хорошей переносимости использованного анестезиологического протокола.

Обсуждение и заключение. Предложенная авторская разработка оптимизирует лабораторный контроль животных при проведении общей анестезии, способствует повышению качества результатов экспериментальных исследований, облегчает работу ученых-исследователей и может быть использована при разработке новых ветеринарных препаратов.

Ключевые слова: общая анестезия, лабораторный контроль, экспериментальные исследования, лабораторные крысы, ингаляционный наркоз, ингаляционная камера, электрофизиологические параметры

Для цитирования. Шебеко С.К. Оптимизация методов контроля общей анестезии лабораторных животных при разработке и экспериментальном изучении ветеринарных препаратов. *Ветеринарная патология*. 2026;25(2):25–33. https://doi.org/10.23947/2949-4826-2026-25-2-25-33

Introduction. General anesthesia in animals is an integral part not only of veterinary practice but also of experimental studies of veterinary drugs. Laboratory monitoring of anesthesia is an important factor for its successful implementation [1]. Due to its specific nature and the need for potent sedatives and hypnotics, anesthesia evidently has always been posing a risk for laboratory animals, especially for young and elderly animal specimens and animals with induced pathologies [2, 3, 4]. Complications resulting from general anesthesia manifest not only in deterioration of animal's physiological functions and the state of all life support systems, but also in exacerbation of the pathological process, which can even lead to death [5].

According to statistics, adverse reaction to anesthesia is a quite widespread phenomenon in veterinary practice [6]. Poor recovery from general anesthesia in dogs is observed in 29.1% of cases, with 55.5% of them requiring sedation to control behavior [7]. In sick animals, anesthesia-related mortality is 3.6 times higher than this figure in the overall animal population (4.80% versus 1.35%) [2], moreover, in sick dogs the probability of cardiac arrest caused by anesthesia is 23 times higher, and the probability of death is 24.5 times higher than in healthy animals [8]. Post-operative mortality is of particular concern in sick animals. According to some data, it reaches 47% in dogs, 61% in cats and 64% in rabbits. In the overall animal population, rab-

bits are the most susceptible to anesthesia-and sedation-related mortality, with the risk of death being 8 times higher than that in dogs (1.39% versus 0.17%) [9].

Currently, the problem of proficient monitoring anesthesia when working with animals, along with proper examination, and adherence to recommendations is acute, both in experimental research and in veterinary medicine [10, 11]. This problem is especially relevant when working with small rodents, which are the main test systems in biomedical research, due to their small size and metabolic characteristics [12]. The opportunities of Russian scientists in the field of experimental veterinary research are considerably limited due to limited access to modern technologies, medicinal products, and equipment, especially those used for monitoring general anesthesia in laboratory rodents. Therefore, improving approaches to administering general anesthesia and laboratory monitoring of the process in the frame of experimental studies is of scientific importance for improving animal safety.

The aim of the study is to develop and optimize the methods for monitoring general anesthesia in laboratory animals to improve the efficiency and safety of experimental studies of new veterinary drugs.

Materials and Methods. The study was conducted at the Pharmacology and Experimental Pathology Research Laboratory of the Institute of Living Systems, DSTU (Rostov-on-Don) from January to May 2024. Twenty Wistar rats of both sexes weighing 300–400 g were involved in the experiment. All animals were kept on a standard diet with free access to water in accordance with acting sanitary standards [13].

The studies were conducted in compliance with the general principles of bioethics [14] and Directive 2010/63/EU of the European Parliament and of the Council "On the Protection of Animals Used for Scientific Purposes" (Brussels, 2010) [15]. All manipulations causing pain and suffering, and the withdrawal of animals from the experiment was conducted using adjusted dosage of anesthesia and analgesia [16]. The protocol of the study was verified by the Local Independent Ethics Committee of DSTU (Resolution No. 4 of 09.10.2023).

General anesthesia of animals was performed using an RWD R520 anesthesia machine for animals (RWD Life Science, USA) and isoflurane (Laboratories Karizoo, S.A., Spain).

Using the KOKS-2 cardiorespiratory complex for small laboratory animals (Medical Computer Systems Ltd., Russian Federation), electrocardiography (ECG) was performed, and heart rate (HR) and respiratory rate (RR) were assessed [17, 18]. Blood pressure (BP) was assessed by non-invasive plethysmometric method [19] using the "Sistola" non-invasive blood pressure measurement system for rodents with the "Phlogiston" heating platform (Neirobiotiks LLC, Russian Federation). Brain activity intensity was assessed by electroencephalography (EEG) [20] using the "Neiron-Spektr-1V" computerized electroencephalograph for veterinary medicine (Neirosoft LLC, Russian Federation). Animal body temperature (T) was measured using a Zamer-1 veterinary digital rectal thermometer (version 2 – rectal, Zamer LLC, Russian Federation). During laboratory observations, the animals' pedal, swallowing, and pupillary reflexes were also assessed.

To assess the functional condition of the organs and systems of animals before and after anesthesia, a series of biochemical studies of blood and urine were performed. Blood was obtained from the caudal vein in an amount of up to 0.5 ml per draw. The glucose concentration in native blood was determined using a OneTouch Verio Reflect glucometer (LifeScan Europe GmbH, Switzerland). Creatinine content, aspartate aminotransferase (AST) and alanine aminotransferase (ALAT) activity were determined in blood serum using "Diacon-DS" kits and a SPECTROstar Nano spectrophotometer (BMG Labtech, Germany) [21]. Urine was obtained using metabolic cages (OpenScience, Russian Federation) with a duration of collection for 2 hours. The creatinine content was also determined in urine, as well as the glomerular filtration rate (GFR) was calculated based on the endogenous creatinine clearance [22].

The obtained results were processed using descriptive statistics methods, tested for normality using the Shapiro-Wilk test, and presented as the arithmetic mean ± standard error of the mean (M ± m). Statistical analysis of intergroup differences was performed using one-way analysis of variance (ANOVA) with Tukey's HSD post hoc test [23]. Calculations were performed using IBM SPSS Statistics v. 22 (IBM Corp., USA) and MS Excel 2016 (Microsoft Corp., USA) software. Differences in figures were considered statistically significant at a probability level of $p < 0.05$.

Results. Inhalation anesthesia is the preferred method of general anesthesia used in experimental studies in terms of efficacy and safety, as it enables complete control over animal's condition through a combination of two key parameters: the concentration of the inhalation anesthetic and the rate of gas mixture flow. This method not only allows quick putting an animal in a state of pharmacological hypnosis but also its immediate recovery after cessation of gas delivery, practically without adverse consequences. Therefore, the study proposes improvement of laboratory monitoring techniques used specifically for this type of anesthesia.

Inhalational anesthetics, especially isoflurane, are known to pose a hazard to professionals who are constantly in contact with them during work. The standard masks supplied with the RWD R520 animal anesthesia machine are not hermetically sealed and are prone to gas leakage. To solve the problem, a sealed inhalation chamber for rats that enabled laboratory monitoring based on measuring the electrophysiological parameters was designed. The design of the chamber had been developed to ensure enough space to place EEG electrodes on the animal's scalp as well as the

respiratory sensor of the cardiorespiratory system with a minimal working volume of a gas mixture required. At the same time, there remained the possibility to place ECG sensors on the animal's torso, a blood pressure cuff on the tail, and a rectal thermometer in the anus. Implementation of all the above-mentioned monitoring elements was possible only using a chamber, where the animal's head was placed, leaving the rest of the body free. The standard inhalation anesthesia induction chambers are not suitable for this purpose.

The chamber was made of transparent polycarbonate with external dimensions of 100 x 100 x 60 mm and an internal volume of 500 cm^3 (Fig. 1). A nozzle adhering to DIN standard with an internal diameter of 6 mm was used to deliver the gas mixture to the chamber, and a nozzle adhering to 22M standard with an internal diameter of 18 mm was used to remove the waste gas. These nozzles were positioned opposite each other to ensure a unidirectional gas flow, so that it could reach the inlets of the animal's respiratory tract. The 1:3 ratio of inlet to outlet nozzle cross-sections ensured the flow of the gas mixture from the entry to evacuation point. Six animals were involved at the stage of inhalation chamber design and assembly.

To solve the problem, it was necessary not just design a chamber itself, develop the method of putting the upper part of the animal's body into it, but also to invent the way of forced gas removal from the chamber using a gas evacuation device and replaceable gas filters supplied with the anesthesia machine. Such devices are designed to absorb and bind excess inhalational anesthetic, thereby ensuring operational safety. In the current experiment, two RWD Life Science gas evacuation apparatuses with the gas filter weighing function were used: R546-Pro with forced gas removal and R548 without it, with corresponding gas filters R510-31-6 and R510-31S-6.

During general anesthesia, the animal was exposed to isoflurane in the induction chamber. The animal was then placed on the experimental heating platform, fixed, and its head was placed in the inhalation chamber. EEG electrodes were attached, a respiration sensor was installed, and the ECG electrodes were applied. The inhalation chamber was then closed, and the gas mixture started to be delivered (Fig. 2). The animal's tail was then placed on a "Phlogiston" heating platform, a blood pressure cuff was applied, and a rectal thermometer was inserted. The animal remained in this position throughout the general anesthesia procedure to enable laboratory monitoring, piloting this technique, and recording the respective physiological parameters. The resulting data were analysed for the efficacy of the proposed monitoring methods and safety of the tested general anesthesia protocol.

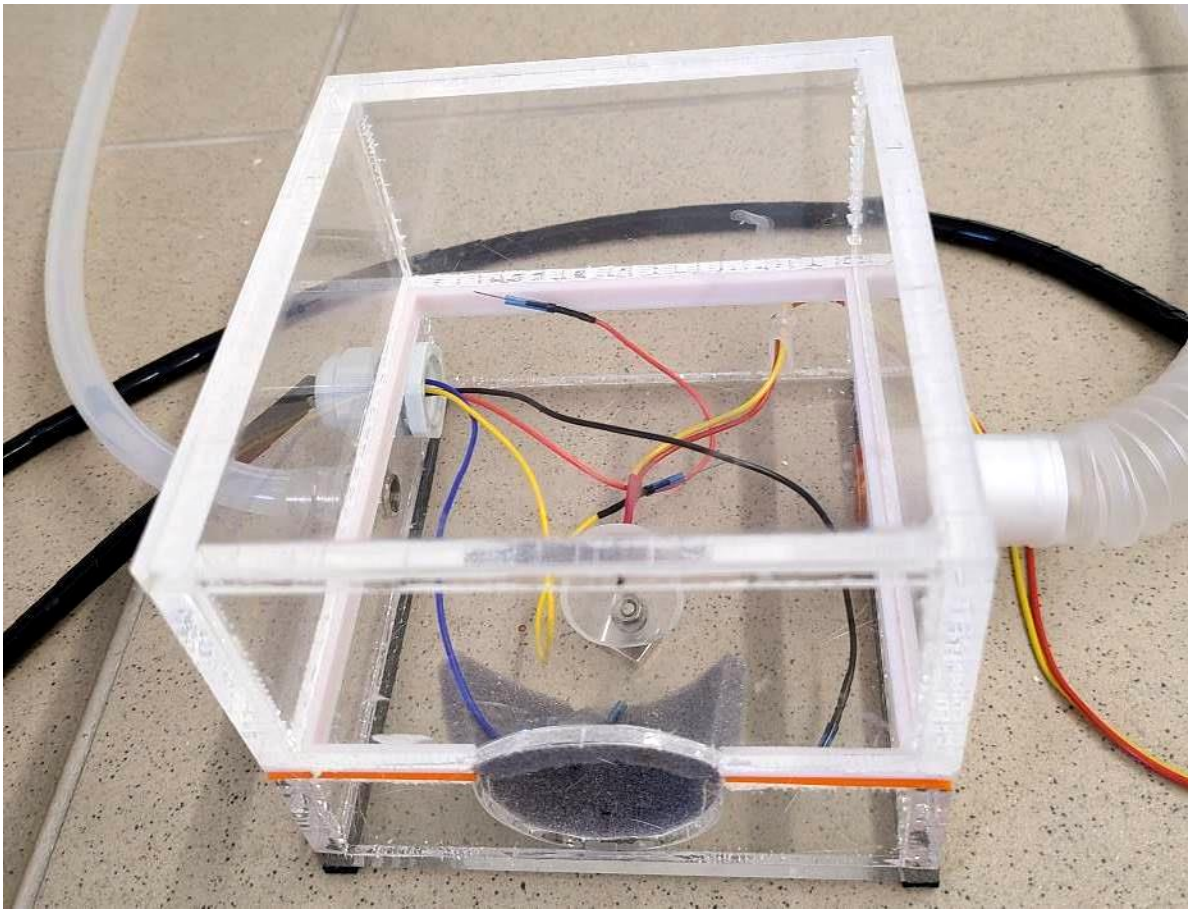

Fig. 1. A prototype of an inhalation chamber for general anesthesia in rats

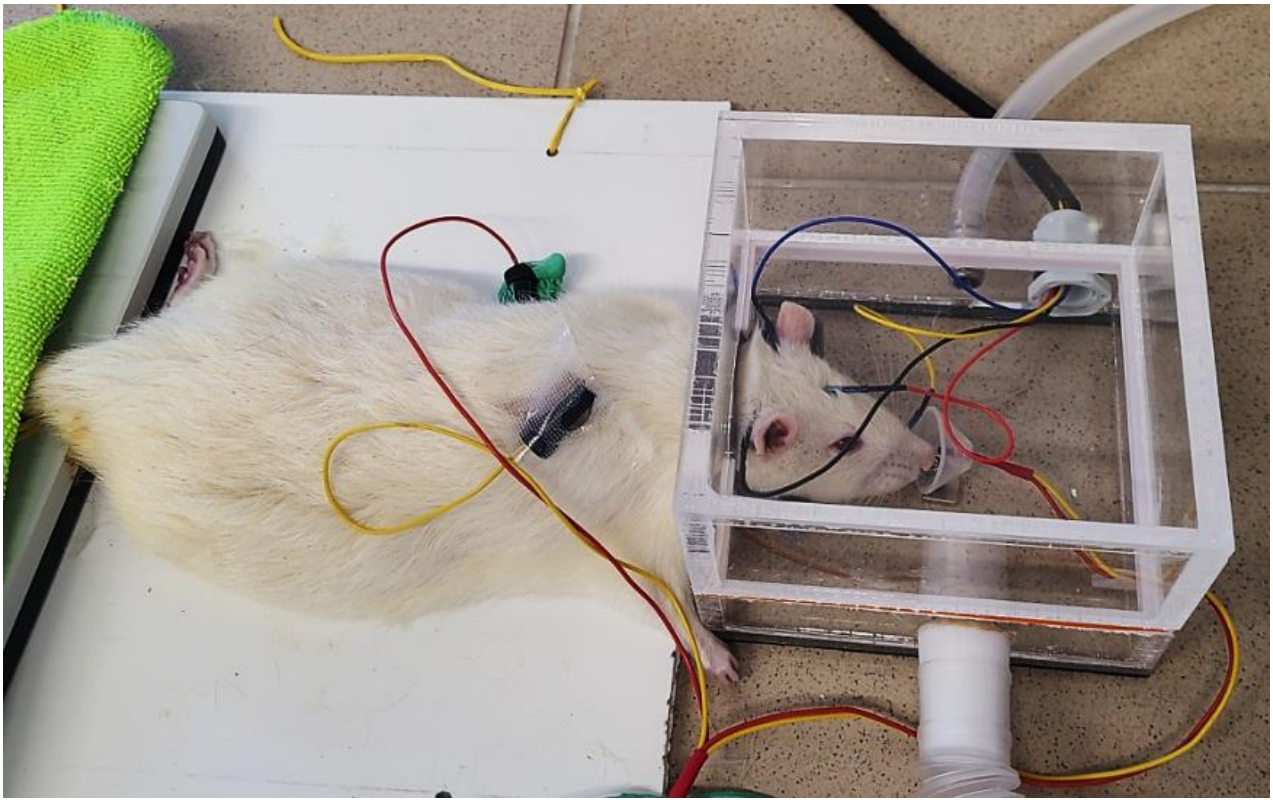

Fig. 2. A Wistar rat monitored during inhalation anesthesia using the developed inhalation chamber

During the study, two modes of anesthesia administration were used — using active and passive gas removal, whereas the concentration ratio and flow rate were adjusted to minimize the effect on the animal. During the adjustment process, we judged about the depth of anesthesia in rats by determining the stages based on the animal condition, the level of reflexes and physiological parameters.

As a result, two gas delivery modes were used:

1st mode: isoflurane concentration 2.0%, flow rate 2.0 l/min, removal rate 8.0 l/min;

2nd mode: isoflurane concentration 1.5%, flow rate 2.0 l/min, without forced gas removal.

With respect to these modes, two groups of seven animals were formed and exposed to general anesthesia with assessment of laboratory monitoring methods based on physiological parameters recorded.

During the study, electroencephalograms (EEG) were continuously recorded in the animals in the state of inhalation anesthesia (Fig. 3), and EEG indices were computed using the software (Table 1).

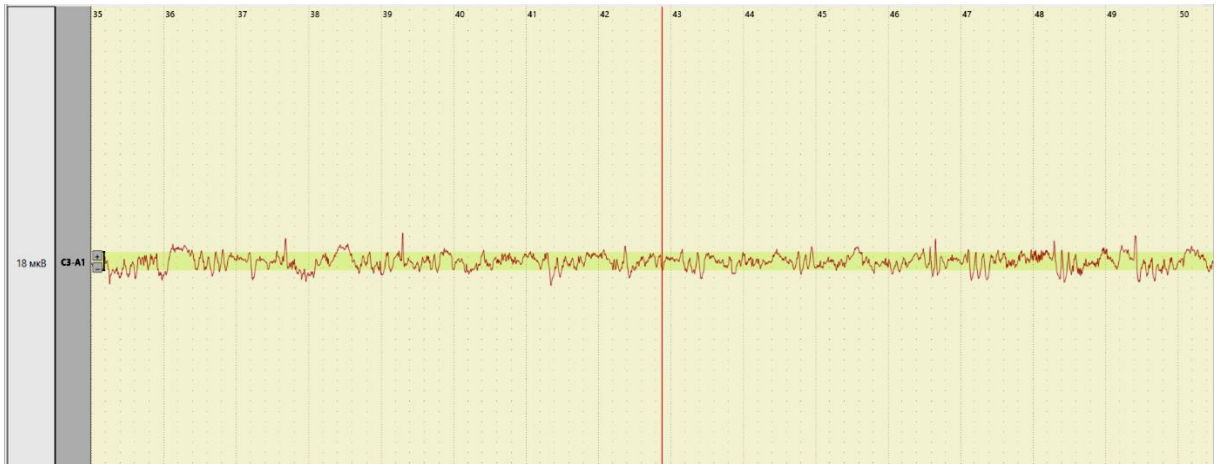

Fig. 3 Example of an electroencephalogram of a rat in the state of general anesthesia

Table 1

Electroencephalogram indices in rats in condition of general anesthesia 30 minutes after induction

EEG indices	1st group (n=7)	2nd group (n=7)
Maximum amplitude, μV	130.2±13.7	112.7±11.0
Mean amplitude, μV	19.3±2.2	15.8±1.6
Delta rhythm, μV	45.6±4.5	58.7±5.5
Theta rhythm, μV	33.5±3.5	37.2±4.0
Alpha rhythm, μV	31.4±3.2	20.3±2.7*
Beta-LF rhythm, μV	11.7±1.5	10.2±1.3
Beta-HF rhythm, μV	10.7±1.2	5.9±1.0*

Note: * – differences are significant relative to animals of the 1st group ($p<0.05$).

The EEG was analysed by the general indices of maximum and mean amplitudes, as well as the indices of mean amplitudes of five main rhythms: delta rhythm with a frequency of 0.5–3.0 Hz, theta rhythm (4.0–6.0 Hz), alpha rhythm (8.0–13.0 Hz), low frequencies of the beta band (13.0–18.0 Hz) and high frequencies of the beta band (18.0-32.0 Hz) [20]. Analysis of the EEG spectral amplitudes makes it possible to determine the predominant type of EEG rhythm and, based on this, draw a conclusion about the degree of animal immersion in anesthesia, weakening the hypnotic effect of anesthetics, or, conversely, excessive depth of anesthesia with the risk of a lethal outcome, as well as to record the moment of agonal phase or clinical death development.

The results presented in Table 1 indicate a greater depth of anesthesia in rats anesthetized with the second mode of gas mixture delivery compared to the first group. This is confirmed by a non-significant decrease in the maximum and mean EEG amplitudes, growing predominance of the delta rhythm ($p>0.05$), and a significant decrease in the amplitudes of the alpha rhythm and beta-high-frequency rhythm ($p<0.05$).

Moreover, during general anesthesia, cardiorespiratory parameters were recorded in rats (Fig. 4), as well as blood pressure and body temperature 10 minutes after induction of anesthesia and after 30 minutes (before the end of the experiment). The data are presented in Table 2.

The obtained results indicate that in animals exposed to general anesthesia using the second experimental mode, the significant decrease in heart rate (HR) by 18.5%, as well as decrease in the R wave voltage by 1.6 times, and respiratory rate (RR) by 20.7% ($p < 0.05$) were observed. This pattern indicates a more pronounced suppression of cardiovascular and respiratory systems than in the first group (Table 2).

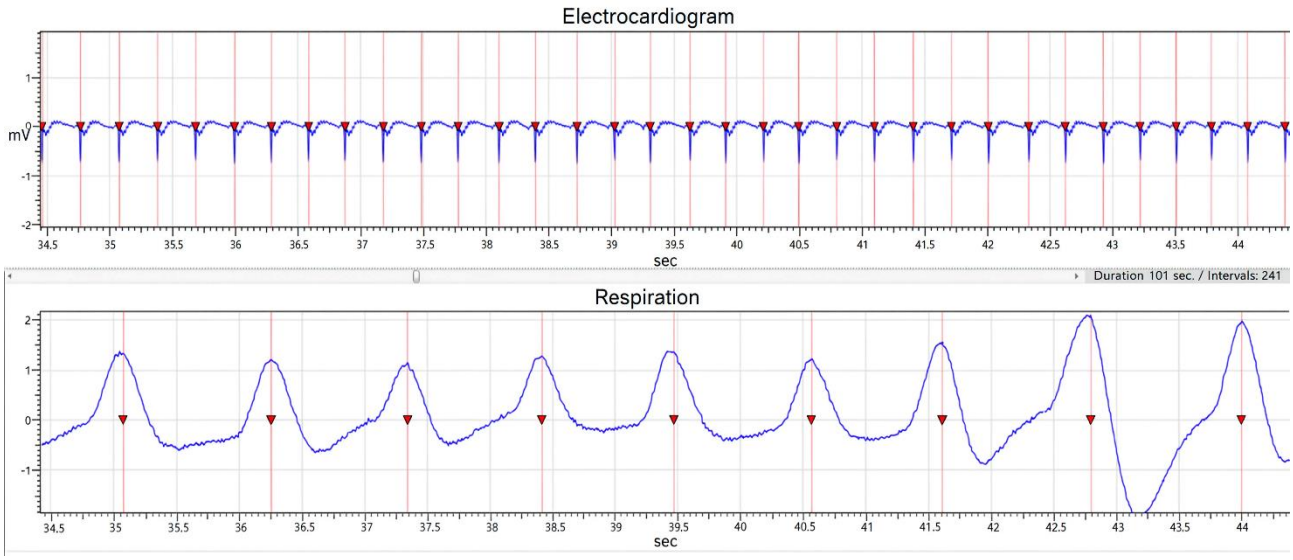

Fig. 4. Example of recording the cardiorespiratory data in rats in the state of general anesthesia

Table 2

The effect of the experimental modes of inhalation anesthesia on cardiorespiratory parameters and temperature in rats

Parameter studied		1st group (n=7)		2nd group (n=7)	
		10 min	30 min	10 min	30 min
HR, beats/min		225±12	215±10	222±13	181±11*/**
R wave voltage, mV		0.85±0.03	0.78±0.05	0.80±0.05	0.52±0.07*/**
RR, breaths/min		55±3	50±4	53±5	42±3*
BP, mmHg	systolic	121.2±4.4	115.1±3.5	119.7±3.8	99.4±2.3*/**
	diastolic	78.1±2.8	75.6±2.5	79.2±3.0	71.3±3.3
	mean	99.6±3.5	95.3±3.1	98.1±4.2	84.9±3.1*/**
T, °C		37.8±0.2	35.2±0.2*	37.5±0.3	33.1±0.5*/**

Notes: *— differences are significant relative to the baseline data (p<0.05);
**— differences are significant relative to animals of the 1st group (p<0.05).

Moreover, in the second group, a significant decrease in systolic and mean blood pressure by 16.7% and 14.3%, respectively, was also observed (p < 0.05). By the end of the experiment, body temperature in rats in this group significantly decreased to 33.1°C, which was statistically lower than in animals in the first group (p < 0.05). This also indicates an impairment in the function of cardiovascular system and general depression of body functions, which was more typical for animals in the second mode of general anesthesia, and correlates with the previous data.

Additionally, a number of biochemical parameters, including the renal function indices, were assessed in animals before and after anesthesia, and are presented in Table 3.

Table 3

Biochemical parameters and renal function indices in rats in the state of general anesthesia

Parameter	1st group (n=7)		2nd group (n=7)	
	before anesthesia	after anesthesia	before anesthesia	after anesthesia
Blood glucose, mmol/l	4.61±0.18	4.24±0.17	4.80±0.19	3.76±0.19*/**
Blood creatinine, μmol/l	45.65±3.17	39.04±2.68	42.15±2.89	55.56±3.86*/**
AST, μkat/l	0.75±0.02	0.71±0.02	0.69±0.07	0.78±0.05
ALT, μkat/L	0.36±0.02	0.38±0.01	0.40±0.03	0.66±0.02*/**
Urine creatinine, mmol/l	2.64±0.37	2.11±0.18	2.26±0.18	3.54±0.32*
GFR, ml/day	410.4±28.5	380.5±18.6	389.4±14.3	315.6±8.2*/**

Notes: * – differences are significant relative to the baseline data (p<0.05);
**– differences are significant relative to animals the 1st group (p<0.05).

The data obtained show that in the state of general anesthesia using the 1st mode of gas mixture delivery, no statistically significant changes in key blood biochemical parameters or renal function indices were observed in animals. Only single trend-based changes were observed. This indicates the good condition of organs and systems, such as the liver, heart, and urinary system, after general anesthesia. This pattern demonstrates good tolerability of the anesthetic protocol used.

At the same time, when using the 2nd mode of gas mixture delivery, a significant decrease in the blood glucose level by 21.7% ($p < 0.05$), an increase in ALT by 1.7 times ($p < 0.05$), an increase in blood creatinine by 31.8% ($p < 0.05$), urine creatinine — by 1.6 times ($p < 0.05$) and a corresponding decrease in the GFR by 18.8% ($p < 0.05$) were observed. All of the above indicates damage to some of the organs and systems of animals as a result of general anesthesia. First of all, it is worth to note the suppression of renal function, as evidenced by the GFR indicator. The activation of cytolysis, which may occur due to liver damage caused by inhalation anesthetic is also worth noting. A drop in glycemia also fits into the overall picture and indicates exhaustion of animals exposed to anesthesia.

This picture correlates with the laboratory observations. The animals were in a very deep phase of anesthesia (approximately 3–4), characterised by pronounced depression of respiratory system, with infrequent and deep breathing, and depression of cardiovascular system. EEG indices were also depressed. On the whole, this indicates poor tolerability of the second mode of anesthesia with the chosen duration time. This effect of isoflurane can be explained by stagnation of the gas mixture in the inhalation chamber due to the lack of forced gas removal, decrease of air content in the chamber, and consequent decrease of partial pressure of oxygen. This ultimately has led to deep hypoxia in the animals and, consequently, to deterioration of organ and tissue resistance to this mode of anesthesia.

Discussion and Conclusion. The obtained results demonstrate the high efficacy of the developed device—an inhalation chamber for rats connected to an anesthesia machine—for laboratory monitoring animals' condition during general anesthesia induced by inhalation. Analysis of the results reveals a significant correlation between animals' electrophysiological, functional, and biochemical parameters, which together enable a comprehensive assessment of the anesthesia protocol safety.

Thus, the proposed inhalation chamber enables monitoring general anesthesia using electrophysiological methods that are objective, sensitive, highly informative, and correlate well with the results of biochemical and functional studies in animals. This approach has good perspective for practical implementation in the experimental study of veterinary drugs, and may contribute to improving the quality of research results, as well as may facilitate the work of researchers.

References

1. Betshart-Wolfensberger R, Stekolnikov AA, Plemyashov KV, Nechaev AYu. *General Anesthesia and Euthanasia In Veterinary Medicine: A Textbook*. Saint Petersburg: Prospect Nauki; 2024. 376 p. (In Russ.).

2. Bille C, Auvigne V, Bomassi E, Durieux P, Libermann S, Rattez E. An Evidence-Based Medicine Approach to Small Animal Anaesthetic Mortality in a Referral Practice: The Influence of Initiating three Recommendations on Subsequent Anaesthetic Deaths. *Veterinary Anaesthesia and Analgesia*. 2014;41(3):249–258. https://doi.org/10.1111/vaa.12116

3. Baetge CL, Matthews NS. Anesthesia and Analgesia for Geriatric Veterinary Patients. *Veterinary Clinics of North America: Small Animal Practice*. 2012;42(4):643–653. https://doi.org/10.1016/j.cvsm.2012.05.001

4. Bille C, Auvigne V, Libermann S, Bomassi E, Durieux P, Rattez E. Risk of Anaesthetic Mortality in Dogs and Cats: An Observational Cohort Study of 3546 Cases. *Veterinary Anaesthesia and Analgesia*. 2012:39(1):59–68. https://doi:10.1111/j.1467-2995.2011.00686.x

5. Grubb T, Sager J, Gaynor JS, Montgomery E, Parker JA, Shafford H, Tearney C. 2020 AAHA Anesthesia and Monitoring Guidelines for Dogs and Cats. *Journal of American Animal Hospital Association*. 2020;56(2):59–82. https://doi.org/10.5326/jaaha-ms-7055

6. Pinho RH, Nasr-Esfahani M, Pang DSJ. Medication Errors in Veterinary Anesthesia: A Literature Review. *Veterinary Anaesthesia and Analgesia*. 2024;51(3):203–226. https://doi.org/10.1016/j.vaa.2024.01.003

7. Jones H, Robson K, Maddox T, Alderson B. Incidence of and Risk Factors for Poor Recovery Quality in Dogs Recovering from General Anaesthesia-A Prospective Case Control Study. *Veterinary Anaesthesia and Analgesia*. 2024;51(3):227–234. https://doi.org/10.1016/j.vaa.2023.12.002

8. Varkoulis K, Savvas I, Anagnostou T, Kazakos G, Pavlidou K. A Retrospective Study on Canine and Feline Mortality during Anaesthesia at a University Clinic in Greece. *Animals.* 2023;13(15):2486. https://doi.org/10.3390/ani13152486

9. Brodbelt DC, Blissitt KJ, Hammond RA, Neath PJ, Young LE, Pfeiffer DU, Pfeiffer DU. The Risk of Death: The Confidential Enquiry into Perioperative Small Animal Fatalities. *Veterinary Anaesthesia and Analgesia*. 2008;35(5):365–373. https://doi.org/10.1111/j.1467-2995.2008.00397.x

10. Reiser K, Schroers M, Reese S, Meyer-Lindenberg A. Gängige veterinärmedizinische Praxis in der Kleintieranästhesie – eine Onlineumfrage unter Kleintierpraktikern in Europa [Common Veterinary Practice in Small Animal

Anesthesia — An Online Survey among Small Animal Practitioners in Europe]. Tierärztliche Praxis Ausgabe K: *Kleintiere Heimtiere*. 2021;49(5):325–334. https://doi.org/10.1055/a-1543-5167

11. Truchetti G, Otis C, Brisville AC, Beauchamp G, Pang D, Troncy E. Management of Veterinary Anesthesia in Small Animals: A Survey of Current Practice in Quebec. *PLoS One*. 2020;15(1):e0227204. https://doi.org/10.1371/journal.pone.0227204

12. Bennett K, Lewis K. Sedation and Anesthesia in Rodents. *Vetterinary Clinics of North America Exotic Animal Practice*. 2022;25(1):211–255. https://doi.org/10.1016/j.cvex.2021.08.013

13. GOST 33216-2014. *Guidelines for the Care and Maintenance of Laboratory Animals. Rules for the Care and Maintenance of Laboratory Rodents and Rabbits*. Official Edition. Moscow: Standartinform; 2016. 16 p. (In Russ.).

14. Kalkan KK, Kekecoglu M. Ethical Principles and Rules in Experimental Animal Studies: A Comprehensive Review. *Duzce Medical Journal*. 2024;26(S1):1–13. https://doi.org/10.18678/dtfd.1497730

15. Directive 2010/63/EU of the European Parliament and of the Council of 22 September 2010 on the Protection of Animals Used for Scientific Purposes. *Official Journal of the European Union*. 2010; Document 32010L0063. URL: https://eur-lex.europa.eu/eli/dir/2010/63/oj

16. Flecknell P. *Laboratory Animal Anesthesia*. 4th Ed. London: Academic Press, 2015. 350p.

17. Lycheva NA, Makarova MN, Makarov VG, Rybakova AV. Effect of Different Species of Anesthesia on Electrocardiogram Parameters in Rats. *Laboratory Animals for Science*. 2018;2:16–23. (In Russ.). https://10.29296/2618723X-2018-02-02

18. Caracciolo SF, Bertran GC, Arini PD. Electrocardiography in Wistar Rat Experimental Model: Analysis and Characterization. *Sistema Nacional de Repositorios Digitales*. 2018. URL: https://repositoriosdigitales.mincyt.gob.ar/vufind/Record/CONICETDig_3359662e317b0cc411c85e6d4108a7da

19. Allen PS, Dell'Italia LJ, Esvelt M, Conte ML, Cadillac JM, Myers DD. Cardiovascular Research. In: Suckow MA, Hankenson FC, Wilson RP, Foley PL (Eds). *The Laboratory Rat*. 3rd Ed: Elsevier; 2020. P. 927–965. https://doi.org/10.1016/B978-0-12-814338-4.00025-8

20. Karkischenko NN, Grachev SV. *Handbook on Laboratory Animals and Alternative Models in Biomedical Technologies*. Moscow; 2010. 344 p. (In Russ.).

21. Rifai N, Horvath AR, Wittwer CT. *Tietz Fundamentals of Clinical Chemistry and Molecular Diagnostics*. 8th Ed. St. Louis: Elsevier Health Science; 2019. 1062 p.

22. Koeppen BM, Stanton BA. *Renal Physiology*. 6th Ed. Philadelphia: Elsevier; 2019. 248 p.

23. Islam MA, Al-Shiha A. *Foundations of Biostatistics*. Singapore: Springer; 2018. 474 p.

24. Pokhrel LR, Grady KD. Risk Assessment of Occupational Exposure to Anesthesia Isoflurane in the Hospital and Veterinary Settings. *Science of the Total Environment*. 2021;783:146894. https://doi.org/10.1016/j.scitotenv.2021.146894

About the Author:

Sergei K. Shebeko, Dr.Sci.(Pharmacy), Professor, Head of the Department of Biotechnical and Medical Systems and Technologies, Don State Technical University (1, Gagarin Square, Rostov-on-Don, 344003, Russian Federation), ORCID, shebeko_sk@mail.ru

Conflict of Interest Statement: **the author declares no conflict of interest.**

The author has read and approved the final manuscript.

Об авторе:

Шебеко Сергей Константинович, доктор фармацевтических наук, профессор, заведующий кафедрой «Биотехнические и медицинские системы и технологии» Донского государственного технического университета (344003, РФ, г. Ростов-на-Дону, пл. Гагарина, 1), ORCID, shebeko_sk@mail.ru

Конфликт интересов: **автор заявляет об отсутствии конфликта интересов.**

Автор прочитал и одобрил окончательный вариант рукописи.

Received / Поступила в редакцию 16.04.2026
Reviewed / Поступила после рецензирования 30.04.2026
Accepted / Принята к публикации 15.05.2026

ANIMAL PATHOLOGY, MORPHOLOGY, PHYSIOLOGY, PHARMACOLOGY AND TOXICOLOGY

ПАТОЛОГИЯ ЖИВОТНЫХ, МОРФОЛОГИЯ, ФИЗИОЛОГИЯ, ФАРМАКОЛОГИЯ И ТОКСИКОЛОГИЯ

UDC 619:616.11:636.7
https://doi.org/10.23947/2949-4826-2026-25-2-34-43

Original Empirical Research

EDN: OWJQGS

Clinical, Echocardiographic and Cytological Characteristics of Pericardial Pathologies Accompanied by Pericardial Effusion in Dogs

Kira V. Kokulenko[1] ✉, Anna V. Goncharova[2], Vladislava K. Illarionova[1,2], Vladislav A. Kostylev[2]

1Veterinary Oncological Research Center "Biocontrol", Moscow, Russian Federation

2Moscow State Academy of Veterinary Medicine and Biotechnology – MVA Named after K. I. Skryabin, Moscow, Russian Federation

✉ magnet.ru@mail.ru

Abstract

Introduction. The majority of pericardial diseases are accompanied by pathological accumulation of fluid in the pericardial cavity (effusion), as well as cardiac tamponade. Physical examination methods combined with transthoracic echocardiography are widely used to diagnose these conditions. An important task for veterinary specialists is to determine characteristic symptoms and specific echocardiographic signs of cardiac tamponade, which is considered to be a life-threatening condition. Cytological examination of pericardial fluid is an integral part in diagnosing the cause of the effusion. A comprehensive approach to diagnosis underpins the efficiency of treatment strategies. The existing studies poorly reveal the relationships between the clinical symptoms and echocardiographic signs, which could enable the diagnosis of disease severity and its prognosis, neither do they fully elucidate the cytological characteristics of effusions that could indicate the causes of effusion occurrence. The aim of the study is to establish the clinical, echocardiographic, and cytological relationships in dogs with pericardial pathologies accompanied by pericardial effusion.

Materials and Methods. The study was conducted at the Department of Veterinary Surgery of Moscow State Academy of Veterinary Medicine and Biotechnology – MVA named after K. I. Skryabin and at the Veterinary Research Center "Biocontrol" in the period from 2018 to 2023. The objects under study were dogs of various breeds, ages, and sexes (n=200). The examination methodology included: collection of patient's medical history, clinical examination, echocardiography, electrocardiography, chest radiography, ultrasonographic visualization of free fluid in the thoracic and abdominal cavities, pericardiocentesis, cytological examination of effusion, and histological examination of pathological material obtained during surgery.

Results. During the echocardiography, a ring-shaped anechoic space of varying diameter was revealed around the heart in all the studied dogs with pericardial effusion. Of 200 patients, cardiac tamponade was registered in 64 animals (32.0%), to whom pericardiocentesis was performed. For further determination of the causes of pericardial effusion, cytological examination of the obtained fluid was performed in 61 patients. According to cytomorphological characteristics, the following types of effusion were identified: transudate (1.6%), modified transudate (4.9%), septic exudate (1.6%), hemorrhagic effusion (which, in turn, was divided into effusion corresponding to: acute hemorrhage (4.9%), chronic hemorrhage (77.0%), hemorrhagic effusion with cytological signs of a tumor (9.8%)).

Discussion and Conclusion. In the presence of pericardial effusion, detection of the cardiac tamponade syndrome is of great clinical importance. We have established the most common echocardiographic signs of tamponade: caudal vena cava dilation and reduction of its collapsibility amplitude to less than 50%, as well as right atrial collapse. A relationship between the clinical symptoms (abdomen volume increase due to accumulation of ascitic fluid, progressing weakness, and exercise tolerance decrease) and echocardiographic signs of cardiac tamponade was revealed. Based on cytological examination results, the hemorrhagic type of pericardial effusion was identified as the most common one, concomitant to cardiac and pericardial tumors in older dogs of medium and large breeds.

Keywords: dogs, pericardial effusion, cardiac tamponade, pericardial cavity, echocardiography, cytological examination of fluid

For Citation: Kokulenko KV, Goncharova AV, Illarionova VK, Kostylev VA. Clinical, Echocardiographic and Cytological Characteristics of Pericardial Pathologies Accompanied by Pericardial Effusion in Dogs. *Russian Journal of Veterinary Pathology*. 2026;25(2):34–43. https://doi.org/10.23947/2949-4826-2026-25-2-34-43

Оригинальное эмпирическое исследование

Клинико-эхокардиографические и цитологические характеристики патологий перикарда собак, сопровождающихся перикардиальным выпотом

К.В. Кокуленко[1]✉, А.В. Гончарова[2], В.К. Илларионова[1,2], В.А. Костылев[2]

[1]Ветеринарный онкологический научный центр «Биоконтроль», г. Москва, Российская Федерация

[2]Московская государственная академия ветеринарной медицины и биотехнологии – МВА имени К.И. Скрябина, г. Москва, Российская Федерация

✉ magnet.ru@mail.ru

Аннотация

Введение. Большинство болезней перикарда сопровождаются патологическим скоплением жидкости в перикардиальной полости (выпот), а также тампонадой сердца. Для диагностики подобных состояний широко используют методы физикального обследования в сочетании с трансторакальной эхокардиографией. Важной задачей ветеринарных специалистов является определение характерных симптомов, а также специфических эхокардиографических признаков тампонады сердца как состояния, угрожающего жизни. Цитологическое исследование перикардиальной жидкости является неотъемлемой частью диагностического поиска причин выпота. Комплексный подход к диагностике определяет эффективную тактику лечения пациента. В существующих исследованиях остаются мало раскрытыми клинико-эхокардиографические взаимосвязи, позволяющие диагностировать тяжесть течения и прогноз заболевания, а также недостаточно освещены цитологические характеристики выпотов, определяющие их причины. Цель исследования — установить клинико-эхокардиографические и цитологические взаимосвязи у собак с патологиями перикарда, сопровождающимися перикардиальным выпотом.

Материалы и методы. Исследование проведено на кафедре ветеринарной хирургии ФГБОУ ВО «Московская государственная академия ветеринарной медицины и биотехнологии – МВА имени К.И. Скрябина», а также на базе ветеринарного научного центра «Биоконтроль» в период с 2018 по 2023 г. Объектом исследования послужили собаки различных пород, возраста и пола (n=200). Методика обследования включала: сбор анамнеза, клинический осмотр, эхокардиографию, электрокардиографию, рентгенографию грудной клетки, ультрасонографическую визуализацию свободной жидкости в грудной и брюшной полостях, перикардиоцентез, цитологическое исследование выпота, гистологическое исследование патологического материала, полученного в ходе хирургического вмешательства.

Результаты исследования. У всех исследуемых собак с перикардиальным выпотом на эхокардиографии выявлено кольцевидное анэхогенное пространство (ободок) разного диаметра вокруг сердца. Из 200 пациентов у 64 животных (32,0 %) зарегистрирована тампонада сердца и выполнен перикардиоцентез. Цитологическое исследование полученной жидкости для дальнейшей диагностики причины перикардиального выпота выполнено у 61 пациента. По цитоморфологическому характеру выявлены следующие виды выпота: транссудат (1,6 %), модифицированный транссудат (4,9 %), септический экссудат (1,6 %), геморрагический (который, в свою очередь, разделялся на выпот, соответствующий: острому кровотечению (4,9 %), хроническому кровотечению (77,0 %), геморрагический выпот с цитологическими признаками опухоли (9,8 %)).

Обсуждение и заключение. При наличии перикардиального выпота важное клиническое значение имеет распознавание синдрома тампонады сердца. Нами установлены самые распространённые эхокардиографические признаки тампонады: расширение и снижение амплитуды спадения каудальной полой вены менее 50 % и коллапс стенки правого предсердия. Выявлена взаимосвязь между клиническими симптомами (увеличение объема живота в результате накопления асцитной жидкости, прогрессирующая слабость и снижение переносимости нагрузок) и эхокардиографическими признаками тампонады сердца. По результатам цитологического исследования самым распространенным видом перикардиального выпота явился геморрагический, сопровождавший опухоли сердца и перикарда у собак старшей возрастной группы средних и крупных пород.

Ключевые слова: собаки, перикардиальный выпот, тампонада сердца, перикардиальная полость, эхокардиография, цитологическое исследование жидкости

Для цитирования: Кокуленко К.В., Гончарова А.В., Илларионова В.К., Костылев В.А. Клинико-эхокардиографические и цитологические характеристики патологий перикарда собак, сопровождающихся

перикардиальным выпотом. *Ветеринарная патология*. 2026;25(2):34–43. https://doi.org/10.23947/2949-4826-2026-25-2-34-43

Introduction. Enhancement of cardiac disease diagnostics in animals is particularly important due to the increasing incidence of pericardial pathologies in dogs of various breeds and sizes. In recent years, significant progress has been made in diagnostics of cardiac diseases in animals, including diagnostics of diseases accompanied by pericardial effusion inducing compression of the heart chambers and hemodynamic disorders. This condition causes reduction of cardiac filling and emptying, provokes venous congestion, and can lead to cardiogenic shock and death of a patient [1–3].

Diagnostic tests for pericardial pathologies accompanied by pericardial effusion include echocardiography, electrocardiography, radiography, computed tomography, cytomorphological examination of effusion, histological examination of the pericardium and neoplasms of the heart and pericardium. Each method has its advantages and limitations, but echocardiography (EchoCG) is the preferred first-line diagnostic test [2]. This visual diagnostic method is highly informative, as it allows one to determine the size of the heart and evaluate its function, the presence and volume of pericardial effusion, the presence of intracardiac thrombi and cardiac and pericardial tumors [3, 5, 6]. EchoCG is the leading method for dynamic monitoring of pericardial effusion during conservative therapy [7]. An important advantage of EchoCG is its non-invasiveness and the absence of the need for animal sedation.

A cytological analysis of pericardial effusion is a necessary diagnostic method for determining the etiology of the pathological process and patient's treatment strategy. In some cases, this test is crucial and reduces the amount of diagnostic procedures required for the patient.

A number of ultrasound criteria for diagnosing canine pericardial diseases accompanied by effusions have been identified in the available national and international literature. However, the relationship between the clinical symptoms and echocardiographic signs that enables diagnosing disease severity and prognosticating its course remains poorly studied, the same as the correlation of pathological changes with the body weight and age of the patients. Furthermore, the cytological characteristics of effusions, which determine effusion causes, are insufficiently described. The aim of the study is to establish clinical, echocardiographic, and cytological relationships in dogs with pericardial pathologies accompanied by pericardial effusions.

Materials and Methods. The study was conducted at the Department of Veterinary Surgery of Moscow State Academy of Veterinary Medicine and Biotechnology – MVA named after K. I. Skryabin and at the Veterinary Research Center "Biocontrol" in the period from 2018 to 2023. The objects of the study were sexually mature dogs of various breeds, ages, and sexes (n=200). The following dog breeds were included in the study: mixed breeds (n=38), French Bulldogs (n=19), Labrador Retrievers (n=12), Chihuahuas (n=11), Yorkshire Terriers (n=10), Golden Retrievers (n=8), Smooth-haired Dachshunds (n=6), American Staffordshire Terriers (n=5), Jack Russell Terriers (n=5), Cane Corso (n=5), German Shepherd Dogs (n=4), Bullmastiffs (n=4), Dogue de Bordeaux (n=4), Siberian Huskies (n=4), German Spitz (n=3), Staffordshire Bull Terriers (n=3), Shiba Inu (n=2), Central Asian Shepherd Dogs (n=2), Russian Spaniels (n=2), Pomeranian Spitz (n=2), German Boxers (n=2), Chinese Crested (n=2), Ca de Bou (n=2), Caucasian Shepherd Dogs (n=2), Dobermans (n=2), East European Shepherd Dogs (n=2), Weimaraners (n=2), Boerboels (n=2), Bernese Mountain Dogs (n=2), American Pit Bull Terriers (n=2), English Bulldogs (n=2), Biewer Yorkshire Terriers (n=2). The following breeds included in the study were represented by a single animal: English Cocker Spaniel, Alaskan Malamute, Dogo Argentino, Beauceron, West Highland White Terrier, Dalmatian, Irish Setter, Keeshond, Maremma Sheepdog, Miniature Poodle, Moscow Toy Terrier, Pug, Neapolitan Mastiff, Pointer, Petit Brabancon, Rhodesian Ridgeback, Russian Hound, Russian Toy Terrier, Samoyed, Skye Terrier, Scottish Terrier, Olde English Bulldogge, Whippet, Fox Terrier, Miniature Pinscher, Shar Pei, Shih Tzu, Entlebucher Mountain Dog, Japanese Chin (Fig. 1).

The distribution of animals by age groups was as follows: Group 1 — from 1 to 5 years (n = 14), Group 2 — from 6 to 9 years (n = 71), Group 3 — from 10 to 15 years (n = 107), Group 4 — from 16 to 17 years (n = 8). Distribution of animals by sex — 134 males and 66 females (Table 1).

For a reliable assessment of the heart structures, the animals were divided into groups depending on body weight: Group 1 — up to 10 kg (n=54), Group 2 — 10–25 kg (n=58), Group 3 — 26–45 kg (n=62), Group 4 — over 45 kg (n=26) (Table 2).

General clinical examination of the dogs was performed according to a standard methodology, including collection of patient's medical history, and physical examination. Echocardiography was performed using Philips Epiq 5 and Philips HD15 ultrasound systems ("Philips", USA) with phased array transducers operating at frequencies of 1–5 MHz, 2–9 MHz, and 4–12 MHz. The animals were positioned in the right and left lateral positions. To ensure direct contact between the transducer and the skin, the dogs' coats were shaved, and 30% isopropyl alcohol and ultrasound gel were applied. During the examination, the structural and functional characteristics of the heart were assessed, including the presence of thrombi in the cardiac chambers, tumors in the heart, pericardium and thoracic cavity, pericardial thickening, and the presence of free fluid in the pericardial cavity.

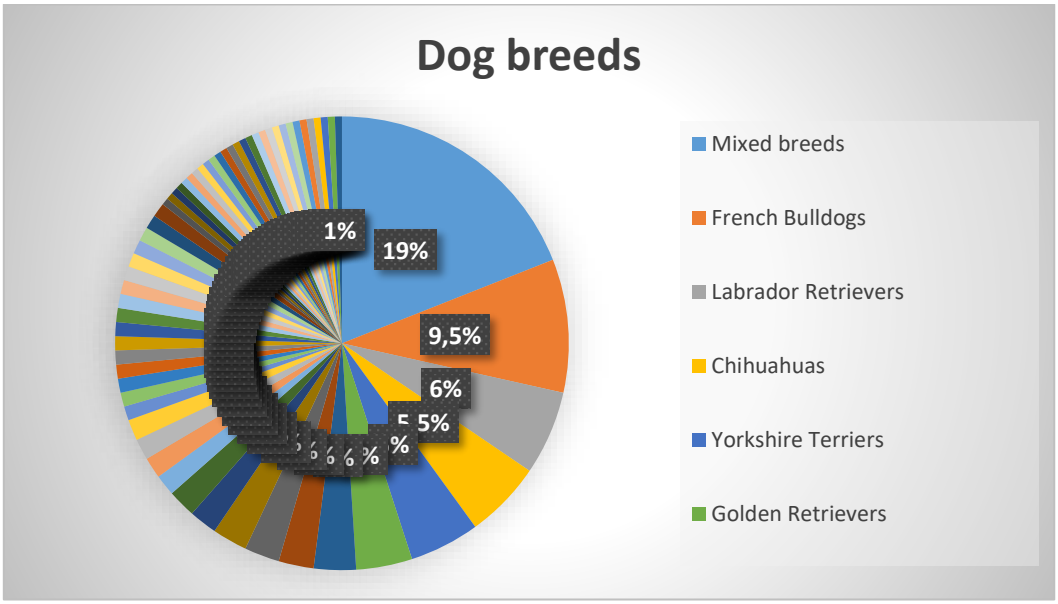

Fig. 1. Distribution of dogs with pericardial effusion by breed

Table 1

Distribution of dogs with pericardial effusion by age and sex

Group/age, years	Absolute number, n	Relative quantity, %	Sex			
Group 1 (1–5)	14	7.0	Males		Females	
Group 2 (6–9)	71	35.5	n	%	n	%
			134	67	66	33
Group 3 (10–15)	107	53.5				
Group 4 (16–17)	8	4.0				
Total	200	100	200	100	200	100

Table 2

Distribution of dogs with pericardial effusion by body weight

Group/body weight, kg	Absolute number, n	Relative quantity, %
Group 1 (up to 10)	54	27.0
Group 2 (10–25)	58	29.0
Group 3 (26–45)	62	31.0
Group 4 (over 45)	26	13.0
Total	200	100

To obtain the material for cytological examination, ultrasound-guided pericardiocentesis was performed through the 3rd–5th intercostal spaces on the right. The patient was given general anesthesia (by intravenous injection of Propofol at a dose of 4–8 mg/kg) and positioned in the left lateral decubitus position. To prepare the surgical site, the coat was shaved, and the skin around the needle insertion site was cleaned with 70% ethyl alcohol.

Cytological examination of pericardial effusion was performed in 61 dogs. Pericardial fluid obtained by pericardiocentesis was transferred to the EDTA tube. For cell count in the Goryaev chamber, 20 µl of fluid was removed from the tube and mixed with 380 µl of a 3–5% acetic acid solution stained with methylene blue. The EDTA tube was then centrifuged for 5 min at 2000 rpm. Direct brush smears were prepared from the sediment. The smears were stained for 20–30 min according to Romanowsky staining technique. The resulting smears were examined at 100×, 200×, and

1000× magnification using an Olympus CX43 microscope ("Olympus", Japan).

A histological examination was performed in 23 patients. The dogs had recurrent cardiac tamponade with pericardial effusion accumulated two or more times. Patients underwent pericardiectomy to collect the pericardial and cardiac tumor specimens for histological examination, or euthanasia followed by pathological autopsy with histological examination. A sample for the study (a 3–5 mm thick section) was excised from the obtained biopsy specimen that had been fixed in 10% buffered formalin (BF). The resulting samples were dehydrated and impregnated with paraffin using a Histo-Tek VP1 histoprocessor ("Sakura Seiki Co." LLC, Japan). Paraffin blocks were then prepared, from which series of sections (2–4 μm thick) were sliced using a HistoCore Biocut rotary microtome ("Leica Biosystems", Germany).

The resulting preparations were then stained with hematoxylin and eosin to visualize tissue components. But prior to this, the preparations were deparaffinized (sequentially through a paraffin solvent (xylene) and alcohols of descending concentration). After staining, the prepared samples were cleared in xylene and mounted under coverslips using a mounting medium. The prepared histological slides were examined using an Olympus CX43 microscope at 100×, 200×, 400×, and 1000× magnification.

Research Results. Based on the anamnesis and clinical examination of 200 patients with pericardial effusion, cardiac tamponade was diagnosed in 64 animals (32.0%). In this group of animals, one or more of the leading clinical symptoms were identified: increase in volume of the abdomen due to the accumulation of ascitic fluid (50.0%), sudden weakness/syncope (37.5%), progressing weakness/decreased activity (62.5%), and dyspnea caused by hydrothorax (32.8%). The remaining patients had nonspecific symptoms (Table 3).

Physical examination of dogs with cardiac tamponade revealed a number of characteristic clinical symptoms: pallor of the mucous membranes (15.6%), muffled heart sounds (75.0%), weak pulse waveform (35.9%), arrhythmic pulse (21.8%), and paradoxical pulse (7.8%) (Table 4). One or more components of Beck's triad (edema of the neck, dewlap, and peripheral edemas) were recorded in 3 dogs (1.5%). Jugular venous distention was not detected, possibly because of the difficulty to identify the characteristic signs due to the thick coats of the patients. In 27 of 64 patients with cardiac tamponade, the tonometry data had been obtained before pericardiocentesis. Hypotension with mean systolic blood pressure of 80 mmHg and lower was detected in 12 dogs (42.0%).

In all dogs (n=200) with pericardial effusion, echocardiography revealed a ring-shaped anechoic space (rim) of varying diameter around the heart. Echocardiographic signs of cardiac tamponade were: right atrial collapse in 42 dogs (65.6%), right ventricular diastolic collapse in 20 dogs (31.2%), reduced cardiac chambers due to insufficient filling with blood in 5 dogs (7.8%), paradoxical septal motion during respiration in 8 dogs (12.5%), dilation of caudal vena cava and reduction of its collapsibility amplitude to less than 50% during inhalation in 34 animals (53.1%) (Table 5).

Table 3

Leading clinical symptoms accompanying cardiac tamponade

Symptoms	Absolute number, n	Relative quantity, %
Dyspnea caused by hydrothorax	21	32.8
Sudden weakness/ syncope/forced posture	24	37.5
Increasing apathy/weakness/decreased activity	40	62.5
Increase in volume of the abdomen (ascitic fluid)	32	50.0

Table 4

Leading symptoms of cardiac tamponade identified during physical examination (n=64)

Symptoms	Absolute number, n	Relative quantity, %
Pallor of the mucous membranes	10	15.6
Muffled heart sounds	48	75.0
Weak pulse waveform	23	35.9
Paradoxical pulse	5	7.8
Arrhythmic pulse	14	21.8

Table 5

Echocardiographic signs of cardiac tamponade in the dogs studied (n=64)

Echocardiographic signs	Absolute number, n	Relative quantity, %
Right atrial collapse	42	65.6
Right ventricular diastolic collapse	20	31.2
Paradoxical septal motion	8	12.5
Reduction of left cardiac chambers (visual assessment)	5	7.8

Dilation and poor collapsibility of caudal vena cava (less than 50%)	34	53.1

Data analysis enabled establishing a relationship between clinical symptoms and structural and functional parameters of the heart: of 34 dogs with signs of dilation of caudal vena cava and reduction of its collapsibility amplitude to less than 50% during inhalation (diagnosed by echocardiography), 29 patients had ascites, 15 dogs — progressing weakness, and 13 dogs — dyspnea. Of 42 patients with right atrial collapse, 22 dogs had ascites, 23 had progressing weakness, and 19 dogs had dyspnea (Table 6).

Pericardiocentesis was performed in 64 dogs with cardiac tamponade, whereas the cytological examination of the obtained fluid for further diagnostics was performed in 61 patients. By the cytomorphological nature of effusion, the following types were identified: transudate (1.6%), modified transudate (4.9%), septic exudate (1.6%), hemorrhagic effusion, which in turn was divided into effusion corresponding to: acute hemorrhage (4.9%), chronic hemorrhage (77%) and hemorrhagic effusion with cytological signs of a tumor (9.8%) (Table 7).

Histological examination of the pericardium was performed in 23 patients with recurrent cardiac tamponade. In 16 dogs, cardiac or pericardial neoplasms were diagnosed by echocardiography, and 2 patients were suspected of having pericardial neoplasia (Table 8).

Table 6

Correlation of clinical symptoms with echocardiography data (n=64)

Symptoms	EchoCG sign				
	Dilation/poor collapsibility of caudal vena cava	Right atrial collapse	Right ventricular diastolic collapse	Reduced left cardiac chambers	Paradoxical septal motion
AscitesАсцит	29	22	10	-	4
Гидроторакс	10	7	1	1	2
Sudden weakness/ syncope	9	14	8	2	5
Hypotension	2	5	5	5	9
Increasing apathy/weakness/decreased activity	15	23	10	–	4
Peripheral edemas	2	1	1	–	
Dyspnea	13	19	10	–	4

Table 7

Correlation between the causes and cytological characteristics of pericardial effusion (n=61)

Causes of effusion	Absolute number, n	Relative quantity, %	Type of effusion by nature					
			Transudate	Modified transudate	Septic exudate	Chronic hemorrhagic effusion	Acute hemorrhagic effusion	Hemorrhagic effusion with cytological signs of a tumor
Cardiac/pericardial neoplasms	34	55.7		1		26	1	4 (lymphoma) 1 (carcinoma) 1 (mesothelioma)
Idiopathic/unknown cause	18	29.5		1		16	1	
Congestive heart failure	2	3.3		1		1		
Pericarditis	5	8.2			1	4		
Left atrial rupture	1	1,6					1	

Protein-losing enteropathy	1	1,6	1					

Table 8

Histological examination of the causes of pericardial effusion (n=23)

Causes of effusion	Absolute number, n	Relative quantity, %
Lymphoplasmacytic pericarditis	1	4.3
Neutrophilic pericarditis	2	8.7
Mixed pericarditis (lymphoplasmacytic and neutrophilic)	6	26
Chemodectoma	6	26
Hemangiosarcoma	5	22
Mesothelioma	1	4.3
Carcinoma	1	4.3
No pathological changes	1	4.3

Discussion and Conclusion. Transthoracic echocardiography is a reliable method for detecting pericardial pathologies and the presence of free fluid in the pericardial cavity. Free fluid in the pericardial cavity is visualized on ultrasonogram as an anechoic rim around the heart. Upon accumulation of a large volume of fluid, a characteristic "floating" or "swinging" heart pattern is observed due to its pendulum-like movements [8].

In the presence of pericardial effusion, recognition of cardiac tamponade syndrome is of major clinical importance; it is diagnosed by comparing the characteristic clinical picture and echocardiographic signs [9]. Of 200 patients participating in the study, cardiac tamponade was diagnosed in 64 animals (32.0%). The diagnostic criteria for diagnosing cardiac tamponade obtained by the authors adhere to the data published in other studies [10]. The most common echocardiographic signs of cardiac tamponade were: right atrial collapse — detected in 65.6% (n=42), dilation of caudal vena cava and reduction of its collapsibility amplitude (to less than 50% during inhalation) — detected in 53.1% (n=34), right ventricular diastolic collapse— detected in 31.2% (n=20).

A comparison of physical examination data and echocardiographic signs revealed that symptoms such as the increase in the volume of the abdomen due to ascitic fluid accumulation, progressing weakness, and exercise tolerance decrease are diagnosed in patients with echocardiographic signs of dilation of caudal vena cava and reduction of its collapsibility amplitude to less than 50% and right atrial collapse. This is explained by impaired venous return in systemic circulation against the background of right ventricular end-diastolic pressure increase resulting from the pericardial fluid pressure. In the presence of all the above listed echocardiographic signs of cardiac tamponade (Table 5), including the paradoxical septal motion and reduction of cardiac chambers due to decrease in venous blood flow, the persistent arterial hypotension (with mean systolic blood pressure of 80 mmHg or lower) was observed in animals. The primary diagnostics of cardiac tamponade is based on a constellation of patient's clinical symptoms and physical examination results. Echocardiography is a confirmatory and expert method that allows visualization of pericardial effusion, assessment of its volume, identification of the signs of cardiac compression and, in some cases, differentiation of the causes of effusion.

When assessing the effusion, the hemorrhagic nature of the fluid was most often diagnosed (91.8%), which is consistent with the literature data [11, 12], whereas signs of acute hemorrhagic effusion were detected only in 4.9% of patients. The most common cause of hemorrhagic effusion in dogs was cardiac neoplasia – 55.7% of cases, of which cardiac hemangiosarcoma was histologically diagnosed in 22%, which, in turn, is considered one of the common neoplastic causes of pericardial effusions [13, 14]. In 26% of cases, histological confirmation of a basal cardiac tumor — chemodectoma was obtained. According to echocardiography, out of 200 patients, cardiac tumors were detected in 86 dogs, of which 32.5% were right heart tumors without histological confirmation, and in 53.5% of cases, basal cardiac tumors were determined. Unknown cause of effusion was the second most common cause and may also include patients with idiopathic pericardial effusion, which is consistent with the previous studies [11, 15]. Modified transudate was recorded in 4.9% of cases, including in cases of congestive heart failure. Transudate caused by protein-losing enteropathy and septic exudate caused by myopericarditis were the rarest types of pericardial effusions. Cytological examination of pericardial fluid is deemed to be less informative and depends on the tumor type and effusion hematocrit [16, 17]. Hemorrhagic effusion with cytological signs of a tumor was observed in 9.8% of cases, with large cell lymphoma being the most commonly diagnosed tumor, which is consistent with the foreign literature data [18, 19]. In this study, in 64 dogs with cardiac tamponade, cardiac neoplasms were diagnosed in 55.7% by echocardiography. The development of cardiac tamponade in such patients may be explained not only by mechanical com-

pression of the vessels by the tumor, but also by their bleeding, which can cause a surge in intrapericardial pressure, acute dilation of pericardial cavity and, as a consequence, cardiac tamponade.

Histological examination of cardiac and pericardial tumors excised during surgery is the "gold standard" for verifying the presence of cancer. According to the results of our study, of 16 dogs with cardiac and pericardial tumors identified by echocardiography, cardiac neoplasia was histologically confirmed in 12 animals: chemodectoma in 26% of cases and hemangiosarcoma in 22%. These types of cardiac tumors are the most common, as described above. In one patient suspected of having pericardial neoplasia, pericardial mesothelioma was diagnosed. In three dogs, histological examination of the cardiac or pericardial tumor turned to be inconclusive, and in one dog, a tumor biopsy was not performed. Pericarditis as a histological diagnosis was found in 39% of cases.

Most dogs with pericardial effusion were male, of medium to large breeds, weighing between 26 and 45 kg: mixed breeds (19%), Labrador Retrievers (6%), Golden Retrievers (4%), Cane Corso (2.5%), American Staffordshire Terriers (2.5%), German Shepherd Dogs (2%) — these breeds have been previously mentioned in other studies too [11, 15, 20]. Small dog breeds were represented by: French Bulldogs (9.5%), Chihuahuas (5.5%) and Yorkshire Terriers (5%). In this study, cardiac tamponade was most commonly diagnosed in mixed breeds (15.6%), French Bulldogs (14%), Golden Retrievers (7.8%), Yorkshire Terriers (6.25%), Siberian Huskies (4.6%), and Jack Russell Terriers (4.6%). It's worth noting that in all French Bulldogs with cardiac tamponade, basal cardiac tumors were detected by echocardiography. In Golden Retrievers, Siberian Huskies, and Yorkshire Terriers, a common cause of cardiac tamponade was right heart tumor. Cases of right heart hemangiosarcoma diagnosed in Golden Retrievers are frequently described in scientific studies [21–23]. The unknown cause, was most common in Labrador Retrievers and Jack Russell Terriers.

Thus, as a result of the data analysis, the following most common clinical, physical and echocardiographic signs of cardiac tamponade were established: an increase in volume of the abdomen (50%), sudden weakness/syncope (37.5%), progressing weakness/decreased activity (62.5%), dyspnea (32.8%), pallor of the mucous membranes (15.6%), muffled heart sounds (75%), weak pulse waveform (35.9%), arrhythmic pulse (21.8%), paradoxical pulse (7.8%), right atrial collapse (65.6%), right ventricular diastolic collapse (31.2%), dilation of caudal vena cava and reduction of its collapsibility amplitude to less than 50% during inhalation (53.1%). A relationship was found between the clinical symptoms such as the increase in the volume of the abdomen due to the accumulation of ascitic fluid, progressing weakness and exercise tolerance decrease, and the echocardiographic signs of cardiac tamponade such as dilation of caudal vena cava and reduction of its collapsibility amplitude to less than 50% and right atrial collapse. The serious condition of a patient with developed arterial hypotension and cardiogenic shock will be accompanied by all EchoCG signs of cardiac tamponade, including paradoxical septal motion and weak filling of the left cardiac chambers. Based on the results of cytological examination, the hemorrhagic type of pericardial effusion was identified to be the most common one, accompanying cardiac and pericardial tumors in dogs of the older age group of medium and large breeds.

References

1. Enders M, Sarani N, Malik A. Isolated Left Ventricular Cardiac Tamponade Diagnosed on Point-of-Care Ultrasound in the Emergency Department: A Case Report and Brief Literature Review. *Journal of the American College of Emergency Physicians Open*. 2023;4(4):e12990. https://doi.org/10.1002/emp2.12990

2. Hanson M, Chan B. The Role of Point-of-Care Ultrasound in the Diagnosis of Pericardial Effusion: A Single Academic Center Retrospective Study. *Ultrasound Journaal*. 2021;13:2. https://doi.org/10.1186/s13089-021-00205-x

3. Kokulenko KV, Kostylev VA, Goncharova AV. Echocardiographic Characteristics of Pericarditis in Small Domestic Animals. In: *Proceedings of the 12th International Interuniversity Conference on Clinical Veterinary Medicine in the Partners Format. Moscow, November 17–18, 2022.* Moscow: Selskokhozyaistvennye tekhnologii Publ.; 2022. P. 589–593. (In Russ.).

4. Klein A, Chair, Abbara S., MD, Agler D., Appleton CP, Asher CR, Hoit B, et al. American Society of Echocardiography Clinical Recommendations for Multimodality Cardiovascular Imaging of Patients with Pericardial Disease: Endorsed by the Society for Cardiovascular Magnetic Resonance and Society of Cardiovascular Computed Tomography. *Journal of the American Society of Echocardiography*. 2013;26:965-1012.e15. https://doi.org/10.1016/j.echo.2013.06.023

5. Arutyunov GP, Paleev FN, Tarlovskaya EI, Moiseeva OM, Arutyunov AG, Koziolova NA, et al. Pericarditis. Clinical Guidelines 2022. *Russian Journal of Cardiology*. 2023;28(3):5398. (In Russ.). https://doi.org/10.15829/1560-4071-2023-5398

6. Adler Y, Charron P, Imazio M, Badano L, Barón-Esquivias G, Bogaert J, et al. 2015 ESC Guidelines for the Diagnosis and Management of Pericardial Diseases: The Task Force for the Diagnosis and Management of Pericardial Diseases of the European Society of Cardiology (ESC) Endorsed by: The European Association for Cardio-Thoracic Surgery (EACTS). *European Heart Journal*. 2015;36(42):2921–2964. https://doi.org/10.1093/eurheartj/ehv318

7. Chiabrando JG, Bonaventura A, Vecchié A, Wohlford GF, Mauro AG, Jordan JH, et al. Management of Acute and Recurrent Pericarditis: JACC State-of-the-Art Review. *Journal of the American College of Cardiology*. 2020;75(1):76–92. https://doi.org/10.1016/j.jacc.2019.11.021

8. Ming Wang TK, Klein A**.** Multi-Modality Cardiac Imaging for Pericardial Diseases: A Contemporary Review**.** *Reviews in Cardiovascular Medicine*. 2022;23(10):336. https://doi.org/10.31083/j.rcm2310336

9. Alerhand S, Adrian RJ, Long B, Avila J. Pericardial Tamponade: A Comprehensive Emergency Medicine and Echocardiography Review. *American Journal of Emergency Medicine*. 2022;58:159–174. https://doi.org/10.1016/j.ajem.2022.05.001

10. Kokulenko KV, Goncharova AV, Kostylev VA. Clinical Characteristics of Dogs with Pericardial Pathologies Accompanied by Pericardial Effusions. *Legal Regulation in Veterinary Medicine*. 2024;(3):63–66. (In Russ.). https://doi.org/10.52419/issn2782-6252.2024.3.63

11. MacDonald KA, Cagney O, Magne ML. Echocardiographic and Clinicopathologic Characterization of Pericardial Effusion in Dogs: 107 Cases (1985–2006). *Journal of the American Veterinary Medical Association.* 2009;235(12):1456–1460. https://doi.org/10.2460/javma.235.12.1456

12. Cagle LA, Epstein SE, Owens SD, Mellema MS, Hopper K, Burton AG. Diagnostic Yield of Cytologic Analysis of Pericardial Effusion in Dogs. *Journal of Veterinary Internal Medicine*. 2014;28(1):66–71. https://doi.org/10.1111/jvim.12253

13. Scheuermann L, Gordon-Evans W, Nault A. Systematic Review of the Treatment Options for Pericardial Effusions in Dogs. Veterinary Surgery. 2021;50(1):20–28. https://doi.org/10.1111/vsu.13475

14. Gunasekaran T, Olivier N, Smedley R, Sanders R. Pericardial Effusion in a Dog with Pericardial Hemangiosarcoma. Journal of Veterinary Cardiology. 2019;23:81–87. https://doi.org/10.1016/j.jvc.2019.01.008

15. Kokulenko KV, Goncharova AV, Kostylev VA. Risk Factors for the Occurrence and Development of Pericardial Effusions in Dogs. Veterinary, Zootechnics and Biotechnology. 2023;(8):35–41. https://doi.org/10.36871/vet.zoo.bio.202308004

16. Cagle LA, Epstein SE, Owens SD, Mellema MS, Hopper K, Burton AG. Diagnostic Yield of Cytologic Analysis of Pericardial Effusion in Dogs. Journal of Veterinary Internal Medicine. 2014;28(1):66–71. https://doi.org/10.1111/jvim.12253

17. Köster L, Newkirk K, Krawec P. A Case Report: Null-Cell Cardiac Lymphoma in An English Bulldog. Frontiers in Veterinary Science. 2024;11:1256442. https://doi.org/10.3389/fvets.2024.1256442

18. Treggiari E, Pedro B, Dukes-McEwan J, Gelzer AR, Blackwood L. A Descriptive Review of Cardiac Tumours in Dogs and Cats. *Veterinary and Comparative Oncology.* 2017;15(2):273–288. https://doi.org/10.1111/vco.12167

19. MacGregor JM, Faria ML, Moore AS, Tobias AH, Brown DJ, de Morais HS. Cardiac Lymphoma and Pericardial Effusion in Dogs: 12 Cases (1994–2004). *Journal of the American Veterinary Medical Association*. 2005;227:1449–1453. https://doi.org/10.2460/javma.2005.227.1449

20. Stafford Johnson M, Martin M, Binns S, Day MJ. A Retrospective Study of Clinical Findings, Treatment and Outcome in 143 Dogs with Pericardial Effusion. *Journal of Small Animal Practice.* 2004;45:546–552. https://doi.org/10.1111/j.1748-5827.2004.tb00202.x

21. Yamamoto S, Hoshi K, Hirakawa A, Chimura S, Kobayashi M, Machidaet. Epidemiological, Clinical and Pathological Features of Primary Cardiac Hemangiosarcoma in Dogs: A Review of 51 Cases. *Journal of Veterinary Medical Science.* 2013;75(11):1433–1441. https://doi.org/10.1292/jvms.13-0064

22. Griffin M, Culp WTN, Rebhun RB. Canine and Feline Haemangiosarcoma. *Veterinary Record.* 2021;189(9):e585. https://doi.org/10.1002/vetr.585

23. Wakamatsu CN, Potter BM, Leary D, Boss M, Martin TW. Retrospective Study Evaluating Outcomes Following Palliative Radiotherapy with or without Chemotherapy for Dogs with Presumed Cardiac Hemangiosarcoma. *Veterinary and Comparative Oncology*. 2025;23(3):432–441. https://doi.org/10.1111/vco.13068

About the Authors:

Kira V. Kokulenko, Veterinary Cardiologist at the Veterinary Oncological Research Center “Biocontrol” (24, building 10, Kashirskoe shosse, Moscow, 115522, Russian Federation), magnet.ru@mail.ru

Anna V. Goncharova, Dr.Sci. (Veterinary), Associate Professor of the Department of Veterinary Surgery, Moscow State Academy of Veterinary Medicine and Biotechnology – MVA named after K. I. Skryabin (23, Akademik Skryabin Str., Moscow, 109472, Russian Federation), ORCID, annatrukhan@mail.ru

Vladislava K. Illarionova, Cand.Sci.(Biology), Associate Professor of the Department of Physiology, Pharmacology, and Toxicology, Moscow State Academy of Veterinary Medicine and Biotechnology – MVA named after K. I. Skryabin, Head of the Cardiology Department, Veterinary Oncology Research Center “Biocontrol” (24, building 10, Kashirskoe shosse, Moscow, 115522, Russian Federation), ORCID, illarionovapq@gmail.com

Vladislav A. Kostylev, Cand.Sci. (Veterinary), Associate Professor of the Department of Veterinary Surgery, Moscow State Academy of Veterinary Medicine and Biotechnology – MVA named after K. I. Skryabin (23, Academician Skryabin Str., Moscow, 109472, Russian Federation), ORCID, vkstylev@rambler.ru

Claimed Contributorship: all authors made an equally relevant contribution to the preparation of the publication.

Conflict of Interest Statement: **the authors declare no conflict of interest.**

All authors have read and approved the final manuscript.

Об авторах:

Кира Владимировна Кокуленко, ветеринарный врач кардиолог ветеринарного онкологического научного центра «Биоконтроль» (115522, Российская Федерация, Москва, Каширское шоссе, дом 24, стр. 10), magnet.ru@mail.ru

Анна Витальевна Гончарова, доктор ветеринарных наук, доцент, доцент кафедры ветеринарной хирургии Московской государственной академии ветеринарной медицины и биотехнологии – МВА имени К. И. Скрябина (109472, Российская Федерация, Москва, ул. Академика Скрябина 23), ORCID, annatrukhan@mail.ru

Владислава Константиновна Илларионова, кандидат биологических наук, доцент кафедры физиологии, фармакологии и токсикологии ФГБОУ ВО МГАВМиБ – МВА имени К. И. Скрябина (109472, Российская Федерация, Москва, ул. Академика Скрябина 23), руководитель отделения кардиологии ветеринарного онкологического научного центра «Биоконтроль» (115522, Российская Федерация, Москва, Каширское шоссе, дом 24, стр. 10), ORCID, illarionovapq@gmail.com

Владислав Алексеевич Костылев, кандидат ветеринарных наук, доцент кафедры ветеринарной хирургии Московской государственной академии ветеринарной медицины и биотехнологии – МВА имени К. И. Скрябина (109472, Российская Федерация, Москва, ул. Академика Скрябина 23), ORCID, vkstylev@rambler.ru

Вклад авторов: все авторы сделали эквивалентный вклад в подготовку публикации.

Конфликт интересов: **авторы заявляют об отсутствии конфликта интересов.**

Все авторы прочитали и одобрили окончательный вариант рукописи.

Received / Поступила в редакцию 11.03.2026
Reviewed / Поступила после рецензирования 07.05.2026
Accepted / Принята к публикации 07.05.2026

ANIMAL PATHOLOGY, MORPHOLOGY, PHYSIOLOGY, PHARMACOLOGY AND TOXICOLOGY

ПАТОЛОГИЯ ЖИВОТНЫХ, МОРФОЛОГИЯ, ФИЗИОЛОГИЯ, ФАРМАКОЛОГИЯ И ТОКСИКОЛОГИЯ

UDC: 636.09:616.12: 636.7:636.8:619:616–073.7
https://doi.org/10.23947/2949-4826-2026-25-2-44-53

Pilot Research

EDN: HBFYFA

Comparison of the Diagnostic Accuracy of Semiautomated and Expert-Based Calculation of the Vertebral Heart Score in Cats and Dogs: First Stage Validation of the "Desktop Application for Automation of the VHS Calculation Based on Radiographs"

Yulia S. Shmarenkova[1] ✉, **Sergey V. Akchurin**[2], **Artem D. Titov**[2], **Vadim V. Demichev**[2], **Irina V. Akchurina**[2]

[1]Kaluga Branch of Russian State Agrarian University – Moscow Timiryazev Agricultural Academy, Kaluga, Russian Federation
[2]Russian State Agrarian University – Moscow Timiryazev Agricultural Academy, Moscow, Russian Federation
✉ 1shmarenkova_11@mail.ru

Abstract

Introduction. Cardiac diseases are considered to be among the main causes of mortality in small domestic animals. Calculation of the vertebral heart score (VHS) is a method used to assess the cardiac silhouette enlargement on radiographs and predict the development of congestive heart failure. However, traditional manual procedure of VHS calculation is characterized by high inter-observer variability, subjectivity, and significant time-consumption. To improve the access to objective cardiac screening in every-day clinical practice, the authors has developed a desktop application for automating VHS calculation using the artificial intelligence (AI) technologies that unifies the assessment standard, minimizes human error, and accelerates processing of radiographs. The aim of the present pilot research is to conduct the first stage validation of the application and compare the diagnostic accuracy of two VHS calculation methods — semiautomated and expert-based.

Materials and Methods. A balanced sample of 30 right lateral chest radiographs of dogs and cats was selected for analysis as a result of simple random sampling. Preliminary VHS was calculated by manual measurements on the radiographs by the Buchanan & Bücheler method: two veterinarians specializing in visual diagnostics measured the short and long axes of the heart on the radiographs and then compared their dimensions against the spinal vertebrae. The semi-automated calculation of VHS was performed by the author-developed "Desktop application for automation of the vertebral heart score (VHS) calculation based on radiographs" using a convolutional neural network. App validation implied a comparison of the results of the two methods of VHS calculation, taking into account the intraclass correlation coefficient (ICC).

Results. The "Desktop application for automation of the vertebral heart score (VHS) calculation based on radiographs" has proved to perform a highly accurate and replicable automated calculation of VHS on lateral chest radiographs of dogs and cats. It also has demonstrated statistically high agreement with the calculations obtained by veterinarians specializing in visual diagnostics (ICC≥0.97), along with less time required for calculation.

Discussion and Conclusion. The first stage of app validation has demonstrated an excellent agreement between the AI and two specialists' results, therefore, the proposed approach can be deemed a future-oriented tool for general practitioners. The present pilot research has several limitations, i.e. it was conducted on a relatively small sample of animals, which may be insufficient for evaluation of app performance in narrow subgroups (e.g., in specific breeds or in severe cardiomegaly cases). Further studies in larger, more heterogeneous cohorts, including patients with severe cardiomegaly and anatomical abnormalities, are required to confirm clinical significance of the results.

Keywords: pilot research, X-ray diagnostics, radiograph, chest, dogs, cats, vertebral heart score, VHS, cardiomegaly, artificial intelligence, desktop application, validation

For Citation. Shmarenkova YS, Akchurin SV, Titov AD, Demichev VV, Akchurina IV. Comparison of the Diagnostic Accuracy of Semiautomated and Expert-Based Calculation of the Vertebral Heart Score in Cats and Dogs: First Stage

Validation of the “Desktop Application for Automation of the VHS Calculation Based on Radiographs”. *Russian Journal of Veterinary Pathology*. 2026;25(2):44–53. https://doi.org/10.23947/2949-4826-2026-25-2-44-53

Пилотное исследование

Сравнение диагностической точности полуавтоматического и экспертного измерения кардиовертебрального индекса у кошек и собак: первый этап валидации «Десктопного приложения для автоматизации расчета VHS на основе рентгенограмм»

Ю.С. Шмаренкова[1] ✉, С.В. Акчурин[2], А.Д. Титов[2], В.В. Демичев[2], И.В. Акчурина[2]

[1] Калужский филиал Российского государственного аграрного университет – МСХА им. К.А. Тимирязева, г. Калуга, Российская Федерация

[2] Российский государственный аграрный университет – МСХА им. К.А. Тимирязева, г. Москва, Российская Федерация

✉ 1shmarenkova_11@mail.ru

Аннотация

Введение. Болезни сердца являются одной из основных причин смертности мелких домашних животных. Расчет кардиовертебрального индекса (КВИ, VHS) — метод оценки увеличения силуэта сердца на рентгенограммах и прогнозирования развития застойной сердечной недостаточности. Однако традиционное ручное измерение КВИ сопряжено с высокой межнаблюдательной вариабельностью, субъективностью и значительными временными затратами. Для повышения доступности объективного кардиологического скрининга в рутинной клинической практике авторами было разработано десктопное приложение для автоматизации расчета КВИ на основе технологий искусственного интеллекта (ИИ), позволяющее стандартизировать оценку, минимизировать человеческий фактор и ускорить обработку рентгенограмм. Цель данного пилотного исследования — провести первый этап валидации приложения и сравнить диагностическую точность двух способов измерения КВИ — полуавтоматического и экспертного.

Материалы и методы. Для анализа сформирована сбалансированная выборка — по 30 рентгенограмм грудной клетки собак и кошек в правой боковой проекции, отобранных методом простой случайной выборки. Предварительная ручная аннотация изображений выполнена по методике Buchanan & Bücheler: два ветеринарных врача визуальной диагностики по рентгенограммам определяли короткую и длинную оси сердца и далее сопоставляли их относительно позвоночного столба. Для полуавтоматического расчёта КВИ использовали авторское «Десктопное приложение для автоматизации расчета кардиовертебрального индекса (VHS) на основе рентгенограмм», разработанное на основе свёрточной нейронной сети. Валидация включала сравнение результатов двух способов расчета КВИ с учетом коэффициента внутриклассовой корреляции (ICC).

Результаты исследования. Установлено, что «Десктопное приложение для автоматизации расчета кардиовертебрального индекса (VHS) на основе рентгенограмм» обеспечивает высокоточное и воспроизводимое автоматическое измерение КВИ на боковых рентгенограммах грудной клетки у собак и кошек. При этом оно имеет статистически высокое соответствие с измерением, полученным ветеринарными врачами визуальной диагностики (ICC≥0,97), причем на расчет затрачено меньше времени.

Обсуждение и заключение. Первый этап валидации приложения продемонстрировал отличную степень согласия между ИИ и двумя специалистами, поэтому предложенный подход представляет собой перспективный вспомогательный инструмент для врачей общей практики. Текущее пилотное исследование имеет несколько ограничений, в частности, выполнено на относительно небольшой выборке животных и может быть недостаточным для оценки его работы в узких подгруппах (например, при специфических породах или выраженной кардиомегалии). Для подтверждения клинической значимости требуются дальнейшие исследования на более крупных и гетерогенных когортах, включая пациентов с выраженной кардиомегалией и анатомическими аномалиями.

Ключевые слова: пилотное исследование, рентгенодиагностика, рентгенограмма, грудная клетка, собаки, кошки, кардиовертебральный индекс, КВИ, VHS, кардиомегалия, искусственный интеллект, десктопное приложение, валидация

Для цитирования. Шмаренкова Ю.С., Акчурин С.В., Титов А.Д., Демичев В.В., Акчурина И.В. Сравнение диагностической точности полуавтоматического и экспертного измерения кардиовертебрального индекса у собак и кошек: первый этап валидации «Десктопного приложения для автоматизации расчета VHS на основе рентгенограмм». *Ветеринарная патология*. 2026;25(2):44–53. https://doi.org/10.23947/2949-4826-2026-25-2-44-53

Introduction. Cardiac diseases are among the main causes of death in older cats and dogs [1]. Although echocardiography is the primary imaging method for assessing the morphological and functional status of the heart, diagnosing by means of radiography also plays a vital role in identifying pathologies. Since cardiac diseases are often associated with the enlargement of cardiac silhouette on radiographs, this inexpensive and widely accessible diagnostic method can be used primarily as a screening method in patients with ambiguous clinical symptoms (cough, fatigue, dyspnea, etc.) [2].

To estimate the size of the heart on radiographs reliably, Buchanan J.W. and Bücheler J. developed a method for determining the size of the cardiac silhouette correlated with the size of the vertebral bodies, known as the Vertebral Heart Score (VHS) [3]. In the original study, published in 1995, the long axis of the heart was measured from the ventral border of the left main bronchus to the most distal point of the apex of the heart. The short axis was measured along a line perpendicular to the long axis, at the widest part of the cardiac silhouette. The lengths of the two axes were compared to the length of the vertebrae, starting from the cranial edge of T4.

An alternative method described by Poad M.H. et al [4], suggests using the ventral edge of the vena cava as a reference point for measurement along short-axis, however, to our knowledge, there are no studies evaluating the effect of this modification on the quality of VHS calculation.

The main benefit of VHS calculation is providing a general practice veterinarian the objective measurements for identifying cardiomegaly. This method is currently recommended by the American College of Veterinary Internal Medicine (ACVIM) for classifying dogs with mitral valve disease [5]. Calculation of VHS is also useful for monitoring patients' heart size over time for screening purposes, particularly among breeds susceptible to acquired heart diseases [6]. Furthermore, modern veterinary radiographic software includes specialized tools for VHS calculation on digital radiographs, making the method more convenient to use.

Advances in diagnostic imaging have provided access to powerful computer aided (CAD) analysis systems that have recently emerged in veterinary medicine. This means that CAD-based systems can be used for identifying key points and predicting their coordinates on the images. This, for example, can be used for determining the severity of osteoarthritis using radiographs of the coxofemoral joints and making a further prognosis [7]. Initially, significant results were shown in key point detection in facial recognition applications, but this technology is now being applied to medical imaging as it allows automated identification of key points on the image based on detection of anatomical landmarks [8].

Previous machine learning methods enabled the estimation of these indices. Nowadays, deep learning and convolutional neural networks (CNNs) are capable of surpassing human capacities. For example, deep learning algorithms were developed to calculate the cardiothoracic ratio (CTR) on human chest X-rays and were found to be more reliable, efficient, and less labor-consuming than manual calculations [9].

VHS widespreading into every-day clinical practices is hindered by the variability and subjectivity of manual measurements. Studies show that interobserver differences in VHS values can reach 0.8–1.2 vertebrae, equivalent to a transition from "norm" to "pathology" [10, 11]. Even with strict adherence to the Buchanan & Bücheler method (detecting the landmarks: ventral border of the left bronchus/tracheobronchial angle, apex of the heart, maximum width perpendicular to the long axis), the accuracy of measurement depends on the operator's experience, physical condition (degree of fatigue), and cognitive biases.

In this regard, automating the calculation of the VHS using artificial intelligence (AI) algorithms, such as convolutional neural networks, is becoming particularly relevant. Modern AI-based systems are capable not only of detecting anatomical landmarks but also of minimizing human error, ensuring standardized, reproducible measurements [7]. The implementation of such tools into veterinary practice will make it possible to:

— increase the sensitivity and specificity of early diagnostics of cardiomegaly;

— ensure objective monitoring of the dynamics of the disease during repeated examinations;

— expand access to quality cardiological assessment in general veterinary practice settings where a cardiologist is not available.

Thus, the development and validation of algorithms for automatic calculation of VHS in small domestic animals is a vital scientific and practical objective aimed at improving the quality of cardiac pathology diagnostics, improving prognostication, and optimising veterinary medicine resources. To achieve the above objective, the authors have recently developed a "Desktop application for automation of the vertebral heart score (VHS) calculation based on radiographs" [12], trained to automatically and independently establish key points for VHS calculation in cats and dogs. The aim of the study is conducting pilot validation of the developed algorithm and comparing the efficiency and diagnostic accuracy of two VHS calculation methods (semi-automated and expert-based) in cats and dogs.

Materials and Methods. The right lateral chest radiographs of dogs and cats obtained using DR digital panels (wikiVET, China) at Kaluga and Moscow veterinary clinics were taken for the study, conducted in the period from November to December 2025. After anonymization, the images

were converted to JPEG format. The exclusion criteria were the significant chest rotation, pleural effusion, neoplasms, and other artifacts that distort the cardiac silhouette.

A balanced group was formed by simple random sampling: 30 images of dogs and 30 of cats (n=60 in total). The sample of animals was determined based on: 1) recommendations for the minimum sample size for calculating the intraclass correlation coefficient (ICC), when upon the expected value of ICC >0.9 and a confidence interval of 95%, a sample of 30–50 observations proves to have sufficient statistical power to assess agreement [8]; 2) the practices described in the similar studies on validation of AI algorithms in veterinary radiology, where samples of 25–40 images per group were recognized as representative for the primary assessment of diagnostic accuracy [7, 9]; 3) the principle of group balance to minimize bias error when comparing the methods. The formal a priori power analysis was not performed due to the lack of preliminary data on the variability of measurements obtained by this particular algorithm, which is a standard practice for first-stage validation studies of new AI tools.

The assessment was performed based on the original Buchanan & Bücheler method [3]: the long axis of the heart was measured from the ventral border of the main left bronchus to the apex of the heart, the short axis was drawn perpendicular to it in the widest part of the silhouette (Fig. 1). The calculations were made by two independent veterinary radiologists (having 4–5 years of experience in visual diagnostics, >8 years of experience in general clinical practice).

Such an approach adheres to the practices of primary AI algorithms validation common for the veterinary imaging that focus on estimating the bias and reproducibility rather than on multicenter consensus. To level out individual subjectivity, the arithmetic mean of the results obtained by both specialists was taken as the reference value, which provides a stable basis for comparing with the automated algorithm.

Automated calculation of VHS was performed using the authors' proprietary desktop application based on a modified YOLOv8-seg model architecture, which enables cardiac silhouette segmentation, detection of vertebrae, and identification of key points. The model was trained using radiographs pre-labelled by the authors. The program interface provides semi-automated calculation with the possibility to manually adjust the axes to increase the accuracy (Fig. 2).

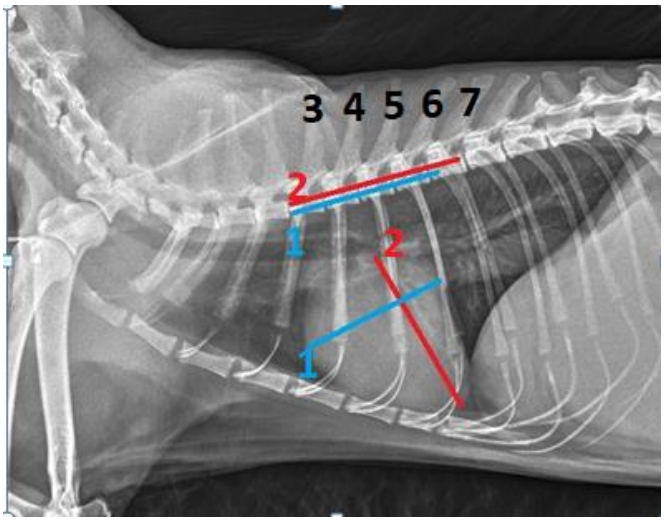

Fig. 1. Principle of the vertebral heart score calculation: 1 — short axis of the heart; 2 — long axis of the heart; 3–7 — thoracic vertebrae, starting from T4

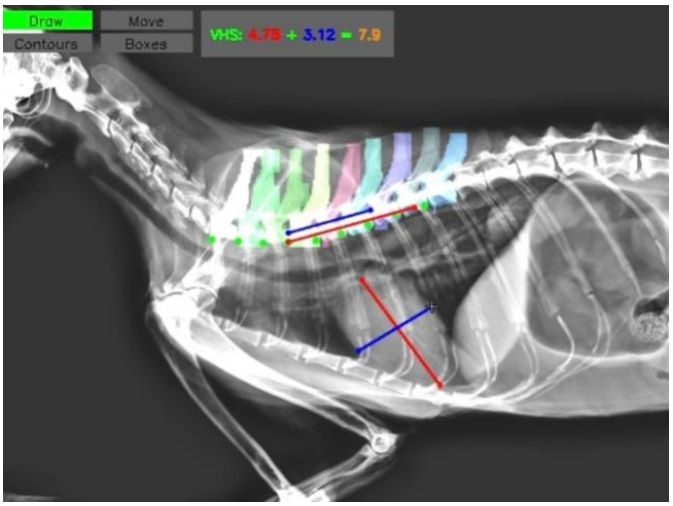

Fig. 2. Screenshot of the application interface in “Drawing” mode

Statistical analysis was performed using MedCalc v.20 (MedCalc Software Ltd., Belgium). Prior to the main analysis, statistical assumptions for the use of parametric methods were verified. The normality of distribution of quantitative variables (long and short axis of the heart, VHS) was assessed using the Shapiro-Wilk test. The homogeneity of variances between measurement groups (two experts and the AI algorithm) was verified using the Brown-Forsythe test, which is robust to deviations from normality. Since no violations of assumptions were detected ($p>0.05$ for all tests), the use of the intraclass correlation coefficient with the absolute agreement model was considered methodologically justified.

To assess the agreement between the experts’ and AI algorithm results, the intraclass correlation coefficient (ICC, absolute agreement model) was calculated with 95% confidence intervals based on the F-distribution, which allows assessing the stability of the obtained agreement indicators. According to the generally accepted classification [8], ICC values <0.5 were interpreted as low, 0.5–0.75 as moderate, 0.75–0.9 as good, and >0.9 as excellent.

Additionally, Bland-Altman plots were constructed to visualize and estimate the bias between measurement methods (expert-based vs. the AI algorithm-based). In these plots, the mean value of the two compared measurements was plotted on the x-axis, and the difference between them (bias) was plotted on the y-axis. The mean bias and limits of agreement (LoA) were calculated as the mean ±1.96 standard deviations of the differences. A bias of no more than 5% of the mean value, as well as the absence of a systematic dependence of the difference from the measured value, were considered clinically acceptable.

To assess the productive capacity of the trained YOLOv8-seg model on a hold-out sample, the standard detection and segmentation metrics were calculated. For the task of detecting anatomical landmarks (borders of the heart, vertebral bodies), the following parameters were used: precision (Precision), completeness (Recall), F1-measure and mean accuracy with a threshold of IoU=0.5 (mAP@50). To assess the quality of segmentation of the cardiac silhouette, the following parameters were used: the Dice similarity coefficient (DSC) and the mAP@50 metric for masks. All metrics were calculated with a model confidence threshold of 0.5. Additionally, the mean inference time per image was recorded.

Research Results. Statistical analysis has revealed that the values of long and short axes, and VHS calculation values obtained using the developed AI-based algorithm and that received by two independent veterinarians specializing in visual diagnostics demonstrated a high degree of agreement both in the dog group (n=30) and the cat group (n=30). Statistical assumptions were verified before calculating the intraclass correlation coefficient (ICC). The normality of distribution of quantitative variables was assessed using the Shapiro-Wilk test, and the homogeneity of variances between measurement methods (two experts and the AI algorithm) — using the Brown-Forsythe test. As shown in Table 1, for all analysed parameters (long axis, short axis, and VHS) in both animal groups, the p values exceeded the significance threshold of 0.05, which doesn’t give the grounds for rejecting the null hypothesis of normal distribution and equality of variances. Thus, the use of parametric ICC with the absolute agreement model is methodologically justified.

For all tests, the significance level was $\alpha=0.05$. P values >0.05 indicate the absense of reason to reject the null hypothesis (normal distribution/homogeneity of variances).

According to the generally accepted interpretation scale, ICC values ≥0.90 are classified as excellent agreement [8], which was the case for all measured parameters (Table 2).

Table 1

Results of verifying statistical assumptions for applying the intraclass correlation coefficient

Parameter	Shapiro–Wilk test (W/p)	Brown-Forsythe test (F/p)	Conclusion
Long axis of the heart in dogs	0.972 / 0.681	1.24 / 0.298	Assumptions are met
Short axis of the heart in dogs	0.965 / 0.412	0.89 / 0.419	Assumptions are met
VHS in dogs	0.981 / 0.893	1.05 / 0.357	Assumptions are met
Long axis of the heart in cats	0.968 / 0.524	1.41 / 0.253	Assumptions are met
Short axis of the heart in cats	0.975 / 0.738	0.76 / 0.474	Assumptions are met

VHS in cats	0.963 / 0.387	1.18 / 0.315	Assumptions are met

Table 2

Summary table of ICC results for the measurements performed and assessment thereof

Parameter	ICC between the experts and AI	Assessment scores
Long axis of the heart in dogs	0.9950	Excellent
Short axis of the heart in dogs	0.9921	Excellent
VHS in dogs	0.9841	Excellent
Long axis of the heart in cats	0.9904	Excellent
Short axis of the heart in cats	0.9953	Excellent
VHS in cats	0.9707	Excellent

The data in Table 2 demonstrate excellent ICC scores between calculation of key VHS parameters made by two veterinarians specialising in visual diagnostics and the desktop application. Furthermore, the calculation performed using the application takes less time: on average, a veterinarian familiar with the VHS method requires 3 to 5 minutes to calculate the value. The use of application reduces twice the examination time.

To further verify the absence of clinically significant bias, Bland-Altman plots were constructed to analyse the difference (bias) between the AI measurements and the mean value obtained by two veterinarians. The mean bias for VHS ranged from -0.34 to +0.15 vertebrae in dogs and from -0.17 to +0.23 vertebrae in cats, which corresponded to acceptable values. The limits of agreement intervals on the Bland-Altman plot were considered acceptable if the standard deviation of the bias was within 5% of the mean value (Fig. 3).

To assess the productive capacity of the developed algorithm, standard detection and segmentation quality metrics were analysed on the test sample. As shown in Table 3, the model demonstrated high performance indicators across all the parameters: the F1-measure exceeded 0.93 for both animal groups, and the Dice similarity coefficient for cardiac silhouette segmentation was 0.92–0.94, indicating precise detection of anatomical structures. The mean processing time for one image was ~1.4 seconds, consistent with the claimed reduction in time compared to manual calculations.

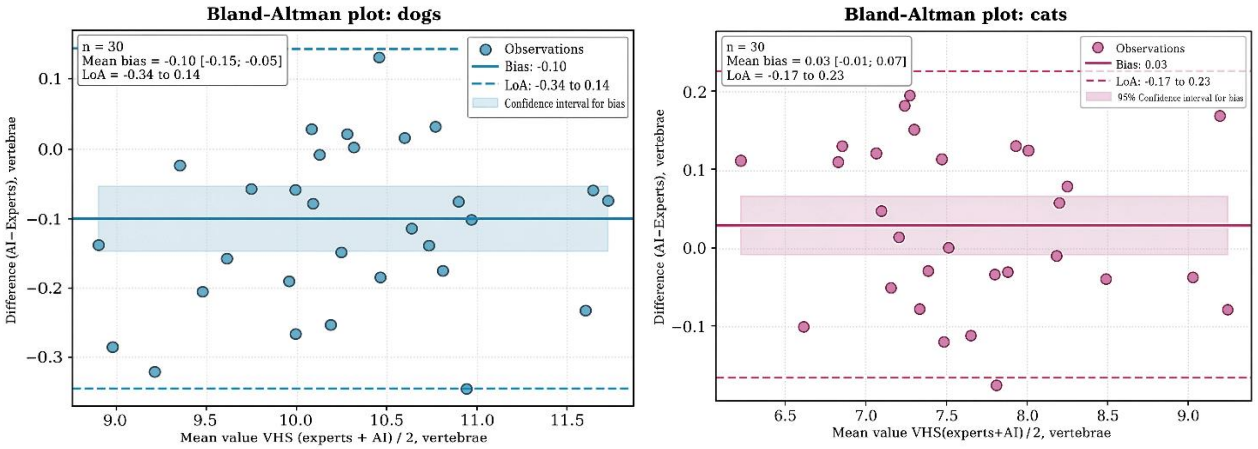

Fig. 3. Bland-Altman plots for assessing agreement between VHS calculation performed by the AI algorithm and VHS mean value obtained by two experts. The x-axis shows the mean VHS value (experts + AI)/2, and the y-axis shows the difference (AI – experts). The solid horizontal line is the mean bias, and the dashed lines are the limits of agreement (LoA: mean ± 1.96 Standard Deviation). The shaded area is the 95% confidence interval for the mean bias.

Table 3

Productive capacity metrics of YOLOv8-seg model on the test sample (n=60)

Metrics	Dogs (n=30)	Cats (n=30)	Interpretation
Detection of objects			
Precision	0.96	0.94	The proportion of correctly detected objects among all predicted ones
Recall	0.95	0.93	The proportion of correctly detected objects among all true ones
F1-measure	0.95	0.93	Harmonic Mean of Precision and Recall
mAP@50	0.97	0.95	Mean accuracy with IoU ≥ 0.5
Segmentation of the cardiac silhouette			
Dice coefficient	0.94	0.92	Measure of the overlap between the predicted and true mask
mAP@50 (mask)	0.93	0.91	Segmentation accuracy with IoU threshold ≥ 0.5
Practical indicators			
Inference time, s	1.4±0.3	1.3±0.2	Mean processing time for one image on a standard PC

Study limitations and directions for further stages of validation. The current study has several limitations. Firstly, it was performed on a relatively small sample of 60 animal chest radiographs. This sample size is sufficient for a pilot assessment of ICC agreement and the detection of gross biases of the algorithm, but may be insufficient for evaluating its performance in narrow subgroups (e.g., specific breeds, severe cardiomegaly, or image artifacts). The representativeness of the general patients' population sample requires confirmation in further multicenter consensus studies. For further validation stages, it is planned to calculate an a priori minimum sample size based on the variances obtained in this pilot study, which will ensure the required power (≥80%) to detect clinically significant differences.

Secondly, only two specialists were involved in the development of reference measurements, although high interobserver variability of VHS is well known. This choice was induced by the objectives of the pilot validation phase: the aim of the study was an initial assessment of the agreement between the algorithm and clinical practice results, rather than a large-scale interlaboratory comparison. The high variability of manual measurements was compensated for by using the intraclass correlation coefficient with the absolute agreement model and Bland-Altman plot analysis that allow for objective identification of discrepancies and confirmation of their clinical insignificance. For further external validation, it is planned to involve a multidisciplinary group of specialists from independent clinics, including veterinarians with varying levels of experience. This will enable assessment of the algorithm's robustness in the real-life practice, where a significant factor of subjectivity is present.

Thirdly, the developed algorithm was validated on images without significant artifacts or anatomical anomalies. In real-life clinical settings, the presence of pleural effusion, significant chest rotation, or spondylosis may affect the accuracy of detecting the cardiac and vertebral silhouettes. Similar limitations are described in the studies on veterinary AI models validation, which note algorithm performance degradation in heterogeneous samples [13, 14, 15]. To overcome this problem, further studies are needed in multicenter cohorts including patients with varying degrees of cardiomegaly, comorbidities, and radiographs of varying quality. It would be interesting to assess the behavior of AI in such cases.

Finally, fourthly, the current study did not evaluate the diagnostic sensitivity and specificity of the algorithm in predicting specific cardiac diseases. Like traditional VHS calculation, the AI tool is designed solely for objective measurement of cardiac silhouette dimensions and not for making an etiological diagnosis. In compliance with the current recommendations for reporting in the field of medical AI (e.g., CLAIM guidelines [16]), the next step should be prospective clinical validation with assessment of the

impact of the automated VHS calculation on medical decision-making and patient treatment outcomes.

Discussion and Conclusion. The results obtained in this pilot study demonstrate excellent agreement (ICC≥0.97) between the VHS calculations based on the YOLOv8-seg model and measurements of two veterinary radiologists. These data are consistent with the current trends for implementing deep learning algorithms in veterinary diagnostic imaging, where AI systems are successfully used for quantitative analysis of radiographs and minimization of subjective factors [7, 10, 13, 14].

High interobserver variability in manual VHS calculation remains one of the main problems of this method. As demonstrated in [11], the difference between the results of calculation made by experienced specialists can equal to the size of more than one vertebra, which can lead to misdiagnosing the patient's condition. Similar limitations have been noted in other studies referring to quantitative radiometric methods, where the subjectivity in selecting the anatomical landmarks directly affects the reproducibility of the results [1, 4]. The implementation of computer vision algorithms makes it possible to standardize the measurement process to identify the key points with high precision and exclude the operator cognitive biases [7, 14].

Thus, this desktop application can be an excellent aid in diagnosing patients' cardiac status, and can be used even by general practice veterinarians lacking the knowledge and experience in VHS calculation. Furthermore, the reduction of VHS calculation time from 3–5 to ~1.5 minutes demonstrated in our study has direct clinical significance. In the context of the high workload of the general practice veterinarians, the automation of the every-day measurements facilitates quicker diagnostic decision-making and optimises the workflow [6, 7]. Furthermore, standardized AI assessments create a reliable foundation for patient monitoring in dynamics, which is particularly important when following-up the progression of mitral valve disease, where even small changes in the cardiac silhouette have prognostic value [5, 6].

References

1. Ward JM, Youssef SA, Treuting PM. Why Animals Die: An Introduction to the Pathology of Aging. *Veterinary Pathology*. 2016;53(2):229–232. https://doi.org/10.1177/0300985815612151

2. Baisan A, Ciocan M, Bîrsan O, Vulpe V. Objective Assessment of the Radiographic Cardiac Size in Dogs – A Review of the Heart Size Measurements. *Lucrari Stiintifice - Universitatea de Stiinte Agricole a Banatului Timisoara, Medicina Veterinara*. 2017;50(2):16–23.

3. Buchanan JW, Bücheler J. Vertebral Scale System to Measure Canine Heart Size in Radiographs. *Journal of the American Veterinary Medical Association.* 1995;206(2):194–199.

4. Poad MH, Manzi TJ, Oyama MA, Gelzer AR. Utility of Radiographic Measurements to Predict Echocardiographic Left Heart Enlargement in Dogs with Preclinical Myxomatous Mitral Valve Disease. *Journal of Veterinary Internal Medicine.* 2020;34(5):1728–1733. https://doi.org/10.1111/jvim.15854

5. Keene BW, Atkins CE, Bonagura JD, Fox PR, Häggström J, Fuentes VL, et al. ACVIM Consensus Guidelines for the Diagnosis and Treatment of Myxomatous Mitral Valve Disease in Dogs. *Journal of Veterinary Internal Medicine*. 2019;33(3):1127–1140. https://doi.org/10.1111/jvim.15488

6. Lord P, Hansson K, Kvart C, Häggström J. Rate of Change of Heart Size before Congestive Heart Failure in Dogs with Mitral Regurgitation. *Journal of Small Animal Practice*. 2010;51(4):210–218. https://doi.org/10.1111/j.1748–5827.2010.00910.x

7. Boissady E, de La Comble A, Zhu X, Hespel AM. Artificial Intelligence Evaluating Primary Thoracic Lesions Has an Overall Lower Error Rate Compared to Veterinarians or Veterinarians in Conjunction with the Artificial Intelligence. *Veterinary Radiology and Ultrasound.* 2020;61(6):619–627. https://doi.org/10.1111/vru.12912

8. Koo TK, Li MY. A Guideline of Selecting and Reporting Intraclass Correlation Coefficients for Reliability Research. *Journal of Chiropractic Medicine*. 2016;15(2):155–163. https://doi.org/10.1016/j.jcm.2016.02.012. Erratum in: *Journal of Chiropractic Medicine.* 2017;16(4):346. https://doi.org/10.1016/j.jcm.2017.10.001

9. Sun Y, Wang X, Tang X. Deep Convolutional Network Cascade for Facial Point Detection. In: *Proceedings of 2013 IEEE Conference on Computer Vision and Pattern Recognition.* Portland, OR, USA: IEEE; 2013. P. 3476–3483. https://doi.org/10.1109/CVPR.2013.446

10. Li Z, Hou Z, Chen C, Hao Z, An Y, Liang S, et al. Automatic Cardiothoracic Ratio Calculation with Deep Learning. *IEEE Access*. 2019;7:37749–37756. https://doi.org/10.1109/ACCESS.2019.2900053

11. Hansson K, Häggström J, Kvart C, Lord P. Interobserver Variability of Vertebral Heart Size Measurements in Dogs with Normal and Enlarged Hearts. *Veterinary Radiology and Ultrasound*. 2005;46(2):122–130. https://doi.org/10.1111/j.1740–8261.2005.00024.x

12. Titov AD, Demichev VV, Akchurin SV, Shmarenkova YuS. Formation and Markup of a Specialized Dataset for Computer Vision Tasks in Veterinary Radiography. *Vestnik of Russian New University (Vestnik of RosNOU). Series:*

Complex Systems: Models, Analysis and Management. 2025;4:129–140. (In Russ.). URL: https://vestnik-rosnou.ru/item/2025/4/129

13. Vasilev ME, Shalimov AS, Savina OA. Overview of Yolo Versions: Single-Stage Convolutional Neural Network Model. *Universum: Technical Sciences.* 2025;6(135):36–45. (In Russ.). URL: https://7universum.com/ru/tech/archive/item/20293

14. Hennessey E, DiFazio M, Hennessey R, Cassel N. Artificial Intelligence in Veterinary Diagnostic Imaging: A literature Review. *Veterinary Radiology & Ultrasound*. 2022;63(Suppl. 1):851–870. https://doi.org/10.1111/vru.13163

15. Levicar C, Nolte I, Granados-Soler JL, Freise F, Raue JF, Bach JP. Methods of Radiographic Measurements of Heart and Left Atrial Size in Dogs with and without Myxomatous Mitral Valve Disease: Intra- and Interobserver Agreement and Practicability of Different Methods. *Animals*. 2022;12(19):2531. https://doi.org/10.3390/ani12192531. Correction in: *Animals*. 2025;15(8):1082. https://doi.org/10.3390/ani15081082

16. Cruz Rivera S, Liu X, Chan AW, Denniston AK, Calvert MJ; SPIRIT-AI and CONSORT-AI Working Group. Guidelines for Clinical Trial Protocols for Interventions Involving Artificial Intelligence: the SPIRIT-AI Extension. *Lancet Digital Health*. 2020;2(10):e549-e560. doi: https://doi.org/10.1016/S2589-7500(20)30219-3

About the Authors:

Yulia S. Shmarenkova, Senior Lecturer of the Veterinary Medicine and Animal Physiology Department, Faculty of Veterinary Medicine and Animal Science, Kaluga Branch of Russian State Agrarian University – Moscow Timiryazev Agricultural Academy (27, Vishnevsky Str., Kaluga, 248007, Russian Federation) ORCID, 1shmarenkova_11@mail.ru

Sergey V. Akchurin, Dr.Sci. (Veterinary), Professor of the Veterinary Medicine Department, Institute of Animal Science and Biology, Russian State Agrarian University – Moscow Timiryazev Agricultural Academy (49, Timiryazevskaya Str., Moscow, 127434, Russian Federation) ORCID, sakchurin@rgau–msha.ru

Artem D. Titov, Assistant at the Statistics and Cybernetics Department, Institute of Economics and Management of Agroindustrial Complex, Russian State Agrarian University – Moscow Timiryazev Agricultural Academy (49, Timiryazevskaya Str., Moscow, 127434, Russian Federation), ORCID, a.titov@rgau-msha.ru

Vadim V. Demichev, Cand.Sci. (Economics), Associate Professor of the Statistics and Cybernetics Department, Institute of Economics and Management of Agroindustrial Complex, Russian State Agrarian University – Moscow Timiryazev Agricultural Academy (49, Timiryazevskaya Str., Moscow, 127434, RF) ORCID, demichev_v@rgau-msha.ru

Irina V. Akchurina, Cand.Sci. (Veterinary), Associate Professor of the Veterinary Medicine Department, Institute of Animal Science and Biology, Russian State Agrarian University – Moscow Timiryazev Agricultural Academy (49, Timiryazevskaya Str., Moscow, 127434, RF) ORCID, akchurinaiv@rgau-msha.ru

Claimed Contributorship:

YS Shmarenkova: collecting the materials, preparing the draft, formulating the conclusions.

SV Akchurin: scientific supervision, formulating the main concept and objectives of the research.

AD Titov: preparing a labeled dataset, developing a modified computer vision model, developing a graphical user interface prototype.

VV Demichev: planning, supervision, and technical support in the development of the computer vision model and the graphical user interface prototype.

IVAkchurina: editing the text and conclusions.

***Conflict of Interest Statement*: the authors declare no conflict of interest.**

All authors have read and approved the final manuscript.

Об авторах:

Шмаренкова Юлия Сергеевна, старший преподаватель кафедры ветеринарии и физиологии животных факультета ветеринарной медицины и зоотехнии Калужского филиала РГАУ–МСХА им. К.А. Тимирязева (248007, РФ, г. Калуга, ул. Вишневского, д. 27) ORCID, 1shmarenkova_11@mail.ru

Акчурин Сергей Владимирович, доктор ветеринарных наук, профессор кафедры ветеринарной медицины института зоотехнии и биологии РГАУ–МСХА им. К.А. Тимирязева (127434, РФ, г. Москва, ул. Тимирязевская, д. 49) ORCID, sakchurin@rgau–msha.ru

Титов Артем Денисович, ассистент кафедры статистики и кибернетики института экономики и управления АПК РГАУ–МСХА им. К.А. Тимирязева (127434, РФ, г. Москва, ул. Тимирязевская, д. 49) ORCID, a.titov@rgau-msha.ru

Демичев Вадим Владимирович, доцент, кандидат экономических наук, доцент кафедры статистики и кибернетики института экономики и управления РГАУ–МСХА им. К.А. Тимирязева (127434, РФ, г. Москва, ул. Тимирязевская, д. 49) ORCID, demichev_v@rgau-msha.ru

Акчурина Ирина Владимировна, кандидат ветеринарных наук, доцент кафедры ветеринарной медицины института зоотехнии и биологии РГАУ–МСХА им. К.А. Тимирязева (127434, РФ, г. Москва, ул. Тимирязевская, д. 49) ORCID, akchurinaiv@rgau-msha.ru

Заявленный вклад авторов:

Ю.С. Шмаренкова: сбор материала, подготовка текста, формирование выводов.

С.В. Акчурин: научное руководство, формирование основной концепции и цели исследования.

А.Д. Титов: подготовка размеченного датасета, разработка модифицированной модели компьютерного зрения, разработка прототипа графического интерфейса.

В.В. Демичев: планирование, руководство и техническая поддержка в разработке модели компьютерного зрения и прототипа графического интерфейса.

И.В. Акчурина: редактирование текста и выводов.

***Конфликт интересов*: авторы заявляют об отсутствии конфликта интересов.**

Все авторы прочитали и одобрили окончательный вариант рукописи

Received / Поступила в редакцию 14.01.2026
Reviewed / Поступила после рецензирования 21.05.2026
Accepted / Принята к публикации 01.06.2026

ANIMAL PATHOLOGY, MORPHOLOGY, PHYSIOLOGY, PHARMACOLOGY AND TOXICOLOGY

ПАТОЛОГИЯ ЖИВОТНЫХ, МОРФОЛОГИЯ, ФИЗИОЛОГИЯ, ФАРМАКОЛОГИЯ И ТОКСИКОЛОГИЯ

UDC: 619:616-006:636.7
https://doi.org/10.23947/2949-4826-2026-25-2-54-60

Original Empirical Research

EDN: GIVVOK

Expression of Vimentin, α-SMA, and CD34 in Malignant Mammary Tumors in Dogs

Alina A. Darbisheva ✉, **Olga V. Dilekova**
Stavropol State Agrarian University, Stavropol, Russian Federation
✉ darbisevaalina@gmail.com

Abstract

Introduction. At the contemporary stage of mammary tumor studies, the microenvironment is considered a key factor contributing to neoplasia formation and metastasis. Therefore, the greatest attention is paid to the cellular composition of the mammary tumor microenvironment, in which the most widespread elements are the stromal cancer-associated fibroblasts (CAFs). However, in veterinary oncology, stromal markers of malignant mammary tumors are insufficiently studied. The aim of the present study is to investigate the expression of tumor marker proteins, i.e. vimentin, α-SMA, and CD34, in the stroma of the malignant mammary tumor microenvironments in dogs.

Materials and Methods. The objects of the study that was conducted in the period from 2022 to 2024 were the female dogs of various breeds and ages (n=26). The materials studied were the mammary tumors. A comprehensive range of histological and immunohistochemical studies was conducted in compliance with the standard techniques.

Results. It has been established that in different histological types and degrees of canine mammary tumor malignancy, the fibroblastic differentiation lineage cells demonstrate a high expression of vimentin and α-SMA and a low expression of CD34, which indicates their differentiation into CAFs.

Discussion and Conclusion. The obtained results can be used as basic applied data in the study of carcinogenesis in veterinary oncology.

Keywords: mammary gland, malignant tumor, immunohistochemistry, dogs, expression, vimentin, α-SMA, CD34.

For Citation: Darbisheva AA, Dilekova OV. Expression of Vimentin, α-SMA, and CD34 in Malignant Mammary Tumors in Dogs. *Russian Journal of Veterinary Pathology.* 2026;25(2):54–60. https://doi.org/10.23947/2949-4826-2026-25-2-54-60

Оригинальное эмпирическое исследование

Экспрессия vimentin, α-SMA и CD34 в злокачественных типах опухолей молочной железы у собак

А.А. Дарбишева ✉, **О.В. Дилекова**
Ставропольский государственный аграрный университет, г. Ставрополь, Российская Федерация
✉ darbisevaalina@gmail.com

Аннотация

Введение. На данном этапе изучения опухолей молочной железы микроокружение рассматривается как ключевой элемент, способствующий формированию и метастазированию неоплазий. В связи с этим наибольшее внимание уделяется клеточному составу микроокружения опухоли молочной железы, в котором наиболее распространены стромальные фибробласты CAFs. Однако в ветеринарной онкологии маркеры стромы злокачественных опухолей молочной железы изучены недостаточно. Цель исследования — изучить экспрессию онкомаркерных белков vimentin, α-SMA, CD34 в стромальном компоненте микроокружения злокачественных опухолей молочной железы у собак.

Материалы и методы. Объектом исследования, проведенного в 2022–2024 гг., являлись самки собак разных пород и возраста (n=26). Материал исследования — опухоль молочной железы. Комплекс гистологических и иммуногистохимических исследований проведен по общепринятым методикам.

Результаты исследования. Установлено, что при разных гистологических типах и степени злокачественности опухолей молочной железы у собак клетки фибробластического дифферона обладают высокой экспрессией виментина и α-SMA и низкой экспрессией CD34, что указывает на их дифференцировку в CAFs.

Обсуждение и заключение. Полученные результаты можно использовать в качестве качестве базовых прикладных данных при изучении канцерогенеза в ветеринарной онкологии.

Ключевые слова: молочная железа, злокачественная опухоль, иммуногистохимия, собаки, экспрессия, виментин, vimentin, α-SMA, CD34

Для цитирования: Дарбишева А.А., Дилекова О.В. Экспрессия vimentin, α-SMA и CD34 в злокачественных типах опухолей молочной железы у собак. *Ветеринарная патология*. 2026;25(2):54–60. https://doi.org/10.23947/2949-4826-2026-25-2-54-60

Introduction. In modern oncology, the mammary tumor microenvironment is considered an important factor influencing the formation of the premetastatic niche in metastasis and contributing to development of a response to nutrient scarcity, lack of oxygen or medicines [1, 2]. Studies [3–5] have established that mammary tumor stroma predominantly consists of cancer-associated fibroblasts (CAFs) — a heterogeneous group of cells participating in a number of processes in tumor microenvironment by fostering the extracellular matrix remodeling, depositing basement membrane components, and by stimulating angiogenesis, development, progression, invasion, and metastasis of cancer.

This cell pool originates from resident fibroblasts, mesenchymal and hematopoietic stem cells, as well as from endothelial cells (endothelial-mesenchymal transition) and epithelial cells (epithelial-mesenchymal transition) [3, 4]. Vimentin, α-SMA and CD34 have been established to be the potential markers of the fibroblastic series cells (including CAFs) and can be used to determine the presence and localization of these cells in the mammary tumors.

Vimentin is an intermediate filament protein expressed in fibroblasts and endothelial cells. It regulates cell migration, differentiation, proliferation, adhesion, and invasion, and modulates the epithelial-mesenchymal transition induced by tumor initiation and development [6].

α-SMA is one of the actin isoforms that stimulates cell motility and is involved in maintaining shape and polarity of cells, as well as in regulating their transcription. Its expression is characteristic of myofibroblasts, known as myofibroblastic CAFs [7, 8, 9].

CD34 is a biomarker of hematopoietic and non-hematopoietic stem cells, including vascular endothelial progenitor cells, embryonic fibroblasts, and multipotent mesenchymal stromal cells [10, 11].

Currently, the problem of expression of tumor marker proteins in the malignant mammary tumor stroma in animals has been insufficiently studied. At the same time, some studies indicate that in the stroma of many invasive malignant tumors with a low degree of differentiation, CD34+ cells are not detected. This is due to the fact that under the influence of soluble factors (especially TGF-β) secreted by tumor cells [12], they differentiate into α-SMA myofibroblasts associated with cancer [13, 14].

The aim of the present study is to investigate the expression of fibroblastic differentiation biomarkers vimentin, α-SMA, and CD34 in the stroma of the canine mammary tumor microenvironment to determine their differentiation in CAFs.

Materials and Methods. The study was conducted in the period from 2022 to 2024 at the Scientific Diagnostic and Treatment Veterinary Center, at the Department of Parasitology and Veterinary-Sanitary Inspection, Anatomy and Pathoanatomy named after Professor S.N. Nikolsky of Stavropol State Agrarian University, and at Stavropol veterinary clinics (“Kolibri”, Sole Proprietor Shalamova E.V., “Pirogov Veterinary Center”, Sole Proprietor Zaichenko I.V.). Medical records of the oncological outpatients registered in the VetAIS, VetDesk, and Vetmanager veterinary practice management systems were analysed. The following aspects of the nosological profile were taken into account: sex, age, breed, castration performed, ridge of mammary glands affected, relapses, as well as the results of instrumental and laboratory examinations for having the pathological conditions indicating the presence of distant metastases.

The material for the study was collected during the unilateral/regional mastectomies and biopsies of mammary tumors in female dogs (n=26). For the study, 1 cm³ specimens were incised from the border of the altered regions of the mammary gland and healthy tissue and skin in compliance with the recommendations of the pathologists’ manual “Macroscopic examination of biopsy and surgical material”. After fixation in 10% neutral buffered formalin (“BioVitrum”, Russia) for 48 hours, the specimens were processed and embedded into the paraffin blocks, which were then sliced into 5-μm-thick sections and mounted on the adhesive slides with the PCI coating, and ground, color-coded edges (CITOTEST, China). To determine the localization of vimentin, anti-Vimentin antibodies (SP20), rabbit monoclonal, 1:25–1:50 (Richard-Allan Scientific Co.,

USA) were used; to determine the localization of α-SMA — anti-α-SMA antibodies (1A4), mouse monoclonal, 1:25–1:50 (Richard-Allan Scientific Co., USA) were used; to determine the localization of CD34 — anti-CD34 antibodies (134M 15), mouse monoclonal, 1:50–1:200 (Cell Marque, USA) were used.

Immunohistochemical studies were performed using a peroxidase polymer-based detection system in compliance with the manufacturer's standard protocol (Dako, USA) by heat-induced antigen retrieval at 100°C in citrate buffer (pH 6.0) for 10 minutes, followed by nuclei staining with Mayer's hematoxylin ("Biovitrum", Russia). For negative control, the primary antibodies were replaced by a diluent (Spring Bioscience, USA).

Microscopic examination of the resulting histological preparations was performed using an Olympus BX45 upright light microscope (Japan) with a built-in C300 photo and video camera and CellSensEntry microscopy software (Japan). Ten digital images were taken from each preparation, taking into account histoarchitecture, for histological analysis at ×400 magnification, covering a HPF of 0.44 mm^2 of the studied tissue.

To assess the expression of vimentin, α-SMA, and CD34 and the prognostic value of these markers, the method proposed by L.E. Gurevich (2003) was used:

— membranous or normal expression type: uniform distribution of immunoreactivity across the entire cell membrane;

— membrane-reduced expression type: distribution of immunoreactivity only in certain areas of the cell membrane;

— mixed membrane-cytoplasmic expression type: uniform cytoplasmic expression combined with membranous expression;

— fine- and coarse-granular cytoplasmic expression type: expression in the form of granules scattered in the cytoplasm of cells;

— clumpy expression type: expression in the cell cytoplasm in the form of randomly localized large clumps and conglomerates of immunoreactive material;

— absence of immunoreactivity.

To assess the prognostic value of the described expression patterns in the cells, immunoreactivity was assessed according to L.E. Gurevich (2003):

— 0 points;

— Membranous type — 1 point;

— Combination of membranous and granular-cytoplasmic — 2 points;

— Coarse-granular — 3 points.

Additionally, the intensity of expression of the immunoreactive material was assessed visually, taking into account the percentage of active cells and the total area of immunopositive structures in compliance with the recommendations of the American Society of Clinical Oncology/College of American Pathologists (ASCO/CAP, 2018):

1. Immunoreactivity is positive (IHC 3+), if complete intense peripheral membranous staining is observed in more than 10% of tumor cells.

2. Immunoreactivity is indeterminate (IHC 2+), if weak to moderate intensity, complete membranous staining is observed in more than 10% of tumor cells.

3. Immunoreactivity is negative (IHC 1+), if incomplete, weak/barely noticeable membranous staining is observed in more than 10% of tumor cells.

4. Immunoreactivity is negative (IHC 0) if no staining is observed or incomplete, weak/barely noticeable membranous staining is observed in 10% or less of the tumor cells.

Research Results. Preliminary, a routine histopathological examination was performed on 26 samples of mammary gland tumors, which revealed the solid carcinoma G3 to be the main histological tumour type (Table 1). Age-related data are presented in Table 2. All samples were obtained from females, two of which were neutered. The analysis revealed that the highest incidence of neoplasms was observed in small-breed dogs — 42.31% of all cases; in medium-breed and in outbred dogs — 15.385%, each; in large-breed dogs — 26.92%. The mammary gland tumor affected both the left mammary ridge (2^{nd} mammary gland — 3.16% of the total amount; 5^{th} mammary gland — 15.79%) and the right mammary ridge (3^{rd} and 5^{th} mammary gland — 13.16%, each, 4^{th} mammary gland — 21.05%). Metastasis to the inguinal lymph nodes was revealed in 30.77% of all cases. One relapse case was identified among 26 patients

.Table 1

Results of histopathological examination of mammary tumors of varying grades of malignancy (G) in dogs (n=26)

Tumour type	G 1, quantity	G 2, quantity	G 3, quantity
Tubular	3	2	-
Papillary	-	4	-
Solid	1	2	5
Mixed	2	4	3

Table 2

Age-related characteristics of mammary tumors in dogs (n=26)

Age, years	Tubular, %	Papillary, %	Solid, %	Tubular-papillary, %
2–2.5	–	–	–	–
6–10	23.08	15.38	11.54	15.38
11–14	–	19.23	7.69	7.69

Vimentin expression in canine mammary tumors is shown in Figure 1. Immunoreactive material was uniformly distributed throughout the cytoplasm in the form of coarse, dark-brown granules (score 3). Although, in some cells, it was visualised in perinuclear pattern as single large foci near the nucleus. Immunopositive areas occupied ≥50% of the total area of the material and biomarker expression was strong (+++). Vimentin-expressing cells had the fibroblastic features— stellate cells with the elongated nuclei. In mammary tumors, they were visualized as a dense network in both the interlobular and intralobular mammary stroma, and were localized around parenchyma in large amounts. This, in our opinion, indicates their paracrine effect on mammary tumor development.

High expression of alpha-smooth muscle actin (α-SMA) in canine mammary tumors is shown in Fig. 2. Dark brown immunoreactive material had perinuclear pattern in papillary, solid, and tubular carcinomas, whereas in mixed tumors, it was uniformly distributed throughout the cell cytoplasm (score 3). Immunopositive areas occupied ≥50% of the total area of the material, and biomarker expression was strong (+++). Cells of a fibroblastic phenotype — stellate cells with the elongated nuclei—were present in the form of cords in the interlobular and intralobular mammary stroma.

Expression of CD34 marker in canine mammary tumors is shown in Fig. 3. A small number of immunopositive cells had a scattered pattern of localization, they were detected in the interlobular stroma of mammary tumor. Areas with these cells demonstrated incomplete, barely noticeable expression, and cytoplasmic staining was negative (+) in more than 10% of tumor cells. The cells had round or elongated form, with nuclei replicating the form of the cells. Immunoreactive material was uniformly distributed throughout the cytoplasm and had the finely- and coarsely granular dark brown structure (score 3). Cells were mostly visualised in the areas where the stroma was subject to fibrosis and sclerosis.

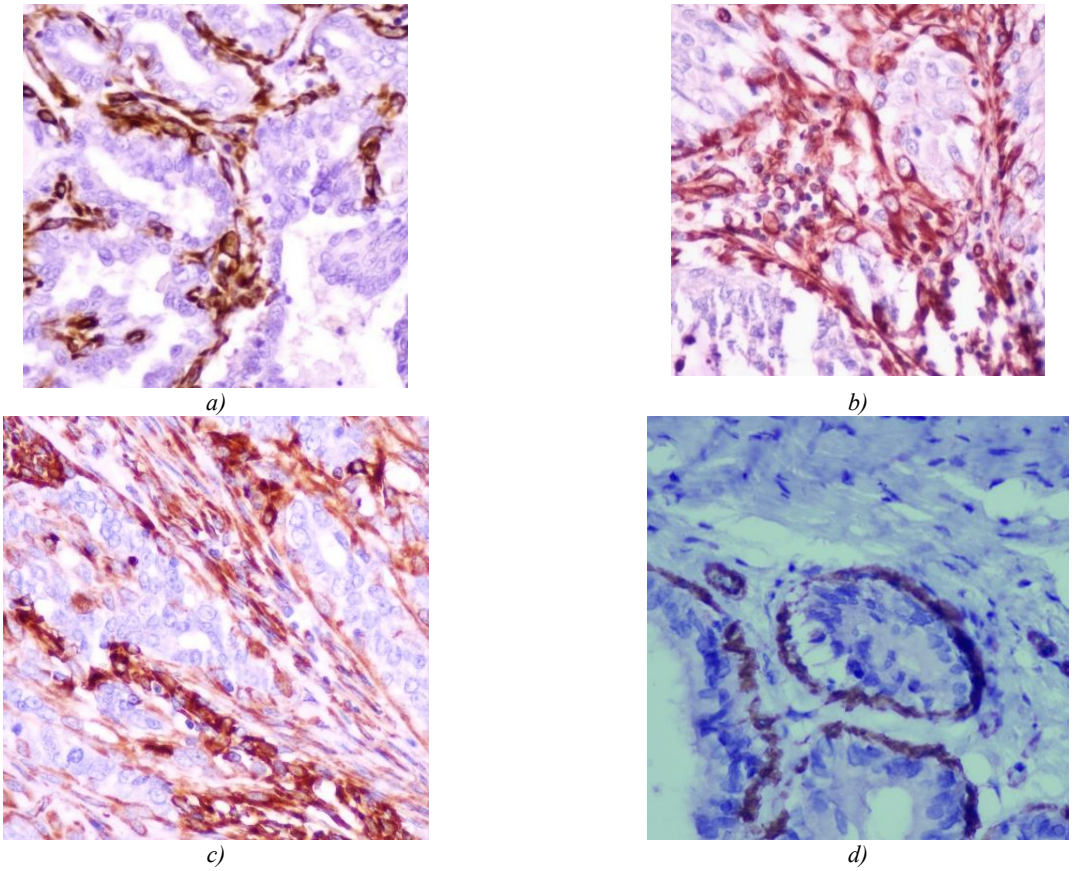

Fig. 1. Expression of vimentin+: a) ductal papillary carcinoma *in situ* G1 (Toy Terrier, 11 years old); b) tubular-papillary moderately differentiated carcinoma G2 (Drahthaar, 6.7 years old); c) solid carcinoma G1 (Yorkshire Terrier, 12.7 years old); d) tubulolobular carcinoma G1 (Toy Terrier, 7.6 years old), ×400 magnification (photos by the authors, here and below)

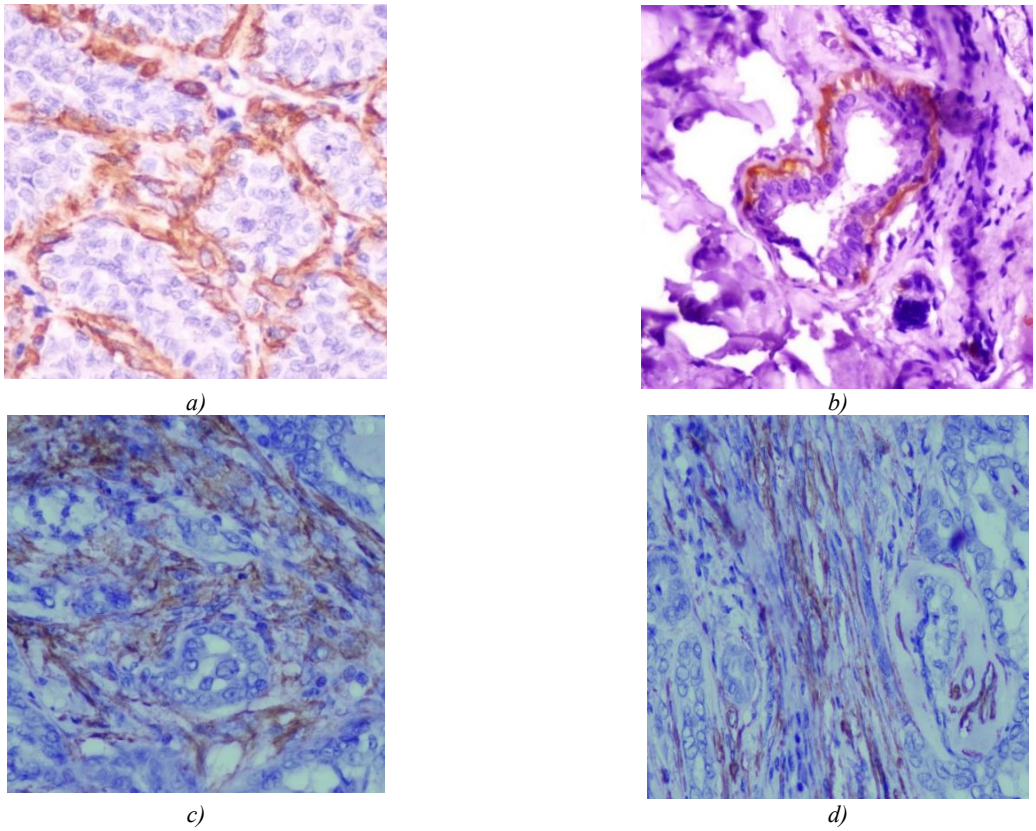

Fig. 2. Expression of α-SMA+: a) ductal papillary carcinoma *in situ* G1 (Toy Terrier, 11 years old); b) tubular-papillary moderately differentiated carcinoma G2 (Drahthaar, 6.7 years old); c) solid carcinoma G1 (Yorkshire Terrier, 12.7 years old); d) tubulolobular carcinoma G1 (Toy Terrier, 7.6 years old), ×400 magnification

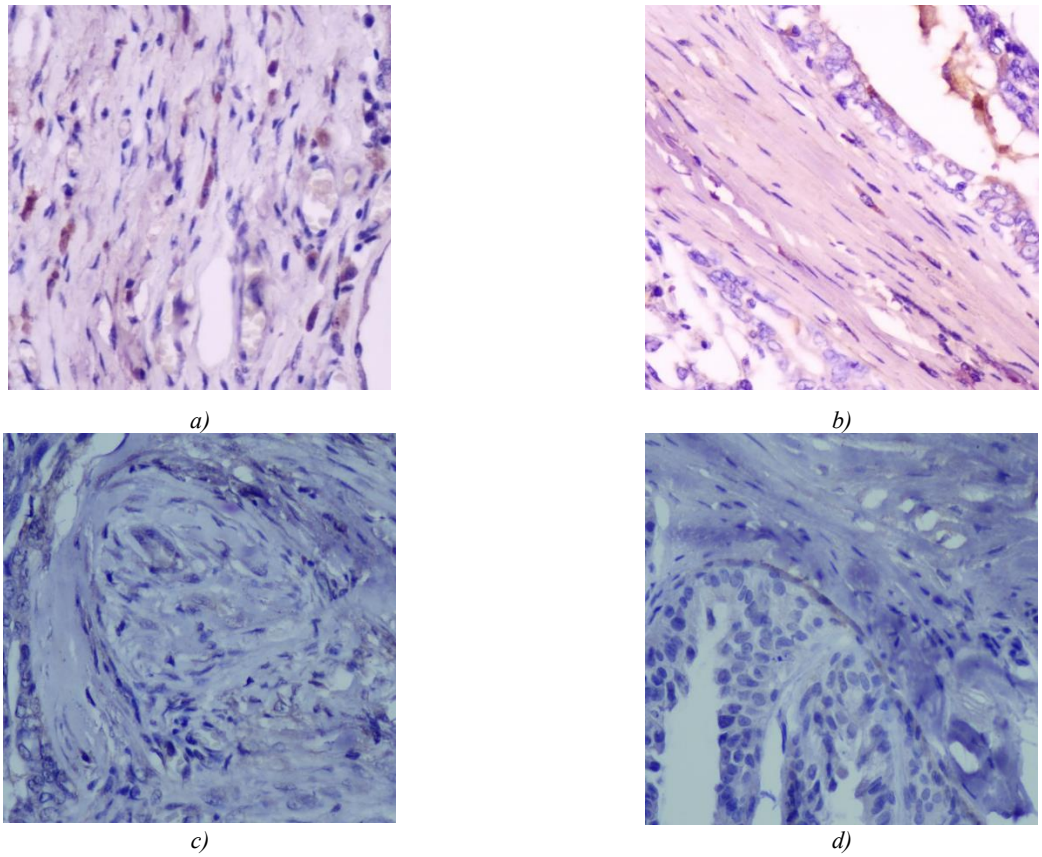

Fig. 3. CD34+ expression: a) ductal papillary carcinoma *in situ* G1 (Toy Terrier, 11 years old); b) tubular-papillary moderately differentiated carcinoma G2 (Drahthaar, 6.7 years old); c) solid carcinoma G1 (Yorkshire Terrier, 12.7 years old); d) tubulolobular carcinoma G1 (Toy Terrier, 7.6 years old), ×400 magnification

Discussion and Conclusion. Based on the conducted research, it is possible to conclude that high expression of vimentin and α-SMA was observed in all neoplasms. As to CD34 marker, its expression in well-differentiated tumors (G1) was low, and in poorly differentiated neoplasms (G3) it was completely absent. Loss of expression of this marker occurred due to the differentiation of the cells in myofibroblasts of the stromal niche of canine mammary tumors. Our data confirm the results of studies [12, 13, 14] indicating that during the development and differentiation of malignant mammary tumors, there occurs a loss of CD34 expression and an increase of α-SMA expression.

Thus, immunohistochemical studies have shown that different types of canine mammary gland tumors have a cell line with a specific biomarker phenotype indicating their affiliation with CAFs. The data obtained by us can be used as basic applied data in the study of carcinogenesis in veterinary oncology.

References

1. Place AE, Huh SJ, Polyak K. The Microenvironment in Breast Cancer Progression: Biology and Implications for Treatment. *Breast Cancer Research*. 2011;13:227. https://doi.org/10.1186/bcr2912

2. Mehraj U, Dar AH, Wani NA, Mir MA. Tumor Microenvironment Promotes Breast Cancer Chemoresistance. *Cancer Chemother Pharmacol*. 2021;87:147–158. https://doi.org/10.1007/s00280-020-04222-w

3. Yu T, Di G. Role of Tumor Microenvironment in Triple-Negative Breast Cancer and Its Prognostic Significance. *Chinese Journal of Cancer Research*. 2017;29(3):237–252. https://doi.org/10.21147/j.issn.1000-9604.2017.03.10

4. Li JJ, Tsang JY, Tse MG. Tumor Microenvironment in Breast Cancer—Updates on Therapeutic Implications and Pathologic Assessment. *Cancers*. 2021;13(16):4233. https://doi.org/10.3390/cancers13164233

5. Giorello MB, Borzone FR, Labovsky V, Piccioni FV, Chasseing NA. Cancer-Associated Fibroblasts in the Breast Tumor Microenvironment. *Journal of Mammary Gland Biology and Neoplasia*. 2021;26:135–155. https://doi.org/10.1007/s10911-020-09475-y

6. Chen Z, Fang Z, Ma J. Regulatory Mechanisms and Clinical Significance of Vimentin in Breast Cancer. *Biomedicine and Pharmacotherapy*. 2021;133:111068. https://doi.org/10.1016/j.biopha.2020.111068

7. Han C, Liu T, Yin R. Biomarkers for Cancer-Associated Fibroblasts. *Biomarker Research*. 2020;8:64. https://doi.org/10.1186/s40364-020-00245-w

8. Dominguez R, Holmes KC. Actin structure and function. *Annual Review of Biophysics*. 2011;40:169–186. https://doi.org/10.1146/annurev-biophys-042910-155359

9. Yoshimura H, Michishita M, Ohkusu-Tsukada K, Takahashi K. Increased Presence of Stromal Myofibroblasts and Tenascin-C with Malignant Progression in Canine Mammary Tumors. *Veterinary Pathology*. 2010;48(1):313–321. https://doi.org/10.1177/0300985810369901

10. Radu P, Zurzu M, Paic V, Bratucu M, Garofil D, Tigora A, et al. CD34—Structure, Functions and Relationship with Cancer Stem Cells . *Medicina*. 2023;*59*(5):938. https://doi.org/10.3390/medicina59050938

11. Sidney LE, Branch MJ, Dunphy SE, Dua HS, Hopkinson A. Concise Review: Evidence for CD34 as a Common Marker for Diverse Progenitors. *Stem Cells*. 2014;32(6):1380–1389. https://doi.org/10.1002/stem.1661

12. Catteau X, Simon P, Noël JC. Myofibroblastic Stromal Reaction and Lymph Node Status in Invasive Breast Carcinoma: Possible Role of the TGF- β1/TGF- βR1 Pathway. *BMC Cancer*. 2014;14:499. https://doi.org/10.1186/1471-2407-14-499

13. Díaz-Flores L, Gutiérrez R, González-Gómez M, García MP, Díaz-Flores L, Carrasco JL, et al. CD34+ Stromal Cells/Telocytes as a Source of Cancer-Associated Fibroblasts (CAFs) in Invasive Lobular Carcinoma of the Breast. *International Journal of Molecular Sciences*. 2021;*22*(7):3686. https://doi.org/10.3390/ijms22073686

14. Khan AA, Alam K, Harris H. A Clinicopathological Study of CD34 Antigen Expression in Benign and Malignant Breast Lesions. *Journal of Clinical and Experimental Pathology*. 2017;07(04). https://doi.org/10.4172/2161-0681.1000321

About the Authors:

Alina A. Darbisheva, Post Graduate Degree Student of the Parasitology and Veterinary-Sanitary Inspection, Anatomy and Pathoanatomy Department Named after S.N. Nikolsky, Stavropol State Agrarian University (12, Zootechnichesky Lane, Stavropol, 355017, Russian Federation), ORCID, darbisevaalina@gmail.com

Olga V. Dilekova, Dr.Sci. (Biology), Associate Professor of the Parasitology and Veterinary-Sanitary Inspection, Anatomy and Pathoanatomy Department Named after S.N. Nikolsky, Stavropol State Agrarian University (12, Zootechnichesky Lane, Stavropol, 355017, Russian Federation), ORCID, dilekova2009@yandex.ru

Claimed Contributorship:

OV Dilekova: scientific supervision, developing the concept and methodology of research.

AA Darbisheva: conducting the research, validating the results, editing the text

Conflict of Interest Statement: **the authors declare no conflict of interest.**

All authors have read and approved the final manuscript.

Об авторах:

Дарбишева Алина Андреевна, аспирант кафедры паразитологии и ветсанэкспертизы, анатомии и патанатомии им. С.Н. Никольского института ветеринарии и биотехнологий Ставропольского аграрного государственного университета (355017, РФ, г. Ставрополь, пер. Зоотехнический, д. 12), ORCID, darbise-vaalina@gmail.com

Дилекова Ольга Владимировна, доктор биологических наук, доцент кафедры паразитологии и ветсанэкспертизы, анатомии и патанатомии им. С.Н. Никольского института ветеринарии и биотехнологий Ставропольского аграрного государственного университета (355017, РФ, г. Ставрополь, пер. Зоотехнический, д. 12), ORCID, dilekova2009@yandex.ru

Заявленный вклад авторов:

О.В. Дилекова: научное руководство, разработка концепции, разработка методологии.

А.А. Дарбишева: проведение исследования, валидация результатов, редактирование

Конфликт интересов: **авторы заявляют об отсутствии конфликта интересов.**

Все авторы прочитали и одобрили окончательный вариант рукописи.

Received / Поступила в редакцию 23.01.2026
Reviewed / Поступила после рецензирования 07.05.2026
Accepted / Принята к публикации 22.05.2026

ANIMAL INFECTIOUS DISEASES AND IMMUNOLOGY
ИНФЕКЦИОННЫЕ БОЛЕЗНИ И ИММУНОЛОГИЯ ЖИВОТНЫХ

UDC: 579.6:60:577.21
https://doi.org/10.23947/2949-4826-2026-25-2-61-67

Original Empirical Research

EDN: EUJXUX

A Comprehensive Analysis of Cytotoxicity of Genetically Modified *Lactobacillus plantarum* 8PA3 (B-11007) Strain Including Identification and Evaluation of Virulence Factors

Viktor S. Samoylenko ✉
North-Caucasus Federal University, Stavropol, Russian Federation
✉ viktor_samoylenko_26@mail.ru

Abstract

Introduction. Active development of biotechnologies and genetic engineering techniques broadens the horizons for engineering the probiotic bacterial strains with tailored functional properties, including the strains based on bacteria of the genus *Lactobacillus* that are traditionally considered safe microorganisms. Genetic modification enhances their antagonist activity, resistance to adverse environmental factors, and boosts metabolic efficiency. However, bacterial genome editing may entail risk of introducing the undesirable traits, including cytotoxicity and expression of virulence factors. Safety concerns are particularly relevant in the frame of veterinary practice, where probiotics are widely used to correct the gastrointestinal microbiocenosis in agricultural animals and improve their productivity. The aim of the study is to conduct a comprehensive analysis of cytotoxicity of the genetically modified *Lactobacillus plantarum* 8PA3 (B-11007) strain including identification and evaluation of the virulence factors responsible for inducing cell death and disruption of cellular functions.

Materials and Methods. A genetically modified *Lactobacillus plantarum* 8PA3 (B-11007) strain was the object of the study conducted in the period from January to February 2026. A comprehensive *in vitro* analysis of its cytotoxicity included: assessment of the cytopathic effect in intestinal cell culture, the effect on the viability and metabolic activity of enterocytes, and the state of intestinal epithelial barrier function. Additionally, the analysis of potential virulence factors was performed, along with the study of the mechanisms of cell death, including signs of apoptosis and necrosis.

Results. The recombinant *Lactobacillus plantarum* 8PA3 (B-11007) strain has demonstrated a high biological safety and pronounced biological activity, which enhanced the intestinal epithelial barrier function by 15.2%, the metabolic activity of cells by 8.7% and simultaneously reduced early apoptosis of enterocytes by 31.1% ($p<0.05$), showing no signs of cytotoxic action or activation of caspase-dependent cell death.

Discussion and Conclusion. The conducted comprehensive analysis allows making the unequivocal conclusion about genetically modified *L. plantarum* 8PA3 (B-11007) strain exhibiting no cytotoxic activity *in vitro.* Moreover, by certain properties (cellular metabolic activity, barrier function), it exceeds the original native strain, which makes it a promising candidate for further preclinical and clinical trials as a potential probiotic agent.

Keywords: comprehensive analysis, *Lactobacillus*, *L. plantarum 8PA3 (B-11007)*, probiotics, genetic engineering, cytotoxicity, intestinal cell culture, enterocytes, virulence factors

For Citation. Samoylenko VS. A Comprehensive Analysis of Cytotoxicity of Genetically Modified *Lactobacillus plantarum* 8PA3 (B-11007) Strain Including Identification and Evaluation of Virulence Factors. *Russian Journal of Veterinary Pathology*. 2026;25(2):61–67. https://doi.org/10.23947/2949-4826-2026-25-2-61-67

Оригинальное эмпирическое исследование

Комплексный анализ цитотоксичности генетически модифицированного штамма *Lactobacillus plantarum* 8РАЗ (В-11007) с выявлением и оценкой факторов вирулентности

В.С. Самойленко
Северо-Кавказский федеральный университет, г. Ставрополь, Российская Федерация
viktor_samoylenko_26@mail.ru

Аннотация

Введение. Активное развитие биотехнологий и методов генной инженерии открывает широкие перспективы для создания пробиотических штаммов с заданными функциональными свойствами, в том числе на основе бактерий рода *Lactobacillus*, традиционно считающихся безопасными микроорганизмами. Генетическая модификация позволяет усиливать их антагонистическую активность, устойчивость к неблагоприятным факторам среды и метаболическую эффективность. Однако вмешательство в бактериальный геном может сопровождаться риском появления нежелательных свойств, включая цитотоксичность и экспрессию факторов вирулентности. Проблема безопасности особенно актуальна в ветеринарной практике, где пробиотики широко применяются для коррекции микробиоценоза желудочно-кишечного тракта сельскохозяйственных животных и повышения их продуктивности. Цель исследования — провести комплексный анализ цитотоксичности генетически модифицированного штамма *Lactobacillus plantarum* 8РАЗ (В-11007) с выявлением и оценкой факторов вирулентности, отвечающих за индуцирование клеточной гибели и нарушение клеточных функций.

Материалы и методы. Объектом исследования, проведенного в период с января по февраль 2026 г., являлся генетически модифицированный штамм *Lactobacillus plantarum* 8РАЗ (В-11007). Комплексный анализ его цитотоксичности с использованием методов *in vitro* включал: оценку цитопатического эффекта на органной культуре кишечника, влияние на жизнеспособность и метаболическую активность энтероцитов, а также состояние барьерной функции кишечного эпителия. Дополнительно выполнялся анализ потенциальных факторов вирулентности и изучались механизмы клеточной гибели, включая признаки апоптоза и некроза.

Результаты исследования. Рекомбинантный штамм *Lactobacillus plantarum* 8РАЗ (В-11007) продемонстрировал высокий профиль биологической безопасности и выраженную биологическую активность, увеличивая барьерную функцию кишечного эпителия на 15,2 %, метаболическую активность клеток на 8,7 % и одновременно снижая ранний апоптоз энтероцитов на 31,1% ($p<0,05$), без признаков цитотоксического действия и активации каспаз-зависимой гибели клеток.

Обсуждение и заключение. Проведённый комплексный анализ позволяет сделать однозначный вывод о том, что генетически модифицированный штамм *L. plantarum* 8РАЗ (В-11007) не обладает цитотоксическим действием в условиях *in vitro*. Более того, по ряду параметров (метаболическая активность клеток, барьерная функция) он превосходит исходный нативный штамм, что делает его перспективным кандидатом для дальнейших доклинических и клинических исследований в качестве потенциального пробиотического средства.

Ключевые слова: комплексный анализ, *Lactobacillus, L. plantarum* 8РАЗ (В-11007), пробиотики, генная инженерия, цитотоксичность, органная культура кишечника, энтероциты, факторы вирулентности

Для цитирования. Самойленко В.С. Комплексный анализ цитотоксичности генетически модифицированного штамма *Lactobacillus plantarum* 8РАЗ (В-11007) с выявлением и оценкой факторов вирулентности. *Ветеринарная патология*. 2026;25(2):61–67. https://doi.org/10.23947/2949-4826-2026-25-2-61-67

Introduction. Active development of biotechnologies and genetic engineering techniques broadens the horizons for engineering the probiotic strains with tailored functional properties. In this context, identification and description of the potential factors of virulence are performed using the specialized databases and taxonomies [1]. Modern understanding of the role of probiotics in maintaining human health and regulating metabolic processes fosters the relevance of targeted modification of bacteria designated to enhance their beneficial properties [2]. At the same time, the results of the phenotypic and genomic analysis of *Lactobacillus reuteri* strains demonstrate the need for a comprehensive safety assessment even for commonly used probiotics [3]. Similar data on the importance of comparing the genomic markers and phenotypic characteristics in the context of assessing safety of a given strain are presented in publication [4]. General reviews emphasize that expansion of the range of probiotic products requires strict control of their biological safety and pathogenic potential absence [5].

A comprehensive approach to assessment of the safety of probiotic cultures, including genotypic and phenotypic

analysis, was implemented in a study of *Lacticaseibacillus paracasei* NTU 101, demonstrating the relevance of multi-level testing of new strains [6]. Similar methodological principles were applied in the analysis of *Lactobacillus bulgaricus* IDCC 3601, where potential risks to humans were assessed [7]. A detailed description of the phenotypic and genotypic characteristics of *Levilactobacillus brevis* KU15006 has also proved the need to exclude the factors of virulence and antibiotic resistance [8]. It is known that molecular signaling pathways regulating cell proliferation and survival in condition of inflammatory stress can be modified by microbial factors, which emphasises the importance of studying the cellular mechanisms of the host response [9].

The problem of safety of genetically modified microorganisms is particularly relevant for veterinary practice, where probiotics are used to normalize the microbiocenosis and increase animal resistance to infections, as confirmed by the studies of *Lactococcus lactis* IDCC 2301 [10]. The assessment of four lactobacilli strains with probiotic properties showed that even closely related microorganisms require individual analysis of genetic stability and the absence of undesirable determinants [11]. The activity of enzymes, such as bile salt hydrolases, is based on the interaction of microbiota and the host organism, and has significant importance [12]. Studies of the *Lactobacillus delbrueckii subsp. lactis* strain CKDB001 confirm the need to evaluate not only safety but also functional metabolic effects [13].

In vitro experimental models are widely used to evaluate the cytotoxicity and safety of encapsulated probiotic cultures, as demonstrated for *Lactiplantibacillus plantarum* CRD7 and *Lacticaseibacillus rhamnosus* CRD11 [14]. Changes in intestinal microbiota and metabolic parameters after administration of *Lacticaseibacillus paracasei* AO356 confirm the importance of studying the systemic effect of probiotics [15]. Analysis of the phenotypic and genotypic characteristics of *Weissellacibaria* JW15 also indicates the need for a comprehensive assessment of safety of the new cultures [16]. An additional stage of preclinical testing is *in silico* analysis of potential genes of virulence and resistance, as shown for representatives of the genus *Bacillus* isolated from the bee products [17].

Particular attention is paid to the ability of strains to produce biogenic amines, which can have a toxic effect when accumulated in food products, as demonstrated for lactic acid bacteria isolated from fish products [18]. Genomic sequencing and evaluation of the probiotic potential of *Lacticaseibacillus paracasei* strain LC86 and *Lacticaseibacillus casei* strain confirm the importance of a comprehensive analysis of their safety [19]. The reviews investigating the biogenic amines in the fermented products emphasise the potential risks of uncontrolled microbial activity for the health [20]. Current data on the oral cavity microbiome and its impact on systemic health also indicate the need for rigorous evaluation of probiotic interventions [21].

Experimental studies using a *Clostridioides difficile* infection model demonstrate that probiotic strains can reduce expression of inflammation and restore barrier function of the intestines, thus, confirm their therapeutic potential subject to proven safety [22]. However, even opportunistic lactobacilli strains can, under certain conditions, exhibit cytopathic effect on intestinal epithelium. Therefore, comprehensive analysis of cytotoxicity is a necessary step in preclinical studies of new probiotic strains.

The aim of the study is to conduct a comprehensive analysis of the cytotoxic properties of the genetically modified strain *Lactobacillus plantarum* 8PA3 (B-11007), aiming to identify and evaluate the virulence factors responsible for inducing the cell death and dysfunction of cellular mechanisms.

Materials and Methods. The experimental part of the study was performed at the Genome Center of the North-Caucasus Federal University (Stavropol) and at the bacteriological laboratory of the Department of Epizootology and Microbiology of Stavropol State Agrarian University in the period from January 23 to February 17, 2026.

In this study, the *Lactobacillus plantarum* strain 8PA3 (B-11007) was genetically modified by introducing a recombinant plasmid containing functionally independent expression cassettes encoding heterologous proteins under the control of constitutive promoters.[1] The cytotoxicity of the genetically modified *L. plantarum* strain 8PA3 (B-11007) was assessed in compliance with the author's method of A.V. Frolov "Method for determining the cytotoxicity of bacteria".[2]

The study was conducted using the genetically modified (GM) *L. plantarum* strain 8PA3 (B-11007) and its native analogue as a control. Such an approach makes it possible not only to identify differences in the cytopathic effect between the GM form and the control one but also to assess the preservation or enhancement of strain's beneficial properties, which is extremely important for the objective assessment of the modified strain's safety and functional activity.

Bacterial strains were cultured in the standard MRS nutrient medium (Difco™) in under anaerobic conditions at 37°C using AnaeroGen gas bags (Oxoid, UK). Bacterial suspensions were prepared in sterile phosphate-buffered saline (PBS), adjusted to optical density of 0.5 McFarland standard, corresponding to a concentration of approximately 1.5×10^8 CFU/ml, and then diluted to a working concentration of 1×10^9 CFU/ml.

[1] At the time of writing this article, the patent is undergoing patent registration (incoming no. W 25039202 Russian Federation. Registration No. 2025116719).

[2] USSR patent SU No. 1747483 A1.

Cytotoxicity was assessed using two parallel approaches. In the first step, jejunal organ culture from clinically healthy 10-day-old calves (n=10) were placed in sterile containers over a cover slip with liquid nutrient medium (RPMI-1640) containing a suspension of the studied *Lactobacillus* strain at a final concentration of 1×10^9 CFU/ml. Incubation with the bacterial suspension was carried out for 30 min at 37°C in an atmosphere of 5% CO_2 and 95% humidity using a CO_2 incubator (Binder GmbH, Germany). After exposure, the containers were centrifuged at the rate of 10 000 rpm for 10 min to sediment the cells detached as a result of the cytopathic effect. Each experiment was performed in 5 biological replicates.

In parallel, cytotoxicity was assessed in primary culture of enterocytes that were isolated from the jejunum of 10-day-old calves. Cells were seeded in 96-well plates coated with type I collagen at density of 3×10^4 cells per well and cultured in RPMI-1640 medium supplemented with 10% fetal calf serum until a monolayer formed. Cytotoxicity was assessed using the MTT assay with 24-hour incubation and subsequent measurement of optical density (OD) at 570 nm. Intestinal barrier integrity was assessed by measuring transepithelial electrical resistance (TEER) using an EVOM2 Volt/Ohm meter, recording readings every 4 hours for 24 hours.

To determine the mechanisms of cytotoxicity, fluorescence microscopy was performed using annexin V-FITC and propidium iodide staining to differentiate apoptosis from necrosis. Caspase 3/7 activity was also assessed using the Caspase-Glo 3/7 Assay kit.

Quantitative cytotoxicity (C) was assessed using the formula:

$$C= N/t\ (1- g1/g0), \quad (1)$$

where N — the number of cells detached during centrifugation, counted per 1.96 mm^2 along the diagonals of the cover glass;

g0 — centrifugal acceleration of cell detachment, not treated with a cytotoxic bacterial suspension;

g1 — centrifugal acceleration of cell detachment, treated with a cytotoxic bacterial suspension;

t — exposure time to cytotoxic bacterial suspension, h.

To more thoroughly assess the impact on the cellular functions, an MTT assay was used on a monolayer of primary enterocytes for 24 hours. The assay is based on the Tetrazolium dye (MTT) reduction by mitochondrial dehydrogenases of viable cells. Cell viability percentage (VC) was calculated using the formula:

$$VC\ (\%) = (OD570\ experiment / OD570control) \times 100\ \%, \quad (2)$$

where OD570 experiment — optical density of formazan solution in wells with cells treated with bacteria;

OD570 control — optical density in wells with cells cultured in a pure nutrient medium.

All numerical data obtained were subjected to statistical processing. Results are presented as the arithmetic mean (M) ± standard deviation (SD) or standard error of the mean (SEM). The Shapiro-Wilk test was used to assess the normality of data distribution. Comparison of means between the experimental and control groups was performed using the Student's t-test for independent samples using the Primer of Biostatistics 4.03 software (McGraw-Hill, USA). Differences were considered statistically significant at $p \leq 0.05$.

Research Results. The primary assessment of the potential cytotoxic effect of the genetically modified *L. plantarum* strain 8PA3 (B-11007) was performed in compliance with A.V. Frolov's method on jejunal organ culture and revealed no statistically significant increase in cytotoxicity between the GM strain and its native analogue (Table 1).

As shown in Table 1, the cytotoxicity index of the GM strain did not differ statistically significantly ($p>0.05$) from that of the native control strain. The number of detached cells in both groups (corresponding to a cytotoxicity index in the range of 0.06–0.12 a.u.) was within the reference values established for this organ culture in the settings free of pathogenic influence (0.05–0.15 a.u.). This indicates the absence of cytopathic effect and disruption of tissue adhesive properties under the influence of the genetically modified strain, even under extreme stress testing conditions. It is important to emphasize that the method is based on a short-term (30 min) exposure to an extremely high bacterial concentration (1×10^9 CFU/ml) followed by the application of centrifugal force, which simulates the tissue resistance limit. These conditions are stressful and extreme, simulating not a standard interaction, but rather the tissue's "resistance limit". In the context of safety assessment, identifying an effect under such conditions is a valuable indicator for further, more in-depth studies, but cannot directly indicate pathogenicity *in vivo*, where bacterial concentrations and interaction conditions are significantly milder.

Table 1

Cytotoxicity index (CI) of native and GM forms of *L. plantarum* strain 8PA3 (B-11007) on jejunal organ culture (M ± SD, n=5)

Studied group	Cytotoxicity index (CI), arbitrary units (a.u.)	Significance level (p)
Native (control) strain	0.08 ± 0.02	–
Genetically modified strain	0.09 ± 0.03	>0.05

Visual assessment of the organ cultures after the experiment confirmed the quantitative data obtained. The jejunal mucosa in both studied groups (both those exposed to the native and GM strains) retained characteristic morphological features consistent with the normal values. The surface of the samples had a uniform pale pink color, indicating preserved microcirculation and the absence of signs of ischemia or hemorrhagic lesions. Macroscopic examination revealed a smooth, moist mucosal surface, characteristic of healthy tissue. The absence of areas of turbidity, focal hyperemia, edema, or massive epithelial desquamation further demonstrates the absence of destructive effects from the GM strain.

The results of the MTT test on a monolayer of primary enterocytes showed that after 24 hours of incubation, the metabolic activity of cells treated with the GM strain was statistically significantly higher than that in the control group (Table 2).

The data obtained in Table 2 indicate that the GM strain has a moderate stimulating effect on enterocyte metabolic activity, significantly ($p < 0.05$) increasing it by 8.7% compared to the control strain. This effect may be associated with targeted changes in bacterial metabolism as a result of genetic modification, such as increased production of specific metabolites (short-chain fatty acids, B vitamins) that have a trophic effect on intestinal epithelial cells.

To assess safety at the level of cell death regulation, the analysis of apoptosis and the activity of executioner caspases 3/7 was performed (Table 3).

As shown in Table 3, the GM strain significantly ($p<0.05$) reduced the proportion of cells undergoing early apoptosis by 31% compared to the control, without affecting caspase 3/7 activity ($p > 0.05$). This indicates an anti-apoptotic effect unrelated to the classical caspase-dependent pathway and confirms the strain's safety.

All quantitative data obtained, demonstrating the balance between the safety and beneficial properties of the GM strain, are summarized in Table 4.

Table 2

Effect of native and GM forms of *L. plantarum* strain 8PA3 (B-11007) on the metabolic activity of primary enterocytes (M ± SD, n=5)

Studied group	Metabolic activity, % of control	Significance level (p)
Native (control) strain	100.0 ± 3.5	–
Genetically modified strain	108.7 ± 4.1	<0.05

Table 3

Effect of native and GM forms of *L. plantarum* strain 8PA3 (B-11007) on apoptosis and caspase 3/7 activity in primary enterocytes (M ± SD, n=5)

Studied group	Cells in early apoptosis, %	Activity of caspases 3/7, a.u.	Significance level (p)
Native (control) strain	4.5 ± 0.6	1.00 ± 0.12	-
Genetically modified strain	3.1 ± 0.4	0.95 ± 0.10	<0.05 (for apoptosis)

Table 4

Summary of the effect of GM form of *L. plantarum* strain 8PA3 (B-11007) on organ culture and primary enterocytes

Parameter	Native (control) strain	GM strain	Difference, %	Statistical Significance (p)
Cytotoxicity index (CI)	0.08 ± 0.02 a.u.	0.09 ± 0.03 a.u.	+12.5	>0.05
Metabolic activity	100.0 ± 3.5 %	108.7 ± 4.1 %	+8.7	<0.05
Transepithelial electrical resistance (TEER)	100 %	115.2 % (by 24th hour)	+15.2	<0.05
Early apoptosis	4.5 ± 0.6 %	3.1 ± 0.4 %	-31.1	<0.05

Discussion and Conclusion. Based on the conducted comprehansive studies, it was established that the genetically modified *L. plantarum* strain 8PA3 (B-11007) does not exhibit a cytotoxic effect on the calf jejunal organ culture. The cytotoxicity index of the GM strain (0.09±0.03 a.u.) did not statistically significantly differ ($p>0.05$) from the index of the native precursor strain (0.08±0.02 a.u.) and was within the physiological norm, indicating the preservation of cellular adhesion and the integrity of the histological structure of the tissue. Macroscopic assessment of the mucous membrane showed the preservation of normal

characteristics — pale pink color and typical surface topography with physiological roughness, which further confirms the absence of pathological changes in the tissue.

The GM strain proved to have a positive effect on the functional activity of enterocytes. A statistically significant ($p<0.05$) increase in cellular metabolic activity by 8.7% compared to the that in the control was detected, as well as a reliable enhancement of barrier function, expressed as an increase in transepithelial electrical resistance by 15.2% by 24th hour of coincubation. It was confirmed that the mechanism of interaction between the GM strain and host cells is not associated with the induction of apoptosis or necrosis. In the experimental group, a statistically significant decrease in the proportion of cells in early apoptosis was recorded (3.1% versus 4.5% in the control; $p<0.05$) with maintained background level of caspase 3/7 activity, indicating the safety of the strain in the context of cell death regulation.

The conducted studies allow us to conclude that the genetic modification of the *L. plantarum* strain 8PA3 (B-11007) did not lead to the acquisition of cytopathic properties or virulence factors. The preservation of normal macroscopic characteristics of the intestinal mucosa, combined with a positive effect on cellular functions, indicates that the GM strain has positive effects, expressed in stimulating enterocyte metabolism and strengthening the intestinal epithelial barrier. The identified properties make this strain a promising candidate for the development of new probiotic medications based on it. To fully understand the mechanisms of the observed positive effects and identify specific bacterial metabolites responsible for the identified effects, it is advisable to conduct further proteomic and metabolomic studies. The results obtained are the basis for moving to the next stage of preclinical testing in laboratory animals.

References

1. Liu B, Zheng D, Zhou S, Chen L, Yang J. VFDB 2022: A General Classification Scheme for Bacterial Virulence Factors. *Nucleic Acids Research*. 2022;50(D1):D912–D917. http://doi.org/10.1093/nar/gkab1107

2. Barrea L, Verde L, Auriemma RS, Vetrani C, Cataldi M, Frias-Toral E, et al. Probiotics and Prebiotics: Any Role in Menopause-Related Diseases? *Current Nutrition Reports.* 2023;12:83–97. https://doi.org/10.1007/s13668-023-00462-3

3. Lee BS, Ban OH, Bang WY, Chae SA, Oh S, Park C, et al. Safety Assessment of *Lactobacillus Reuteri* IDCC 3701 Based on Phenotypic and Genomic Analysis. *Annals of Microbiology.* 2021;71:10. https://doi.org/10.1186/s13213-021-01622-y

4. Sarita B, Samadhan D, Hassan MZ, Kovaleva EG. A Comprehensive Review Of Probiotics and Human Health — Current Perspective and Applications. *Frontiers in Microbiology*. 2025;15:1487641. https://doi.org/10.3389/fmicb.2024.1487641

5. Chen CT, Chao WY, Lin CH, Shih TW, Pan TM. Comprehensive Safety Assessment of *Lacticaseibacillus Paracasei Subsp. Paracasei* NTU 101 through Integrated Genotypic and Phenotypic Analysis. *Current Issues in Molecular Biology*. 2024;46(11):12354–12374. https://doi.org/10.3390/cimb46110734

6. Lee M, Bang WY, Lee HB, Yang SY, Lee KS, Kang HJ, et al. Safety Assessment and Evaluation of Probiotic Potential of *Lactobacillus Bulgaricus* IDCC 3601 for Human Use. *Microorganisms*. 2024;12(10):2063. https://doi.org/10.3390/microorganisms12102063

7. Lee MG, Kang MJ, Kim S, Jeong H, Kang DK, Paik HD, et al. Safety Assessment of *Levilactobacillus Brevis* KU15006: A Comprehensive Analysis of Its Phenotypic and Genotypic Properties. *Probiotics and Antimicrobial Proteins*. 2025;17(3):1117–1131. https://doi.org/10.1007/s12602-024-10237-z

8. Tail M, Zhang H, Zheng G, Hatami M, Skutella T, Unterberg A, et al. The Sonic Hedgehog Pathway Modulates Survival, Proliferation, and Differentiation of Neural Progenitor Cells under Inflammatory Stress in Vitro. *Cells*. 2022;11(4):736. https://doi.org/10.3390/cells11040736

9. Kim T, Mondal SC, Jeong CR, Kim SR, Ban OH, Jung YH, et al. Safety Evaluation of *Lactococcus lactis* IDCC 2301 Isolated from Homemade Cheese. *Food Science and Nutrition*. 2022;10(1):67–74. https://doi.org/10.1002/fsn3.2648

10. Lee YR, Bang WY, Baek KR, Kim GH, Kang MJ, Yang J, et al. Safety Evaluation by Phenotypic and Genomic Characterization of Four *Lactobacilli* Strains with Probiotic Properties. *Microorganisms*. 2022;10(11):2218. https://doi.org/10.3390/microorganisms10112218

11. Bourgin M, Kriaa A, Mkaouar H, Mariaule V, Jablaoui A, Maguin E, et al. Bile Salt Hydrolases: at the Crossroads of Microbiota and Human Health. *Microorganisms*. 2021;9(6):1122. https://doi.org/10.3390/microorganisms9061122

12. Joung H, Chu J, Kwon YJ, Kim KH, Shin CH, Ha JH. Assessment of the Safety and Hepatic Lipid-Lowering Effects of *Lactobacillus Delbrueckii Subsp. Lactis* CKDB001. *Applied Biological Chemistry*. 2024;67:101. https://doi.org/10.1186/s13765-024-00949-9

13. Varada VV, Panneerselvam D, Pushpadass HA, Mallapa RH, Ram C, Kumar S. In Vitro Safety Assessment of Electrohydrodynamically Encapsulated *Lactiplantibacillus Plantarum* CRD7 and *Lacticaseibacillus Rhamnosus* CRD11 for Probiotics Use. *Current Research in Food Science.* 2023;6:100507. https://doi.org/10.1016/j.crfs.2023.100507

14. Song EJ, Lee ES, Kim YI, Shin DU, Eom JE, Shin HS, et al. Gut Microbial Change after Administration of *Lacticaseibacillus Paracasei* AO356 Is Associated with Anti-Obesity in a Mouse Model. *Frontiers in Endocrinology*. 2023;14:1224636. https://doi.org/10.3389/fendo.2023.1224636

15. Jang YJ, Gwon HM, Jeong WS, Yeo SH, Kim SY. Safety Evaluation of *Weissella Cibaria* JW15 by Phenotypic and Genotypic Property Analysis. *Microorganisms*. 2021;9(12):2450. https://doi.org/10.3390/microorganisms9122450

16. Bin Hafeez A, Pełka K, Worobo R, Szweda P. In Silico Safety Assessment of Bacillus Isolated from Polish Bee Pollen and Bee Bread as Novel Probiotic Candidates. *International Journal of Molecular Sciences*. 2024;25(1):666. https://doi.org/10.3390/ijms25010666

17. Yilmaz N. Quantitative Analysis of Biogenic Amine Production of Different Lactic Acid Bacteria Isolated from Ready-to-Eat Packaged Fish Products. *Veterinary Research Forum*. 2024;15:537–543. https://doi.org/10.30466/vrf.2024.2024103.4193

18. Chen T, Zhao Y, Fan Y, Dong Y, Gai Z. Genome Sequence and Evaluation of Safety and Probiotic Potential of *Lacticaseibacillus Paracasei* LC86 and *Lacticaseibacillus Casei* LC89. *Frontiers in Microbiology*. 2025;15:1501502. https://doi.org/10.3389/fmicb.2024.1501502

19. Turna NS, Chung R, McIntyre L. A Review of Biogenic Amines in Fermented Foods: Occurrence and Health Effects. *Heliyon*. 2024;10(2):e24501. https://doi.org/10.1016/j.heliyon.2024.e24501

20. Rajasekaran JJ, Krishnamurthy HK, Bosco J, Jayaraman V, Krishna K, Wang T, et al. Oral Microbiome: A Review of Its Impact on Oral and Systemic Health. *Microorganisms*. 2024;12(9):1797. https://doi.org/10.3390/microorganisms12091797

21. Panpetch W, Phuengmaung P, Cheibchalard T, Somboonna N, Leelahavanichkul A, Tumwasorn S. *Lacticaseibacillus Casei* Strain T21 Attenuates Clostridioides Difficile Infection in a Murine Model through Reduction of Inflammation and Gut Dysbiosis with Decreased Toxin Lethality and Enhanced Mucin Production. *Frontiers in Microbiology*. 2021;12:745299. https://doi.org/10.3389/fmicb.2021.745299

About the Author:

Viktor S. Samoylenko, Cand.Sci. (Veterinary), Head of the Department of Zoology and Parasitology, North-Caucasus Federal University (1, Pushkin Str., Stavropol, 355017, Russian Federation), ORCID, SPIN-code, viktor_samoylenko_26@mail.ru

Conflict of Interest Statement: **the author declares no conflict of interest.**

The author has read and approved the final manuscript.

Об авторе:

Самойленко Виктор Сергеевич, кандидат ветеринарных наук, заведующий кафедрой зоологии и паразитологии, Северо-Кавказский федеральный университет, 355017, Российская Федерация, г. Ставрополь, ул. Пушкина, 1, ORCID, SPIN-код, viktor_samoylenko_26@mail.ru

Конфликт интересов: **автор заявляет об отсутствии конфликта интересов.**

Автор прочитал и одобрил окончательный вариант рукописи.

Received / Поступила в редакцию 24.04.2026
Reviewed / Поступила после рецензирования 06.05.2026
Accepted / Принята к публикации 03.06.2026